DEMONSTRATION OF OPENFMB ENABLED POWER SYSTEM OPERATIONS USING HARDWARE - IN - LOOP (HIL) REAL TIME SIMULATOR

by

Rasik Sarup

A thesis submitted to the faculty of
The University of North Carolina at Charlotte
in partial fulfillment of the requirements
for the degree of Master of Science in
Electrical Engineering

Charlotte

2019

Approved by:

____

Dr. Madhav Manjrekar

____

Dr. Sukumar Kamalasadan

____

Dr. Babak Parkhideh

ABSTRACT

RASIK SARUP. Demonstration of OpenFMB Enabled Power System Operations Using Hardware - in - Loop (HIL) Real Time Simulator. (Under the direction of DR. MADHAV MANJREKAR)

The United States Department of Energy defines Microgrid as a group of interconnected loads and distributed energy resources within clearly defined electrical boundaries that acts as a single controllable entity with respect to the grid. A microgrid can connect and disconnect from the grid to operate in grid-connected or islanded mode. This attribute of microgrid is of key importance in the real-time simulations performed for distribution feeder system. The problem statement is to simulate a microgrid connected distribution feeder model in controller hardware in loop and implement grid connected and islanded mode use-cases for 61850-GOOSE protocol using OpenFMB framework. The feasibility of configuring analog inputs and outputs of simulation in Protection and Control (P&C) Intelligent Electronic Device (IED) and communicate data to Remote Terminal Unit (RTU) using 61850-GOOSE protocol is researched and evaluated. The contribution of this thesis is embedded in converting RTU output data into respective understandable language for HILs subscriber and publisher block. To perform this operation, a new North American Energy Standard interoperability framework known as Open Field Message Bus (OpenFMB) is used. The validation of protection and performance of real-time grid following and forming mode in a microgrid with 800kW of Distributed Energy Resources is the overall purpose of this work.

DEDICATION

This work is dedicated to my sister: Harshita Sarup and my parents: Shailendra Sarup and Nandita Sarup, who have always loved me unconditionally and whose good examples have taught me to work hard for the things that I aspire to achieve.

ACKNOWLEDGEMENTS

I would first like to thank my faculty advisor Dr. Madhav Manjrekar at Dept. of Electrical & Computer Engineering, UNC Charlotte. He helped me a lot academically and non-academically from my very first day at this university. The door to Prof. Manjrekar's office was always open whenever I felt out of track or had questions related to a particular course or research topic. He consistently allowed this research to be my own work, but guided me in the right direction whenever he thought I needed it. Under his guidance, I learnt how to be disciplined, hard-working and most importantly - a focused student.

I would also like to thank my advisory committee members who were present at every step during the period of this research: Dr.Babak Parkhideh and Dr. Sukumar Kamalasadan. Taking the courses taught by them aided the advancement of my research work. Without their responsive input, the implementation process would not have been successfully conducted.

I would also like to acknowledge the tremendous support from Mr. David Mulder, Mr. Michael Groomes, Mr. Wade Malcolm of Open Energy Solutions Inc. and Dr. Stuart Laval, Mr. Aleksandar Vukojevic, Mr. Dwayne Bradley, Mr. David Lawrence, Mr. Randy Brown, Mr. Jason Handley of Duke Energy, ETO. They provided me with the best technical environment and most advanced equipment to use for my research.

Finally, I must express my very profound gratitude to my friends and peers: Darshita Parekh, Rakesh Belchandan, Prasanth Sahu, Kiran Lalwani, Sumedh Halbe, Arunodai Chanda, Dr. Somasundaram Essakiappan for providing me with unfailing support and continuous encouragement throughout my years of study and through the process of researching and writing this thesis. This accomplishment would not have been possible without them. Thank you.

TABLE OF CONTENTS

LIST OF TABLES

LIST OF FIGURES

LIST OF ABBREVIATIONS

Generic Object Oriented Substation Event (GOOSE)

Distributed Energy Resources (DERs)

Photovoltaics (PV)

Maximum Power Point Tracking (MPPT)

Super Capacitor (SC)

Distributed Generation (DG)

Point of Common Coupling (PCC)

Intelligent Electronic Device (IED)

Remote Terminal Unit (RTU)

Protection & Control (P&C)

Hardware in loop (HIL)

Department of Energy (DOE)

Open Field Message Bus (OpenFMB)

Microgrids (MGs)

Energy Storage Systems (ESS)

Point of Common Coupling (PCC)

Smart Energy Management Systems (SEMS)

Hybrid Energy Storage System (HESS)

Battery Energy Storage System (BESS)

Heat Storage System (HSS)

Kilo-Volt (kV)

kilo-Watt (kW)

kilo-Watt-Hour (kWh)

Ampere (A)

Power Conversion System (PCS)

Current Source Inverter (CSI)

Voltage Source Inverter (VSI)

Insulated Gate Bipolar Transistor (IGBT)

Pulse Width Modulation (PWM)

Active Power (P)

Reactive Power (Q)

Isosynchronous (ISO)

Schweitzer Engineering Laboratories (SEL)

Virtual Machine (VM)

Distributed Network Protocol (DNP3)

Message Queuing Telemetry Transport (MQTT)

Network Address Translation (NATS)

Input/Output (I/O)

Real Time Automatic Controller (RTAC)

Circuit Breaker (CB)

Microgrid Point of Interconnection (MPOI)

Gypsum Point of Interconnection (GPOI)

Hybrid Energy Storage Point of Interconnection (HPOI)

Utility Point of Interconnection (UPOI)

Digital Output (DO)

Digital Input (DI)

Analog Output (AO)

Analog Input (AI)

North American Energy Standards Board (NAESB)

Standards Development Organization (SDO)

American National Standards Institute (ANSI)

International Users Group (UCAIug)

Smart Grid interoperability Panel (SGIP)

Smart Electric Power Alliance (SEPA)

Industrial Internet of Things (IIoT)

Supervisory Control And Data Acquisition (SCADA)

CHAPTER 1: INTRODUCTION

1.1 Renewable Energy and Distributed Energy Resources

Wood, coal, petroleum and natural gas have been used since the nineteenth century and has now reached a point where if we keep using these sources of energy at the same rate, the fossil fuels will come to extinction in coming few years. Due to the rapid increase in global energy consumption, diminishing of fossil fuels reserves and environmental pollution, there is an all-time rise in clean energy generation, transmission and utilization. Distributed generation, energy resources/renewable energy is a step forward and has forced the human mankind to switch to technologies which support emission free environment. Green energy technologies along with distributed energy resources (DERs) [4] including solar power PV (photovoltaics) and wind power have attracted significant attention in smart grid [2] because of their ability to produce electricity without carbon emissions Solar photovoltaics is one of the fastest growing distributed power resources due to which its market price is exponentially increasing. The advantages of having photovoltaic system which are known to all include compact system size, noise-free operation and feed in tariff. Their robust design, fuel free operation, less maintenance and longtime service has attracted a lot of customers. However the high installation cost of PV systems and the low conversion efficiency of PV modules are the main hurdles to using solar energy at large scale. The performance of the PV varies with the weather changes, especially solar irradiance and temperature. In order to get maximum PV power, Maximum Power Point Tracking (MPPT) techniques are often used. The main objective of the MPPT algorithms is to find the corresponding voltage (Vmpp) and current (Impp) at which maximum output power (Pmpp) can be generated from PV panel at a given temperature and irradiance [7]. Though the MPP is reliable, the nature of these type of natural resources are intermittent. The fluctuating behavior of the weather (irradiation and temperature) makes it almost a necessity to bring in the concept of storage devices. The availability of a storage device like battery and super capacitor (SC) when integrated with the renewable resources acts as a backup and ensures the continuous power supply to the critical loads when the renewable source is unable to function at its full potential. However, due to the intermittent nature and volatility of distributed generation (DG), there exist challenges to the operation, protection, and power quality of the traditional power systems due to large scale integration [9]. With the ever growing demand for power and accessible renewable energy technologies, the concepts of distributed generation and microgrids are quickly coming to the forefront. The concept of microgrid answers most of the questions about DERs integration to distribution network. It improves power quality and reliability of power supply.

1.2 Importance of Microgrids

A microgrid comprises of sources and loads. Sources are usually distributed, PV panels, fuel cell and wind turbines. Loads can be sensitive, adjustable or shiftable loads. Usually a microgrid also has an energy storage system like batteries and supercapacitors. A microgrid is a locally controlled system. In its normal operation, it is connected with the centralized grid through Point of Common Coupling (PCC). During faults, blackouts, surges, the microgrid is expected to disconnect and function autonomously as a separate unit.

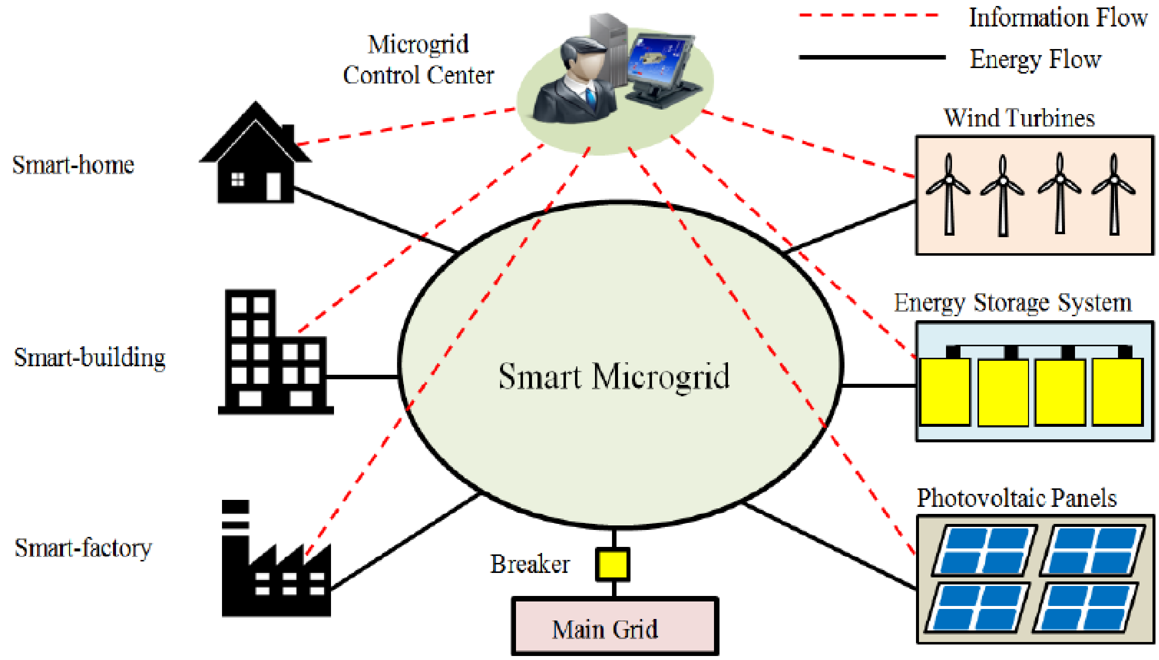

Figure 1.1: Communication Network Architecture for integration with DER's [1]

The reduction in energy loss at the transmission level and higher reliability are the main advantages of microgrid during a blackout as it is able to supply power to the loads especially critical loads. For microgrids to work properly, a switch must open and the DER must be able to carry the load on the islanded section. The two types of microgrid operation include grid following (connected) and grid forming (islanded) modes. Microgrid is known for its ability to separate, island and isolate itself from the utility grid seamlessly without any changes to the loads during a fault or disturbance. In other words, a microgrid can connect and disconnect from the grid to enable it to operate in both grid-connected or island-mode. Once the grid is restored, the microgrid automatically resynchronizes and reconnects itself to the grid seamlessly or after black start.

1.3 Problem Statement and Motivation

The Department of Energy defines Microgrid as a group of interconnected loads and distributed energy resources within clearly defined electrical boundaries that acts as a single controllable entity with respect to the grid. A microgrid can connect and disconnect from the grid to operate in grid-connected or island mode. This application of microgrid is of key importance in the real-time simulation performed for simulated feeder system. The problem statement is to manage the process of grid connection, islanding and grid resynchronization in a microgrid while developing and simulating model of the microgrid connected distribution feeder in a real-time platform. The setup will be used as a testbed to implement use-cases for 61850-GOOSE protocol for the proposed architecture using Open Field Message Bus(OpenFMB) framework. The idea to configure analog inputs and outputs of simulation in Protection and Control (P&C) Intelligent Electronic Device (IED) and communicate data to Remote Technical Unit (RTU) using 61850-GOOSE protocol is researched and implemented. The real work is embedded in converting RTU′s output data into respective understandable language for HIL subscriber and publisher block. To perform this operation, a new North American Energy Standard interoperability framework known as Open Field Message Bus (OpenFMB) is used. The validation of protection and performance of real-time grid following and forming mode in a microgrid with 800kW of Distributed Energy Resources is the goal of this detailed research work.

1.4 Organization of Thesis

This section presents an overview of the organization of thesis:

Chapter 1: Introduction

The chapter portrays the importance of transition from convention energy sources like wood, fossil fuels, natural gas to renewable energy like solar energy photovoltaics (PV). The advantages of using Maximum Power Point Tracking is further discussed. It focuses on using energy source like batteries and super capacitors along with renewable energy resources. It introduces the concept of microgrid briefly.

Section 1.2 presents the importance of using having microgrids and Section 1.3 summarizes the Problem Statement and Motivation for the thesis.

Section 1.4 presents the organization of the thesis.

Chapter 2: Literature Review

Section 2.1 This section compares the DC Microgrid topology with that of AC Microgrids.

Section 2.2 describes different types of DC-DC Converters and DC-AC converter. The technical specification for each converter, their impedance selection and operational functions.

Section 2.3 describes various control methodologies for inverters present in the microgrid.

Section 2.4 presents the P/Q control of inverters and Section 2.5 portrays the design of microgrid controller.

Chapter 3: System Description

Section 3.1 displays the microgrid system configuration and Section 3.2 describes the different components of microgrid system including Hybrid Energy Storage System, Battery Energy Storage System, Distributed Energy Resources (DERs), Current Controlled Current Generating Source, Grounding Transformer

Chapter 4: Typhoon HIL Modeling

This chapter describes the simulation model and the way feeder components are modeled inside Hardware-in-loop simulator used, i.e., Typhoon HIL. The functionality of each modeled component is explained and transition modes of the microgrid are demonstrated step by step. The chapter describes the interconnections of the simulation with Hardware-in-loop and also explains the methodology behind flow of information between different vendors based devices.

Chapter 5: Proposed Use Case

Section 5.1 describes the Classical Approach of Traditional Centralized Systems whereas Section 5.2 describes the Proposed Approach of using OpenFMB nodes.

Chapter 6: Configuration of Hardware Components

Section 6.1 serves as an introduction of the chapter. Section 6.2 demonstrates the detailed configuration of the proposed approach. It describes the configuration of RTU and P&C Section 6.3 defines the configuration of Substation Configuration Description (.scd file). Section 6.4 demonstrates the use cases of proposed approach and the process flow of events. Section 6.5 explains the importance of having OpenFMB, and Section 6.6 gives a detailed comparative analysis between classical and proposed approach.

Chapter 7: Simulation Results

Section 7.1 discusses the results from microgrid and its functionality. Section 7.2 portrays the all the case studies like grid connected mode, grid forming mode and re syncing to the grid

Section 7.3 presents the actual difference in the results from simulation and the proposed approach loop.

Chapter 8: Conclusion & Future Scope

Section 8.1 concludes the research work done and the results achieved. Section 8.2 defines the possible future work that can be extended to get better real-time results.

Chapter 9: References

All the references used to aid this work have been cited here in chapter 9.

CHAPTER 2: LITERATURE REVIEW

2.1 Introduction

This chapter presents the literature study required to perform and verify the research work. It discusses various advantages, disadvantages and application of DC Microgrids and AC Microgrids. The chapters reviews the basics of power electronics converters inclusing DC/DC and DC/AC converters. It explains the working of a three phase inverter and the way Pulse Width Modulation is implemented for the required switching. The chapter also defines the P/Q control method of the three phase inverters, describing the importance of filters. To conclude the chapter, the applications and advantages of microgrid controllers are discussed.

A smart-grid can simply be defined as the one comprising of at least one renewable energy resource like PV, wind, tidal energy and the grid which uses digitized and automated controls for its daily operation [2]. The Department of Energy (D.O.E) defines smart grid as a smarter grid which applies technologies, tools and techniques available now to bring knowledge to power − knowledge capable of making the grid work far more efficiently which ensures reliability to extended degrees, maintains its affordability, fully accommodates renewable and traditional energy sources and introduces advancements and efficiencies yet to be envisioned. If PV is used as the renewable resource in the DER, a suitable panel/module is selected and number of these panels are arranged in an array of series and parallel format. This is often termed as a PV farm. Throughout the day, there is a variation in irradiation falling on the PV farm. Due to this variation, the output voltage does not remain constant. To control this, Maximum Power Point Tracking concept is used where in the farm tries to capture the maximum irradiation and outputs maximum power [8]. The maximum power point block inputs irradiance and temperature. Perturb and Observe as well as incremental conductance are the two highly used algorithms in MPP. The incremental conductance determines the exact time of achieving maximum power point while perturb and observe only oscillates around maximum power point. The output DC link voltage in most of the utility applications is constant 800-1200V DC. So to meet the power conditioning requirement, the PV interconnect is taken by the DC-DC converter. In most cases, to meet the DC link voltage requirement, a boost converter which converts (boosts) the input voltage to a higher required voltage. These type of DC-DC converters use proportional-integrator controllers to make voltage and current in sync and inject/draw power from the grid. It is very well known that renewable energy (Photovoltaics) play a major role in making utility grid a smart one. It is observed that with variation in irradiance, the voltage remains constant but the power varies directly with the irradiance [20] This cannot be the case in real time. The voltage and the power should remain constant throughout. But no PV farm can do this standalone. Hence there is a need an external supply to maintain the voltage at the rated value. Hence a source of energy is needed to take care of the DC link regulation. The power conditioning requirements are taken care by the DC-DC converters. As far as to reach the DC link voltage from batteries terminal voltage a boost converter is sufficient enough to boost the voltage, but to provide the remaining power to PV for constant value throughout, the power needs to be stepped down or we can say that the voltage needs to be brought down. This can be done by using a buck-boost converter. In the initial stages a constant DC source is used but to advance the process, a renewable PV source is used. After discussing the various limitations of PV let alone, it was concluded that PV along with battery would be a powerful mean to supply the regulated DC Link. But this is not enough. In the world of grid cutting technology, the need to use this PV+Battery storage system as a source to feed the grid is exponentially increasing. As discussions pertain towards grid, it need to be noted that everything will be simulated in AC. Hence, there is a need to convert from DC to AC. This can be done using an inverter. As mentioned, an inverter converts the incoming DC to grid connected AC. The voltage , current and phase are the three key parameters to keep in mind while designing an inverter. To smoothen the effect of the conversion, a combination of resistor and inductor (RL) filter is added and the system is then grid tied.

2.2 DC Microgrids vs AC Microgrids

With the increasing future energy demands, an intelligent and flexible energy system in the distribution networks is required. This is one of the main reasons for emerging microgrids (MGs) and their integration with renewable based Distributed Generation (DG) units and Energy Storage Systems (ESS). The DG units usually consist of photovoltaic (PV), wind turbines and fuel cells while the ESSs include batteries, flywheels and supercapacitors [12]. Both the customers and the utility companies benefit from Microgrids. The MGs are treated as controllable entities that operate as a single dispatchable unit (load or generator) to provide ancillary services and meet the needs of the upstream networks. This way the utility can generate and supply back to the grid. The MGs involve alternative energy sources which can offer far higher efficiency and reduce environmental degradation contrary to most conventional power generation units. They are also strategically installed near the loads to provide a variety of benefits such as network voltage and frequency regulation if properly operated. The MGs can provide both thermal and electricity needs to meet special demands such as local reliability, critical load availability and can improve power quality by supporting local voltage and frequency. They reduce the effects of voltage sags and also offer seamless transition functions as may be needed in the areas with critical loads, such as hospitals and data centers. Electrical System consists of three key aspects: Generation, Transmission and Distribution. The electricity is transmitted from the point of generation to consumers, and the electricity network operates by two primary systems, i.e. (i) transmission system and (ii) distribution system. The transmission system delivers power from the plants to the distribution substations and the distribution system delivers power from distribution substations to the consumers. Hence, the power stations are situated far from the load centers. This makes it even more difficult to catch any irregularities or disturbances occurring at the load centers. However, the DG units connected to the grid at low voltage level in the form of microgrids are slowly changing the structure of the conventional grid from passive to active distribution networks. The energy system in present times try to include more intelligence devices installed in the generation units, transmission lines, substations, and distribution networks and some controllable loads. It is a combination of both power system and information and communication system networks. Depending on the combination of the DG units, flexible loads and storage units, customer's participation in different electricity markets will be possible. The stored energy may be discharged during peak demand to earn income. Therefore, with the AC and DC microgrid systems equipped with the DG units, ESS and mixed controllable AC and DC loads, customers are expected to have information access of every unit connected to the given microgrid system [11]. This reflects the idea of the future energy system of which the electrical and communication infrastructures expected to be embedded together. Based on voltage and current in the system, microgrids can be categorized in three ways:

1. AC
2. DC
3. Hybrid

In AC microgrids, the distributed energy resources and loads are integrated to a common AC bus. DG′s and ESS are integrated to the AC bus through converters which convert DC /AC and are referred to as inverters and then integrated with AC/DC converters, referred to as rectifiers which are used for supplying DC loads. However, DC bus is the common bus in a typical DC microgrid where AC generating units are integrated through rectifiers and inverters are used for supplying AC loads. Hybrid microgrids are a combination of AC and DC microgrids wherein the common bus could be either AC or DC [5].The connection of inverters and rectifiers to each bus depends on the proximity of the DER or load to the bus. Through prior studies, it has been demonstrated that DC microgrids offer several advantages over AC microgrids. The use of less converters due to easy integration with the DC loads yields increased efficiency and reduced losses. With DC microgrids in place, there is easier integration of DC DERs, including ESS and solar photovoltaic (PV) to the common bus and enabling bus ties to be operated without the need for synchronizing the buses. DC microgrids allow increase in DC loads such as personal computers, data and telecommunication centers, and other applications where the typical 50- and 60-Hz ac systems are not available, make it an optimal solution when compared with AC microgrids.

2.3 Converters: DC/DC and DC/AC

A boost converter is classified under the category of DC-DC converter whose main function is to step up the voltage eventually stepping down the current as seen from the input to the output. It consists of a diode, transistor and one energy storage element, usually a capacitor, inductor, or both. Mostly LC or LCL filters are added at the load side to reduce the voltage ripple. When PV is integrated to the grid system, there is usually an increase in the power and this power conditioning requirements for the PV interconnect are taken care by these DC-DC converters [6]. Based on the voltage rating of the PV and that of the DC link, a decision is made if there is a need to step up or down the input voltage using the DC-DC converter. For example, if the system requires 100 V at the DC link and the PV voltage ratings is only 60V, a boost converter is placed in order to boost the output voltage from power sources to 60V to 100V for the DC link interconnection. If the system comprises of battery storage system, it needs to be kept in mind that battery would charge as well as discharge depending on the state of charge. Hence, there needs to be a power flow in both directions to enable charging and discharging. To enable this operation, a bidirectional boost converter comes handy, wherein the boosting action would correspond to battery discharge and the bucking action from the opposite direction will cause the battery to charge with surplus current supplied by the PV system.

2.4 Three Phase Inverter

For energy processing of PV and wind power, DC / AC inverters are needed to be controlled. A three-phase inverter has three legs, one for each phase as shown in Figure 2.3. Each inverter leg operates as a single-phase inverter. The output voltage of each leg Van, Vbn, Vcn where n refers to negative dc bus voltage is computed from Vidc and the switch position.

1. Three phase inverters have 3 terminals: Input DC, Output terminals and Control terminal
2. In each of the 3 legs, when one of the switches is ON, the other is OFF
3. The modulation is done such that the fundamental component of the modulated output voltage has the desired magnitude and frequency
4. The variation of magnitude is achieved by Pulse Width Modulation (PWM) as demonstrated by Figure 2.5
5. One of the 3 legs of the inverter is taken for analysis
6. The harmonics in the voltage wave is assumed to be filtered off harmonics.
7. Therefore, the output voltage is assumed sinusoidal

The inductive nature of the load filters out the harmonics in the voltage to give sinusoidal lagging current.

1. In Figure 2.4, During mode 1 operation, both Vout and Iout are positive. Therefore, the converter operates as an inverter and Pout flows from DC side to AC side
2. During mode 2, iout is positive and is negative. In this mode, the converter operates as a rectifier, since the Pout flows from AC side to DC side
3. During mode3, iout and Vout are both negative. Again, converter operates as an inverter, since the Pout flows from DC side to AC side
4. During mode 4, Vout is positive and iout is negative and this mode of operation can be designated as rectifier operation. Since Pout flows from the AC side to the DC side of the converter
5. Hence, inverter can operate in all 4 quadrants
6. The sequence of switching policy for SW1+ and SW1- can be generated by comparing the VC with a triangular wave form VT

1. The desired output voltage, Vc = Vc(max) sin Ωet is compared with a triangular wave vT of frequency fs = 1/Ts
2. When Vc > vT , SW1$\hat{+}$ is turned ON, Va0 = 0.25 * Vidc
3. When Vc < vT , SW1$\hat{-}$ is turned ON, Va0 = -0.25 * Vidc
4. Two terms are defined: Amplitude modulation index= Ma = Vc(max)/vT(max) Frequency modulation index= Mf = fs/fe
5. As in a full − bridge DC − DC converter, the average output voltage over one switching time period, depends on the ratio of Vc to vT for specified Vidc : Va0 = Vc(max)/vT(max) *0.5Vidc
6. For high Mf , Vc remains almost constant and the fundamental of the modulated wave is equal to Vc

2.5 P/Q Control of inverters

Figure 2.6 shows power circuit schematic of a three-phase inverter interfaced with utility power grid via inductances La, Lb, and Lc. Owing to these interfacing inductors, such inverters are modeled as current sinks whereas the grid is represented as three-phase voltage source (denoted by ean, ebn, and ecn) in series with grid inductances Lga, Lgb, and Lgc, magnitudes of which determine stiffness (strong v/s weak) of the grid. The inverter inverts dc voltage Vdc into three-phase ac voltages van, vbn, and vcn by operating switches S1-S6 as explained in the previous section. Capacitor Cdc is employed to maintain dc bus and the box Energy Source represents any distributed energy resource such as photovoltaic array, battery energy storage etc.

Alternatively, L-filter in the above grid-tied inverter may be replaced by a L-C-L filter as shown in Figure 2.7 Such third order filter offers better filtering with smaller components, however, is vulnerable to L-C resonance issues and requires damping. As is well-known, dc bus voltage, and hence q-axis current, iq, is a metric of real power (P) that is exchanged between dc and ac side. Similarly, d-axis current, id, is a measure of reactive power (Q). Thus, one can construct a power control architecture around the classical current control loops in synchronous frame of reference. A simplified block schematic illustrating such indirect P−Q control.

It may be noted that one may achieve identical dynamic performance of a synchronous frame proportional integral current regulator by employing a proportional resonant controller in stationary reference frame. In both these cases, current control loops result in ac voltage references van*, vbn*, and vcn* which are compared with high frequency carrier waveforms to perform pulse width modulation of the switches. This then generates inverter output voltages that are necessary to synthesize required currents to sink into the utility power grid.

2.6 Microgrid Controller

A microgrid control system is a system that can operate autonomously, connect and disconnect from the main distribution grid for the exchange of power and the supply of ancillary services. The electrical point at which the microgrid connects to the main distribution grid is called the point of interconnection (POI). The connection and disconnection of a microgrid to and from the larger grid accomplished without voltage and frequency transients that exceed the specifications of the microgrid design and the interconnection requirements is referred to as seamless transition [3]. The goal of the controller is to a) operate in grid-connected and islanded modes b) Automatically transition from grid-connected to islanded mode by providing a managed transition to islanded mode for microgrid loads during abnormal power system conditions and planned interruptions of the system c) Resynchronize and reconnect from islanded mode to grid-connected mode d) manage energy to optimize both real and reactive power generation and consumption. Dispatch function and Transition functions are the core features of the controller as shown in Figure 2.8. The transition function includes:

1. Unplanned Islanding (T1)
2. Planned Islanding (T2)
3. Black Start (T3)
4. Reconnect (T4)

Secondary Control: Operate at nominal frequency and voltage, share real and reactive demand in proportion to distributed generation Primary Control: Maintain power balance between loads and sources.

Grid Connected Operation Tertiary Control: Optimization of energy and economics Secondary Control: share real and reactive demand in proportion to distributed generation [21] Primary Control: Match power command at point of intersection.

Phase lock loop (PLL) is used to find the correct Frequency (f) and phase angle (Îž) reference value at point of common coupling. The power factor is maintained at unity. The grid current reference signal (Iref) is checked if it is in phase with grid voltage (Vs).

During CSI mode operation, the synchronous frame is changed from abc frame to dq frame. The error signal passed to PI controller to generate inverter reference voltage (Vd, Vq). The voltage references are retransformed from dq to abc. By performing this process, the end goal is to get PWM voltages as the output.

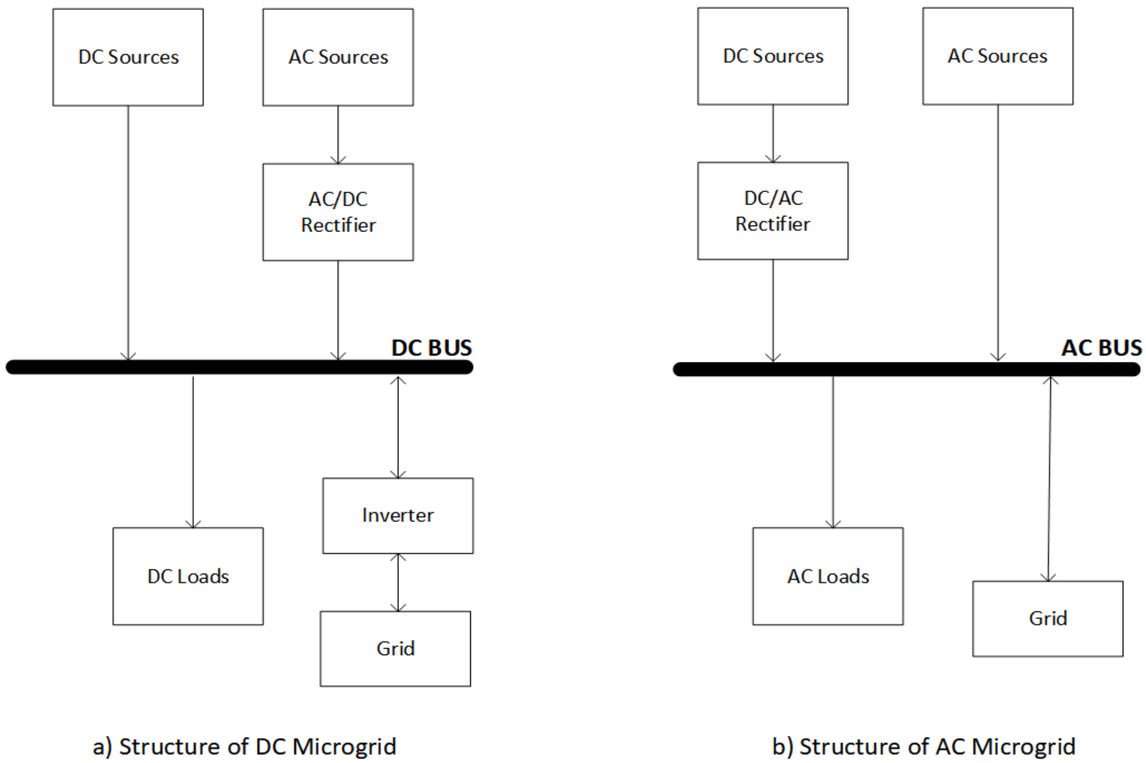

Figure 2.1: DC Microgrids vs AC Microgrids

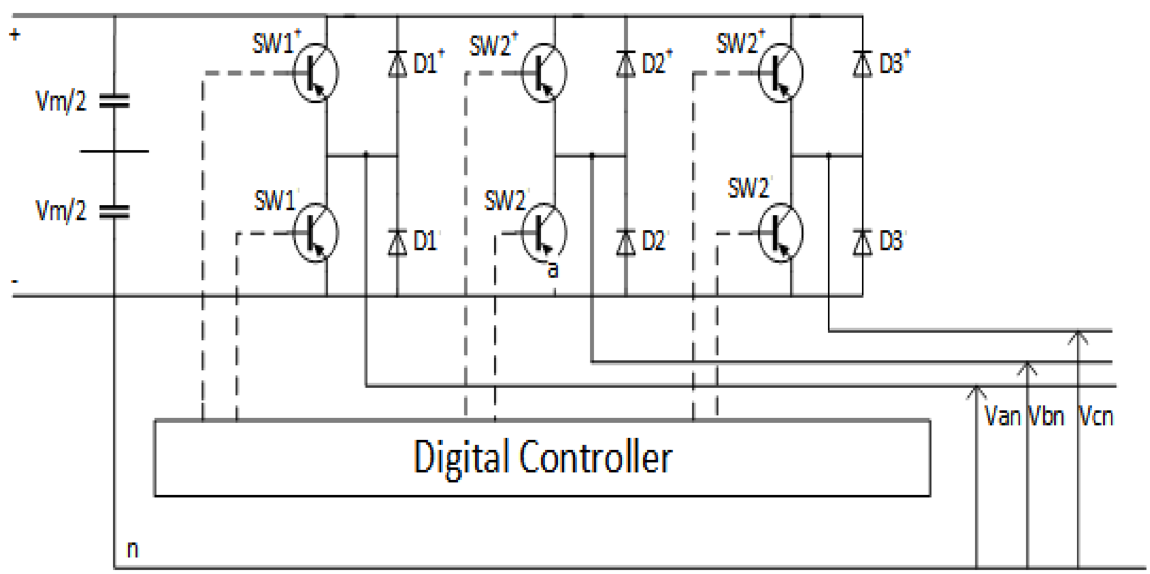

Figure 2.2: Three Phase Inverter

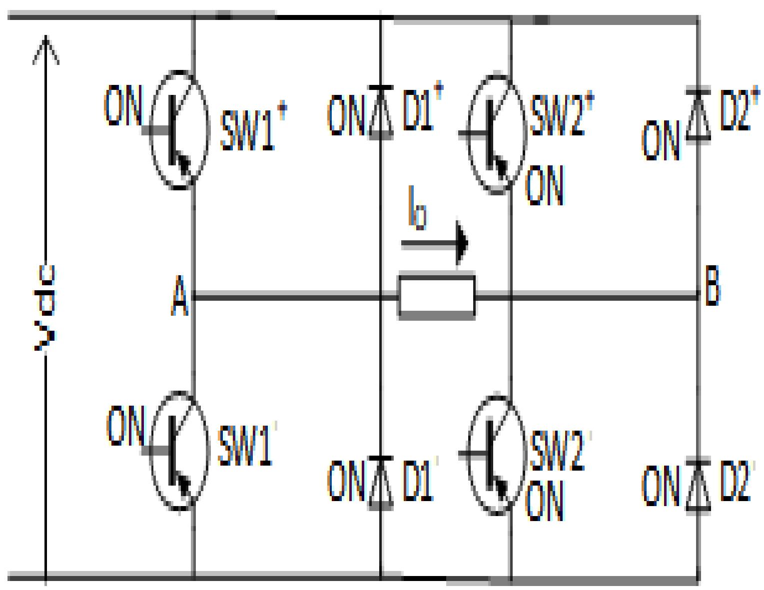

Figure 2.3: Switching Operation-1

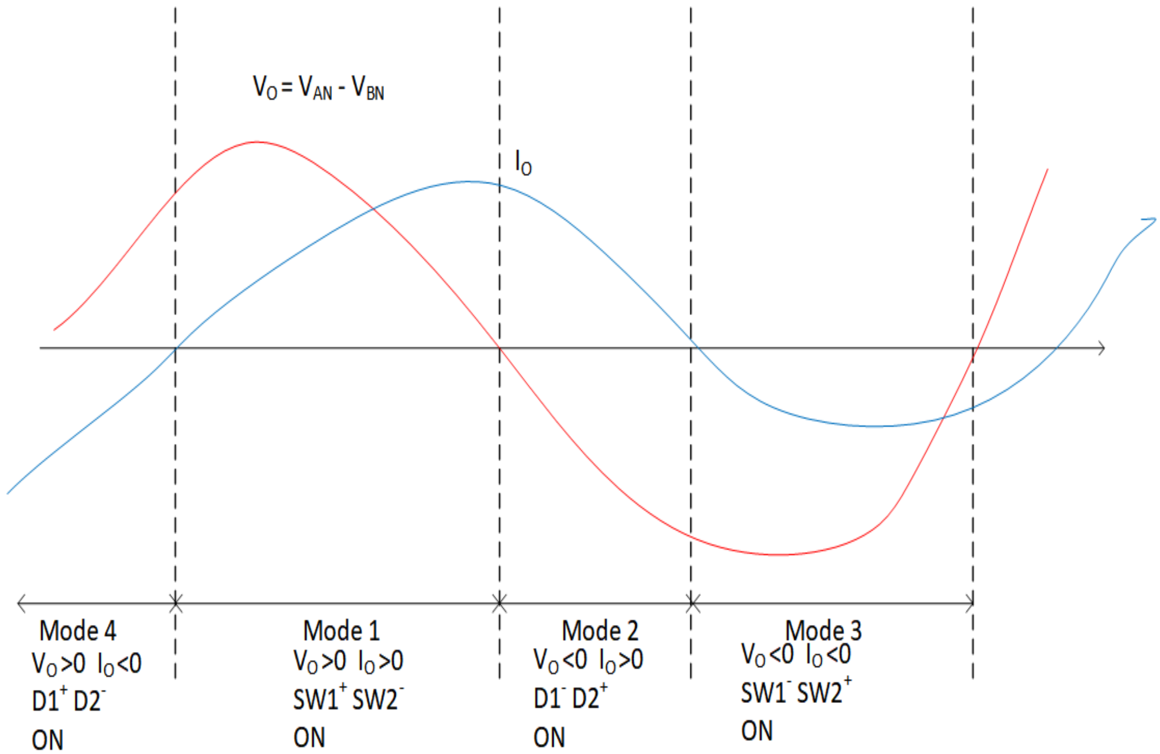

Figure 2.4: Four modes of operation

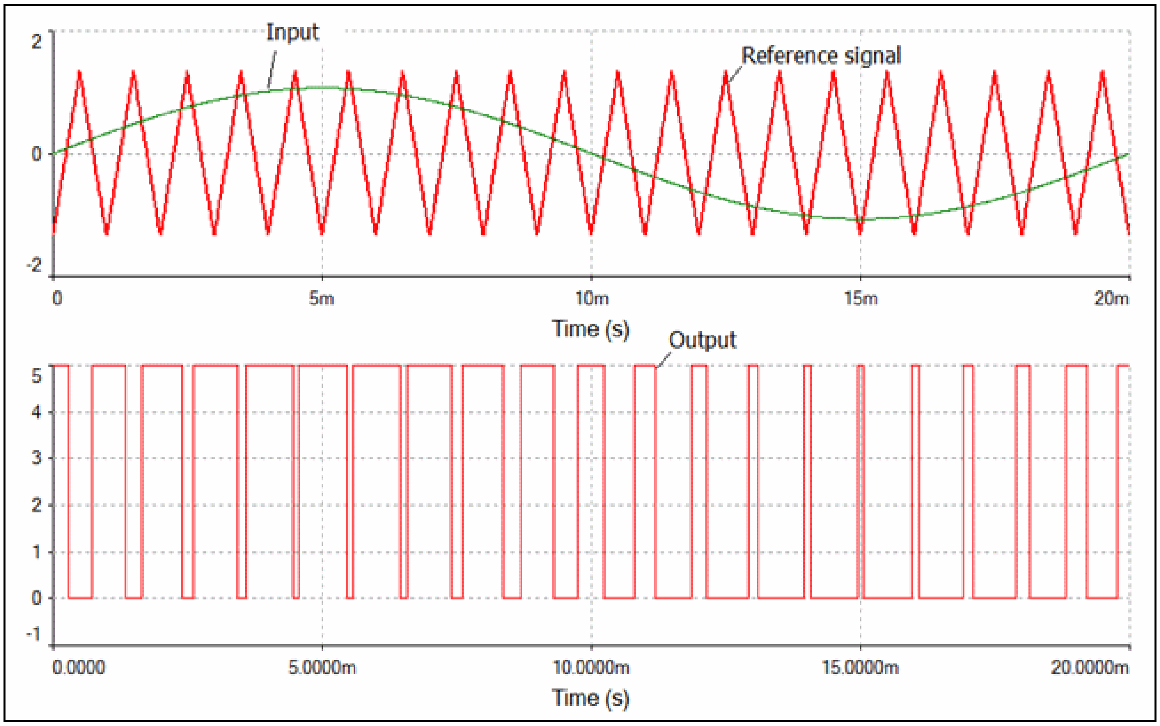

Figure 2.5: Pulse Width Modulation [37]

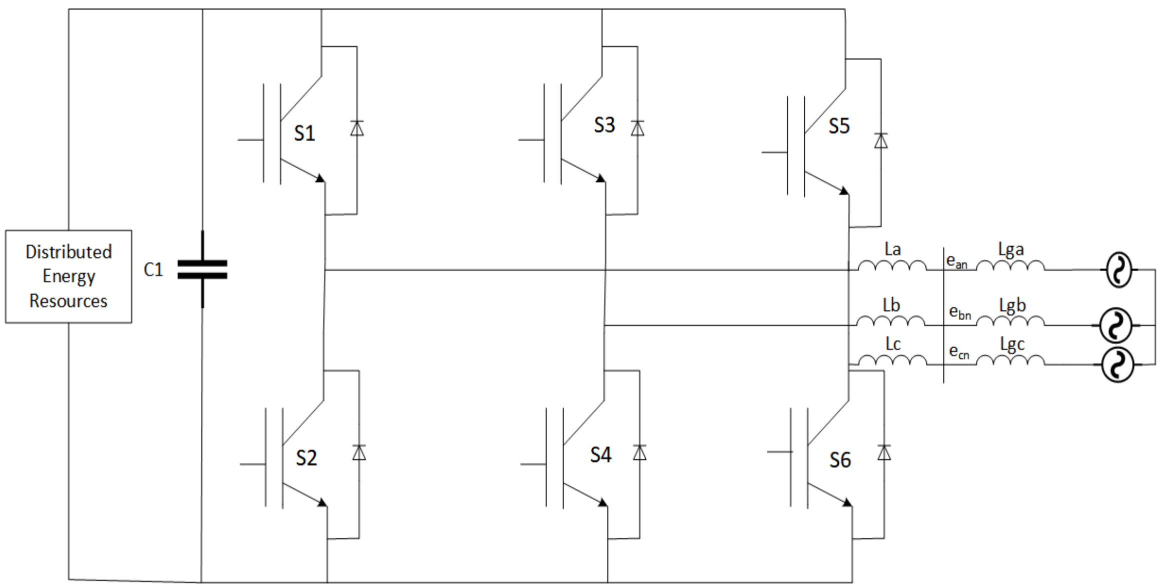

Figure 2.6: Grid Tied Inverter with L filter

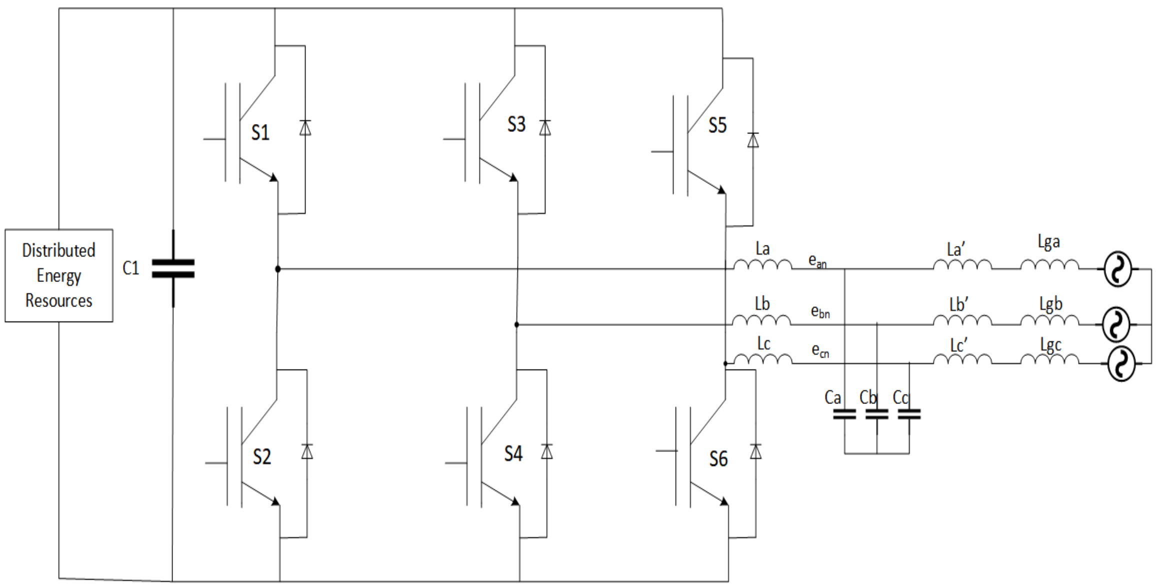

Figure 2.7: Grid Tied Inverter with L-C-L filter

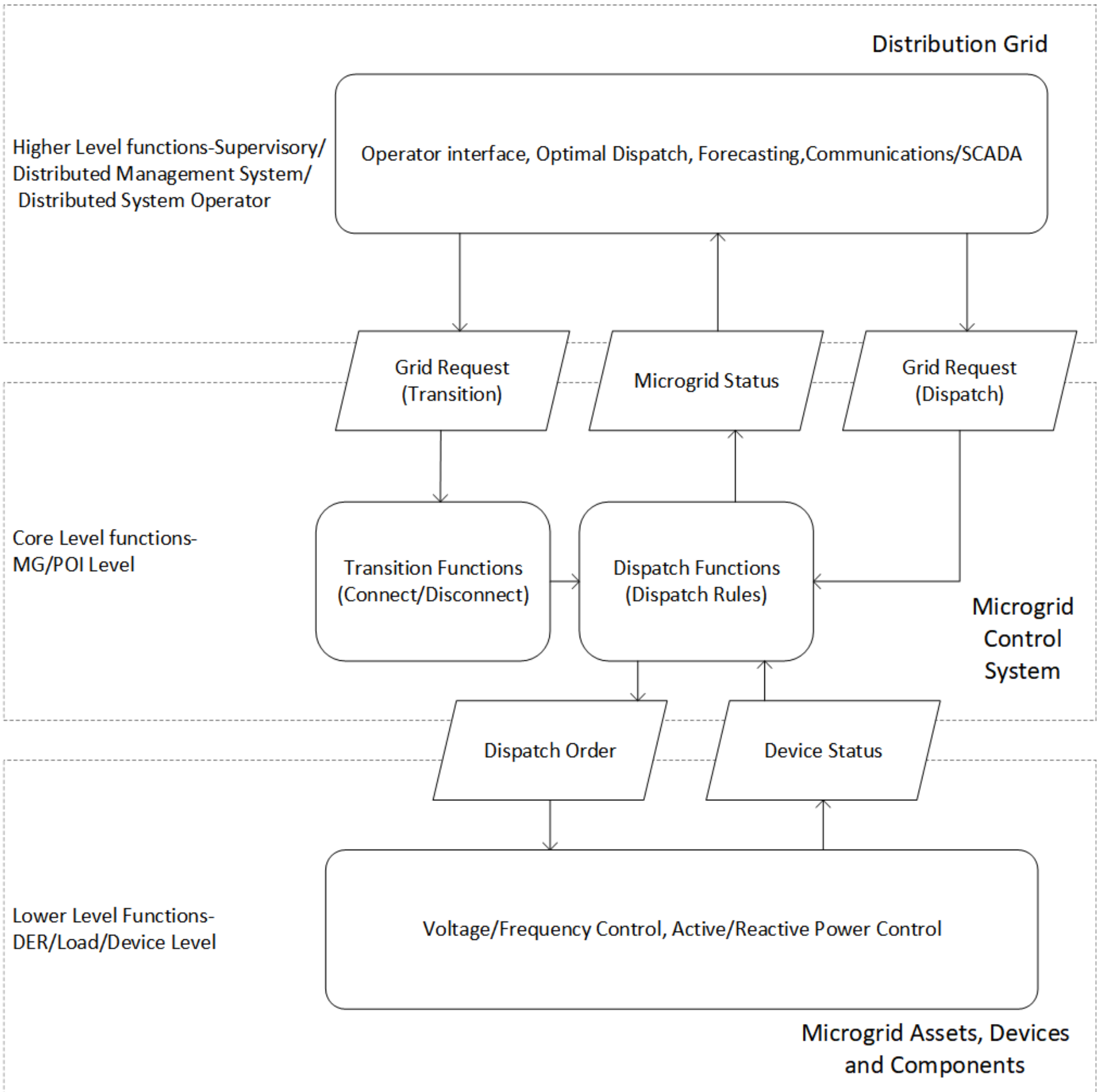

Figure 2.8: Microgrid Control System Framework

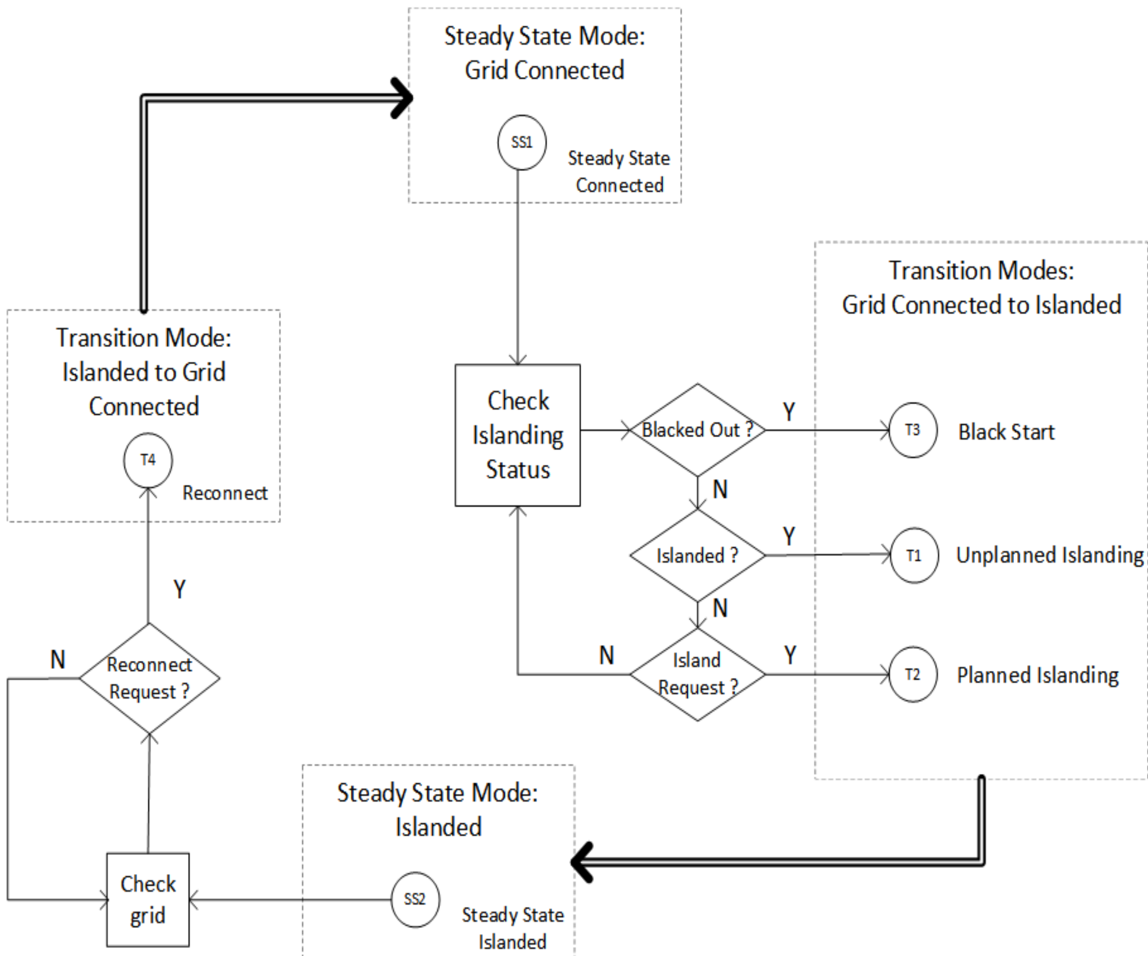

Figure 2.9: Microgrid Synchronization Control Diagram

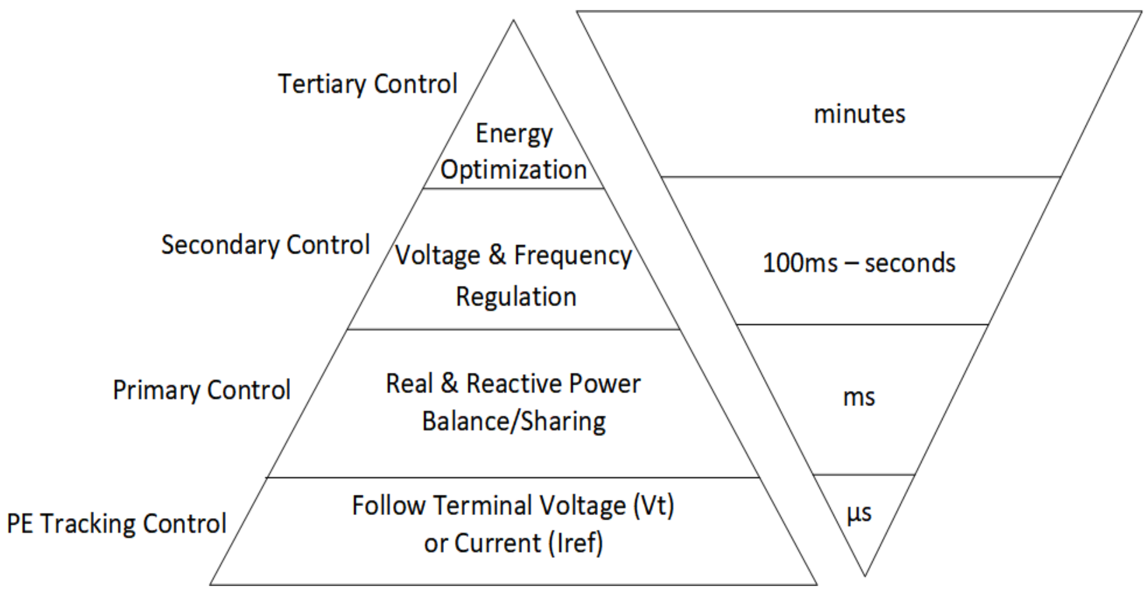

Figure 2.10: Types of control and their Time-Scale

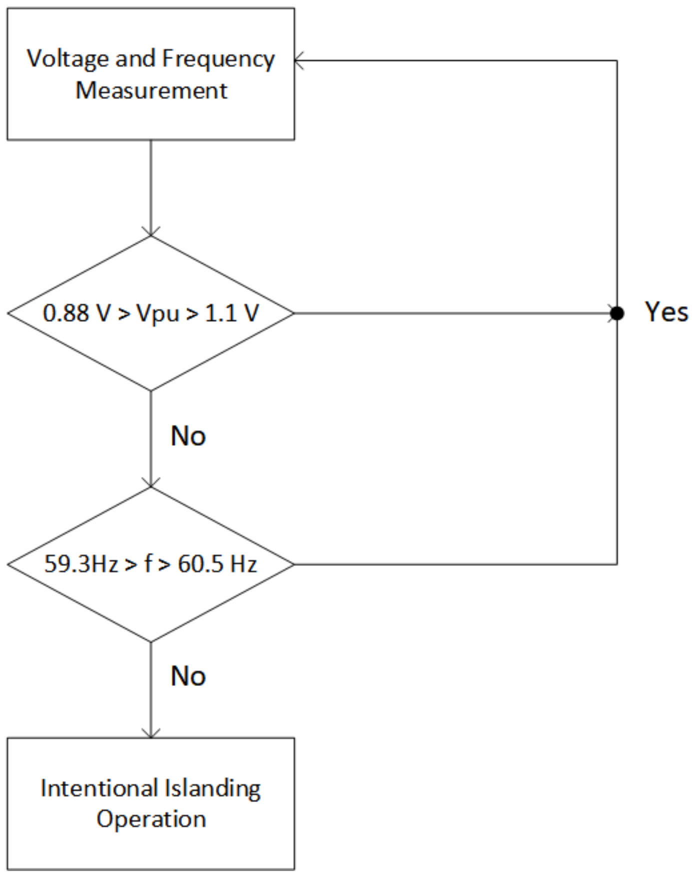

Figure 2.11: Islanding Algorithm

CHAPTER 3: SYSTEM DESCRIPTION

3.1 Introduction

This chapter describes the distribution feeder, microgrid and the Hardware-in-loop (HIL) setup under consideration. The single line diagram of the distribution feeder shows the bus location of the inter-connected utility grid, microgrid, regulator and the nine dynamically varying loads. The single line diagram of the microgrid portrays the placement of its major components including battery energy storage system, PV and DC Coupled battery, grounding transformer and the microgrid controller. The chapter explains the digital real time HIL setup and the way that the HIL devices are connected for utility applications.

3.2 Distribution Feeder

The distribution feeder comprises of 12 buses connected with underground cables between them. The main electrical utility grid is a few miles away and is connected to the distribution feeder at Bus 1. The utility grid [13] is rated at 115kV and is stepped down to 12.47kV AC for microgrid applications. There are nine dynamically-varying loads connected at Bus 2, 4, 5, 6, 7, 8, 9, 10 and 12 as seen from the Figure 3.1 The voltage regulator is located between Bus 5 and Bus 6. The microgrid is strategically placed in the middle of the distribution feeder at Bus 6. The switches S1, S2, S3, S4 and S5 operate as protective elements and can normally open and closed based on the occurring event. The current controlled current source represents a local PV generation source and is modeled as a three-phase external current source which feeds power to the distribution feeder and is connected at bus 12.

3.3 Electric Utility Microgrid

The distribution feeder rated at 12.47kV is tied to the 4-Way Switchgear cabinet present inside the microgrid. The 4-Way Switchgear comprises of 4 switches- Way 1, Way 2, Way 3 and Way 4. The Way 2 switch is connected to two transformers: a) 75kVA - 12.47kV/120V which is then connected to an auxiliary load power; b) 1000kVA - 12.47kV Yg/480V Yg which is connected to 1200A switch. The 125kVA transformer steps down the voltage from 480V to 315V for the 100kVA PV inverter at the AC bus.

The 150kW solar farm is connected with 240kW - 122kWh battery using a 250kW DC/DC converter. The AC bus has two critical loads connected to it: a) 500kW load bank and b) 250kW building load. The Way 3 switch is connected to the grounding transformer which is rated at 500kVA-12.47kV Yg/347V Δ. The Way 4 is connected to the battery energy storage system (combination of 650kVA inverter and 650kW-326kWh battery) through two transformers: a) 1000kVA-12.47kV Yg/347V Y and b) Auxiliary 25kVA - 347V Y/480V Δ

3.4 Hardware-in-loop (HIL) Setup

The figure 3.4 represents the schematic for HIL setup developed in the electrical utility. The simulation model is compiled and simulated in the two Hardware-in-loop platforms.

The feeder model is simulated using two same hardware-in-loop simulators which have an application software embedded inside that helps the simulators to integrate seamlessly with the FPGA based processor. The two simulators allow the use of maximum 8 standard processing cores (SPC's) out of which only 7 cores are used in the simulated model. This is done in order to compile the model and run it in real-time. The analog and digital pins of the simulation are configured to the controller HIL. The Protection & Controlled Intelligent Electronic Device (P&C IED) comprises of virtual machine and analog modules which interconnect with the Remote Terminal Unit (RTU). The unmanaged switch communicates with all the devices over Ethernet. The quad core computer powers the whole HIL Setup and houses the Supervisory Control and Data Acquisition (SCADA) system.

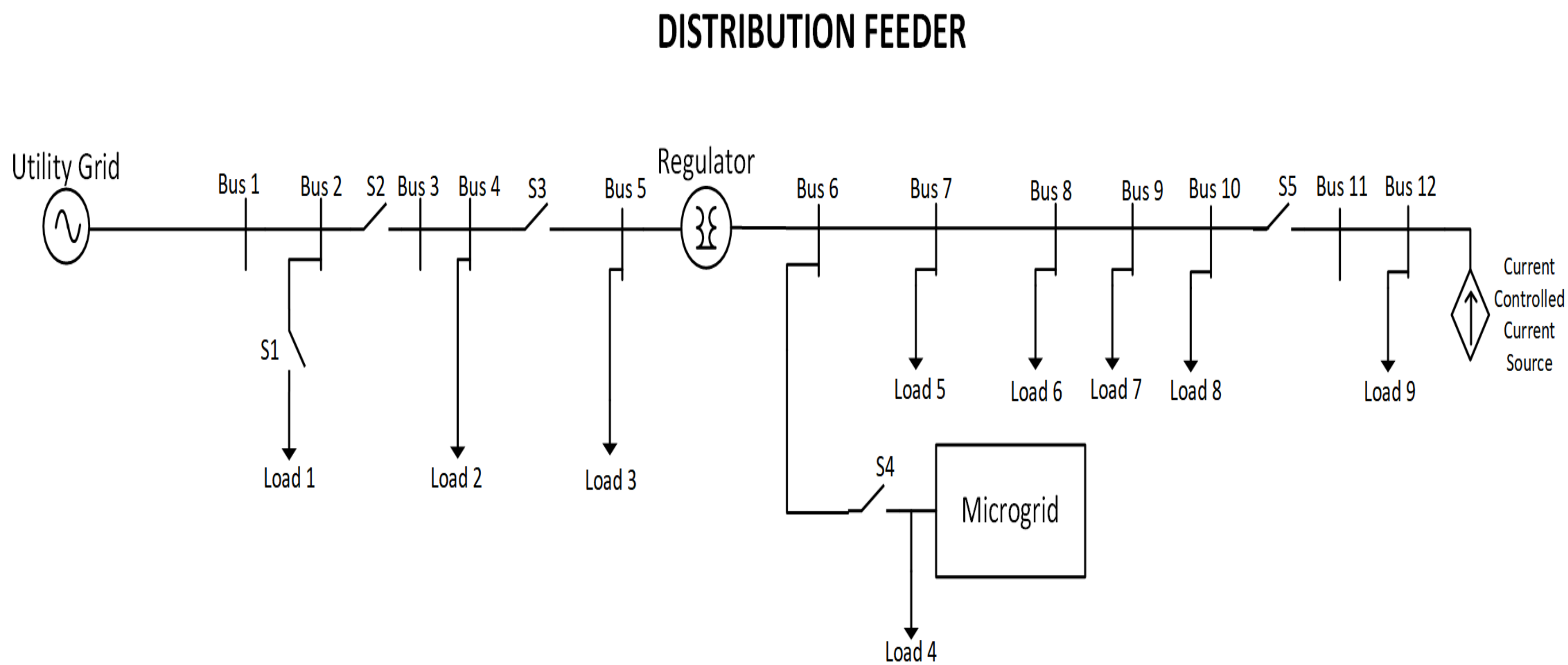

Figure 3.1: Single Line diagram of the Distribution Feeder

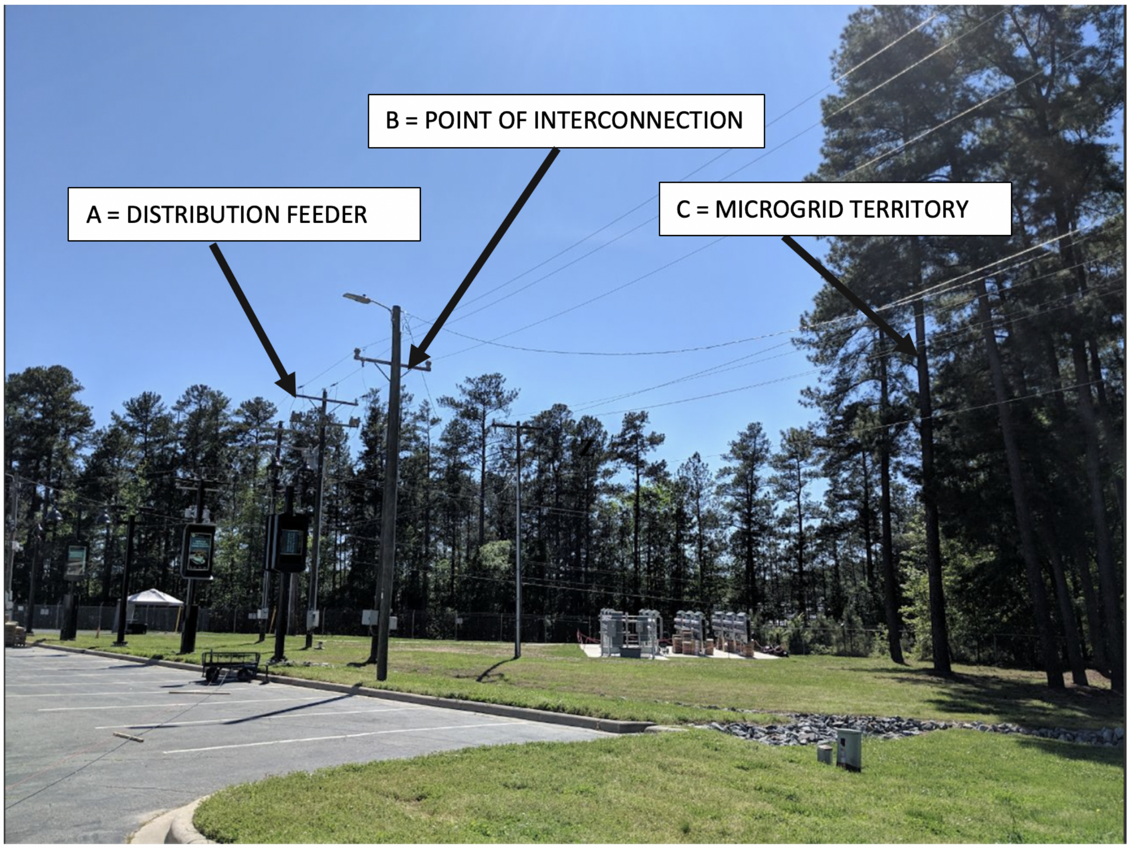

Figure 3.2: Photograph of the Distribution Feeder

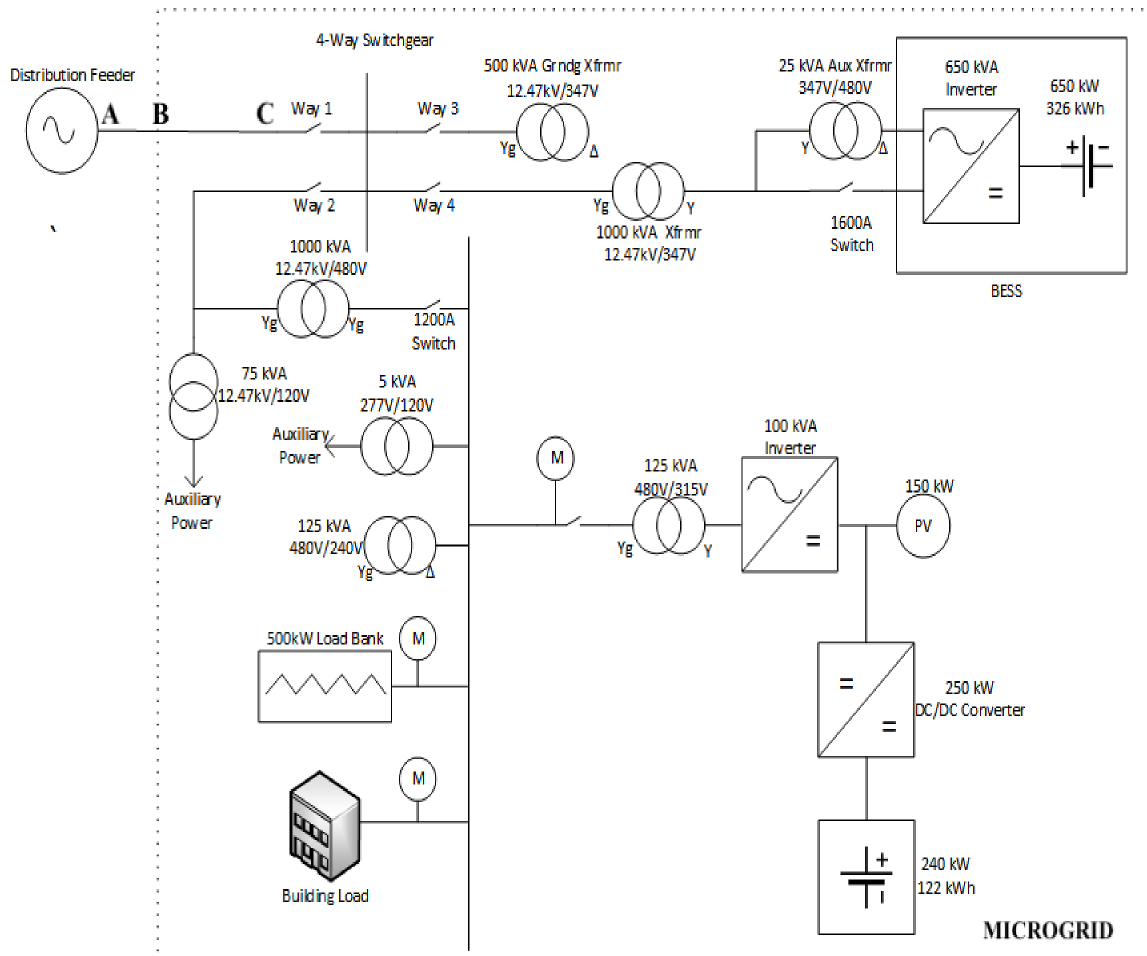

Figure 3.3: Single Line Diagram of Electric Utility Microgrid

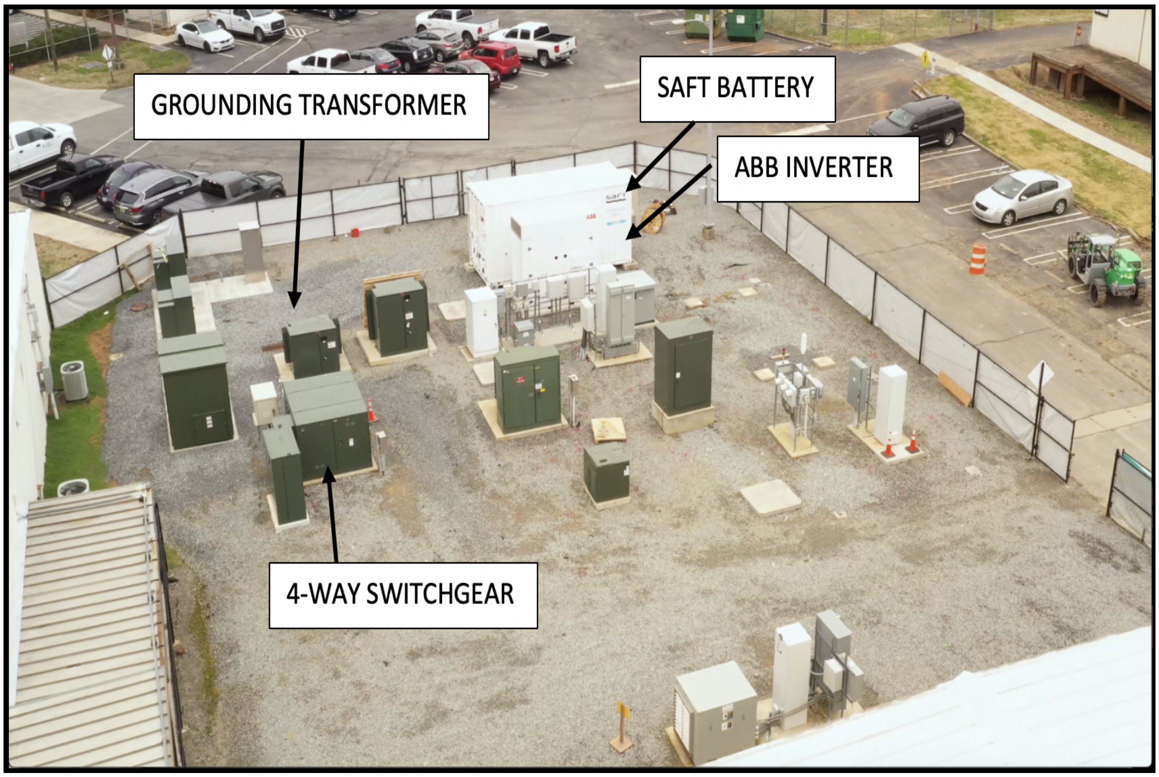

Figure 3.4: Photograph of Electrical Utility Microgrid Yard with Battery inverter and 4-Way Switchgear

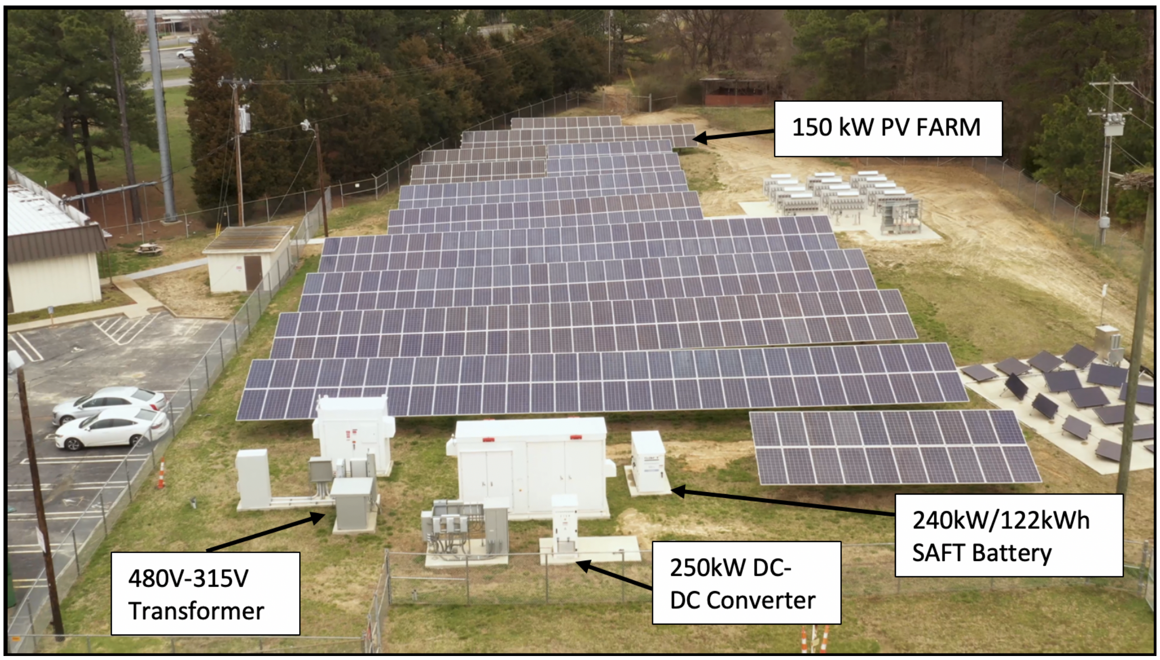

Figure 3.5: Photograph of Solar Farm with integrated Inverter and Battery

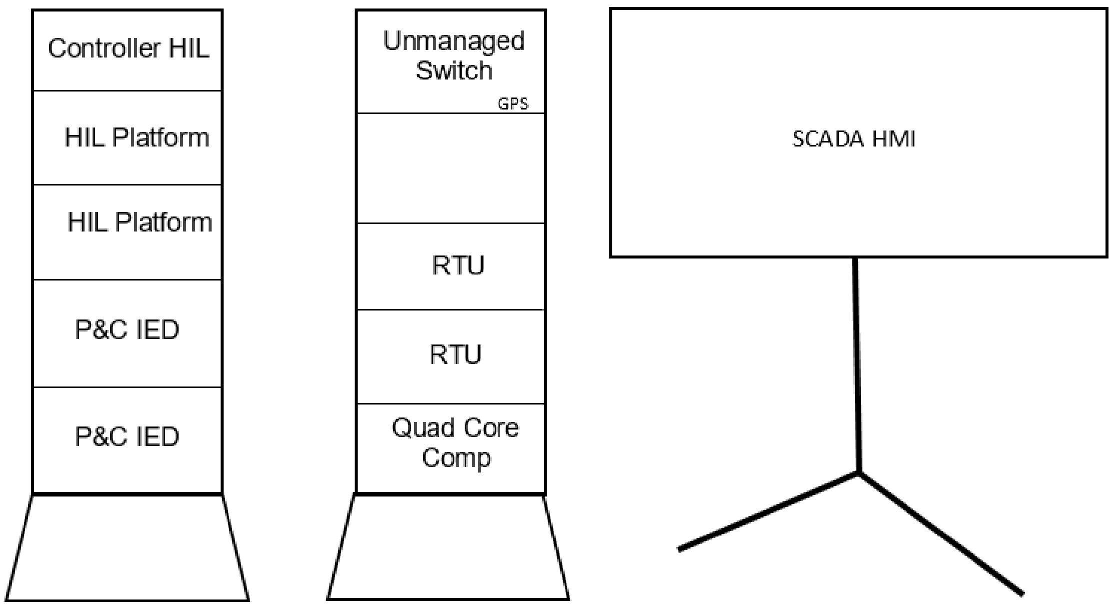

Figure 3.6: Schematic for Hardware-in-loop (HIL) setup

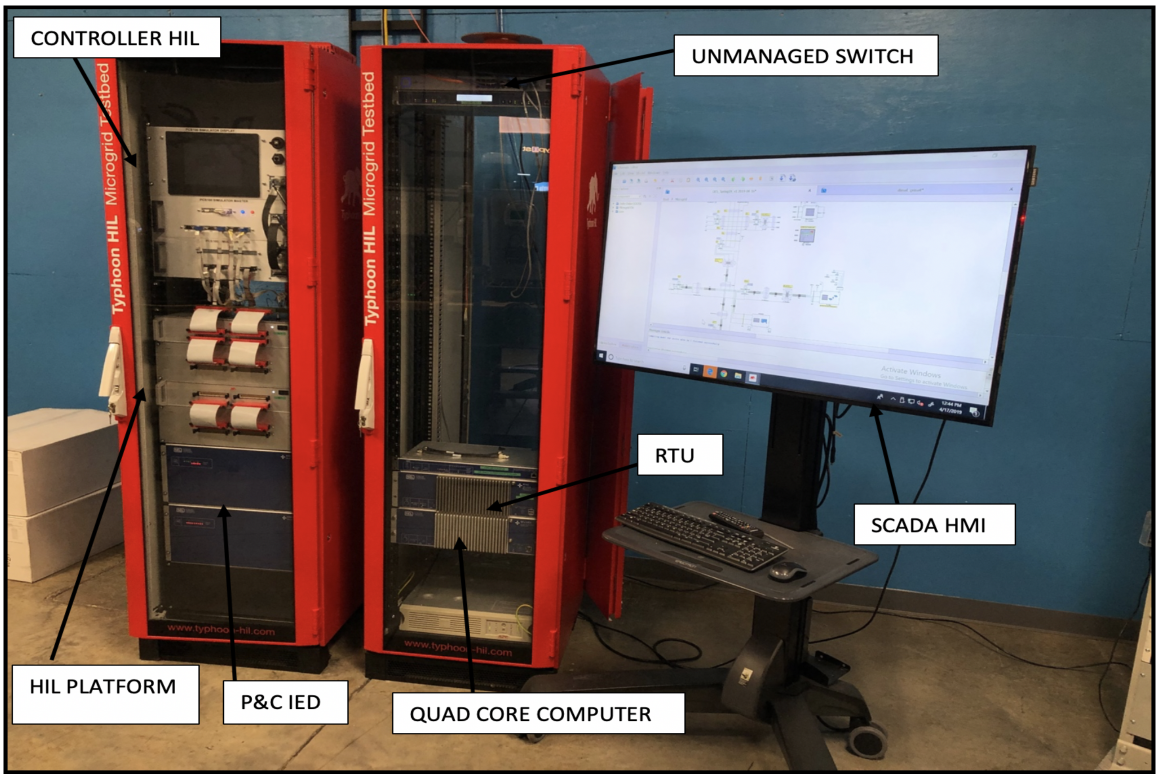

Figure 3.7: Hardware-in-loop (HIL) setup developed at Electrical Utility

CHAPTER 4: HARDWARE-IN-LOOP SIMULATION MODEL

4.1 Introduction

This chapter describes the simulation model and the way feeder components are modeled inside Hardware-in-loop simulator used, i.e., Typhoon HIL. The functionality of each modeled component is explained and transition modes of the microgrid are demonstrated step by step. The chapter describes the interconnections of the simulation with Hardware-in-loop and also explains the methodology behind flow of information between different vendors based devices.

4.2 Feeder Model

The distribution feeder comprises of 12.47kV utility grid, regulator, nine dynamically-varying loads, and current controlled current source. This is modeled and compiled in a real-time platform Typhoon HIL. The feeder model is simulated using two same hardware-in-loop simulators which have an application software embedded inside which help the simulators to integrate seamlessly with the FPGA based processor. The two simulators allow the use of maximum 8 Standard Processing Cores (SPC's) out of which only 7 cores are used in the simulated model. The device coupling is used to divide the model in two halves, one for each HIL simulator device. This device coupling divides the model such that one device simulates all the microgrid components and the other device simulates all the other feeder components including utility grid, regulator, eight dynamically-varying loads and the current controlled current source.

4.2.1 Electrical Utility Grid

The electrical utility grid is considered as the main source of power to the microgrid as well as the nine loads on the distribution feeder.

The voltage and frequency are the key factors which categorize the grid as strong or weak. The main substation is rated at 115kV and is stepped down to 12.47kV using a step down transformer for microgrid applications.

4.2.2 Regulator

Voltage regulators are used to raise or lower the voltage on the distribution line to provide a constant voltage as the amount of load on the line changes.

The nominal voltage of the regulator is rated at 12.47kV/1.73 = 7199.5V and is placed between bus 5 and bus 6 since the distance between them is comparatively larger than other transmission lines.

4.2.3 Local PV Generation Source modeled as Signal Controlled Current Source

This component is modeled as a signal controlled current source which is used to provide the required amount of current and power to the loads. The current reference signals are obtained by the operation of phase lock loop and converting from three phase plane (abc) to two phase plane (α-β). This is done to reduce the complexity of performing the control operation of three separate quantities. The reference signal obtained are used to provide current and power to the nine loads on the feeder.

4.3 Microgrid Simulation Model

Unlike distribution feeder, the microgrid is modeled in the second HIL simulator device. This device uses 4 out of 7 SPC's. The first core contains one remaining varying load, 4-Way Switchgear and the grounding transformer. The second core contains battery and its corresponding inverter while the third core contains PV farm and its corresponding inverter. The last core of the second device consists of building load and the load bank.

4.3.1 4-Way Switchgear

4-way switchgear cabinet comprises of four switches- Way 1, Way 2, Way 3 and Way 4. This switchgear is considered one of the main components as it ensures the proper islanding of microgrid from the electrical utility grid. Before simulating the model, the status of switches is as follows: Way 1=Close, Way 2 = Close, Way 3 = Open and Way 4 =Close.As soon as the microgrid controller detects that the frequency and voltage between battery inverter and the grid is out of the range: 59.3 Hz<f<60.5 Hz and 0.88<Vpu<1.1 respectively, the switchgear operates by opening Way 1 and closing Way 3. Once the voltage and frequency are restored back and in the normal range of operation, the Way 1 closes and Way 3 opens.

4.3.2 Grounding Transformer

The intermittent nature of Distributed Energy Resources (DERs) makes it important to protect microgrid components in case of faults [23] If DERs (like batteries and PV farms) within the microgrid are connected to ungrounded Y side of the Yg - Y transformer, then it is necessary to install a grounding transformer on grounded side of the Yg - Y transformer. If a line to ground fault occurs on a system that is ungrounded or floating, then there is no path for the fault current to return, and as a result, there is no current flow.[24] Power system in such case can continue to operate, except the two phases that are not faulted will see the increase the voltage by 1.73, which will put additional stress on all power system components. In order to prevent this occurrence, grounding transformer needs to be installed on the Yg side of the Yg - Y transformer. There are several purposes for installing the grounding transformer. First, grounding transformer provides a source of ground fault during line to ground faults. Second, if the re-strike of the fault occurs, the grounding transformer limits the magnitude of the transient over-voltages [34]. Third, it provides the low ground path impedance, which in turns keeps the neutral near the ground potential. Fourth, it allows the connection of phase to neutral loads if such loads exist. The grounding transformer is modeled for a rating of 100kVA - 12.47kV Yg/347V Y.

4.3.3 Photovoltaic Farm with inverter (PV)

PV inverter-based systems act as a voltage controlled current sources and cannot form the grid just by themselves. In order for PV system to be able to be operational, it needs a source of voltage and frequency, which is provided by the main electrical utility grid. Hence, to design a microgrid with PV system, it is necessary to have a DER with it that can provide the source of voltage/frequency during islanding []. Battery Energy Storage System (BESS) inverter-based DER is chosen as DERs that provide the voltage/frequency for the PV system. For the simulation purposes, a constant irradiation of 1000 W/m$\hat{2}$ is used. The nominal voltage of the PV plant is 315V, with inverter switching frequency of 10 kHz and nominal DC voltage of 750V. The PV plant is modeled for a plant area of 500 m$\hat{2}$.

4.3.4 Battery Energy Storage System

The Battery Energy Storage System (BESS) is modeled as a combination of a battery inverter and battery. The 150 kW solar farm is connected with 240kW - 122kWh battery using a 250kW DC/DC converter. The inverter system consists of inverter controller (PLC) and Power Conversion System (PCS) which is the real hardware in-the-loop used to generate pulses using Pulse Width Modulation (PWM) for the simulated battery inverter model. Inverter can operate in two modes: Current Source Inverter (CSI) mode and Voltage Source Inverter (VSI) mode. This inverter is not capable to change between two modes while the IGBTs are switching, so in order to make that transition, inverter has four basic operating modes:

1. Current Source Inverter (CSI Mode) Represented as voltage controlled current source with high current impedance source to the grid. To get a quick current output response, the user inputs active power (P) and reactive power (Q) reference points.

2.Voltage Source Inverter (VSI Mode-P/Q) Similar to CSI mode, represented by high current impedance but low voltage impedance, this mode is also a voltage controlled current source but outputs relatively slower current response than CSI mode.

3. VSI-V/f VSI-V/f mode regulates the voltage and frequency at the inverter AC terminals based on the voltage and frequency user defined set-points. The inverter response is defined based on the droop control for both voltage and frequency. This mode is typically used in islanded operation when the DER with the inverter is not the largest unit used for forming the grid, and is rather used for operation in parallel with other DERs.

4. VSI-ISO This mode regulates both voltage and frequency at the inverter AC terminals. The set-points do not include any droop levels i.e. both voltage and frequency droops are zero.

4.3.5 Data Flow and Communication between Real-Time HIL Platform, P&C IED, RTU and HIL SCADA

The distribution feeder is simulated on HIL platform and the analog inputs and outputs (I/O) of the simulation are configured in the Protection and Control (P&C) Intelligent Electronic Device (IED). Table A1 through A5 describes the nomenclature of analog and digital I/O's which are used to configure the simulation and the hardware devices. The P&C IED houses a virtual machine (VM) and to increase the response time, data is being communicated to the Remote Terminal Unit using protocols including DNP3 and IEC 61850 Generic Object-Oriented Substation Events (GOOSE). This RTU is a real-time automation controller and a powerful real-time operating system that ensures deterministic and uninterrupted automation. The device yields an output data using communication protocol,namely GOOSE_RTU. For the subscriber and publisher block inside the HIL model to communicate using GOOSE, the data from RTU needs to be converted into a respective understandable language. To perform this operation, a new North American Energy Standard interoperability framework known as Open Field Message Bus (OpenFMB) is used. GOOSE publisher and subscriber blocks are modeled inside the HIL model and configured with their respective Substation Configuration Description (scd) file. The scd file allows the mapping of a server model with dataset that communicates between IED and RTU using IEC 61850-GOOSE. The subscriber requests data from RTU which sends out data GOOSE_RTU. The data goes through the OpenFMB adapters which converts the data for the Goose publisher block inside Typhoon HIL schematic. This data is received by GOOSE subscriber block and is termed as GOOSE_HIL. This ensures, verifies and validates the architecture if the data coming from the simulation and GOOSE publisher are the same.

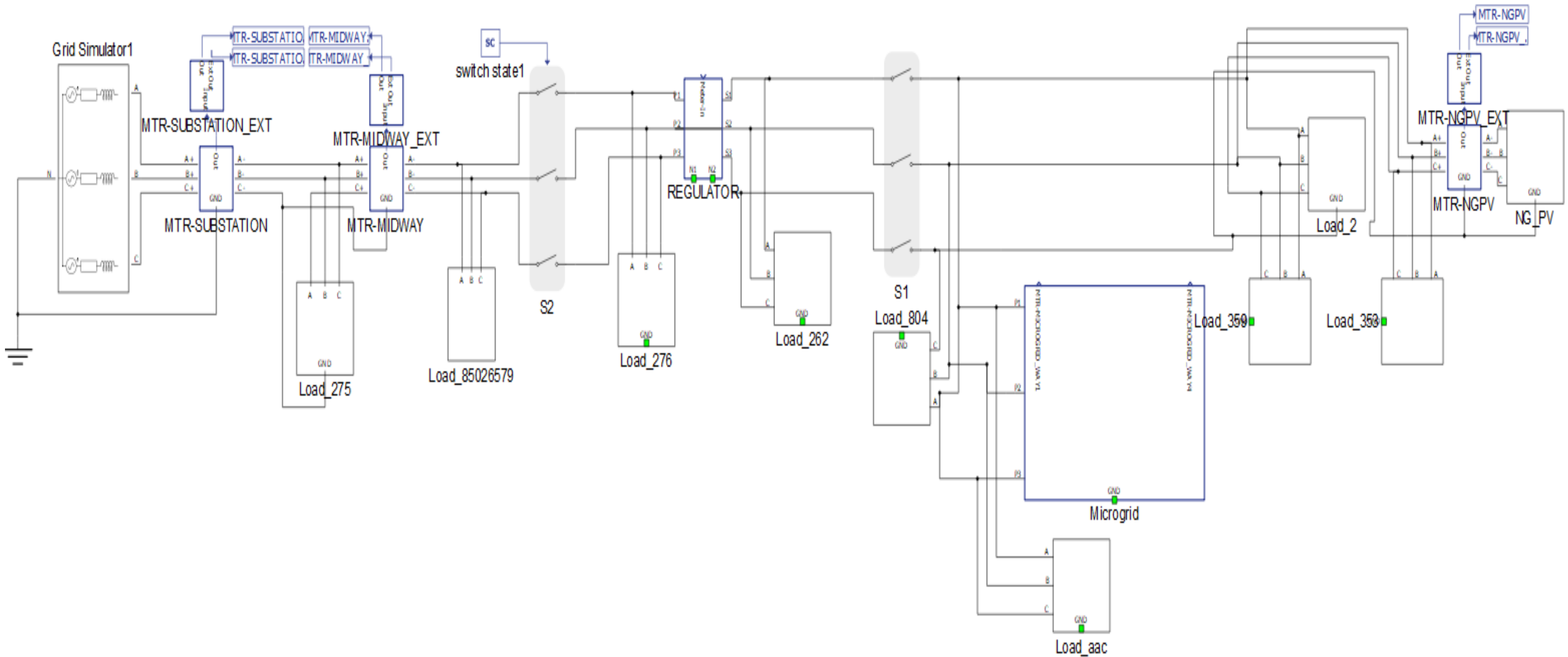

Figure 4.1: Simulation Diagram of Feeder Model

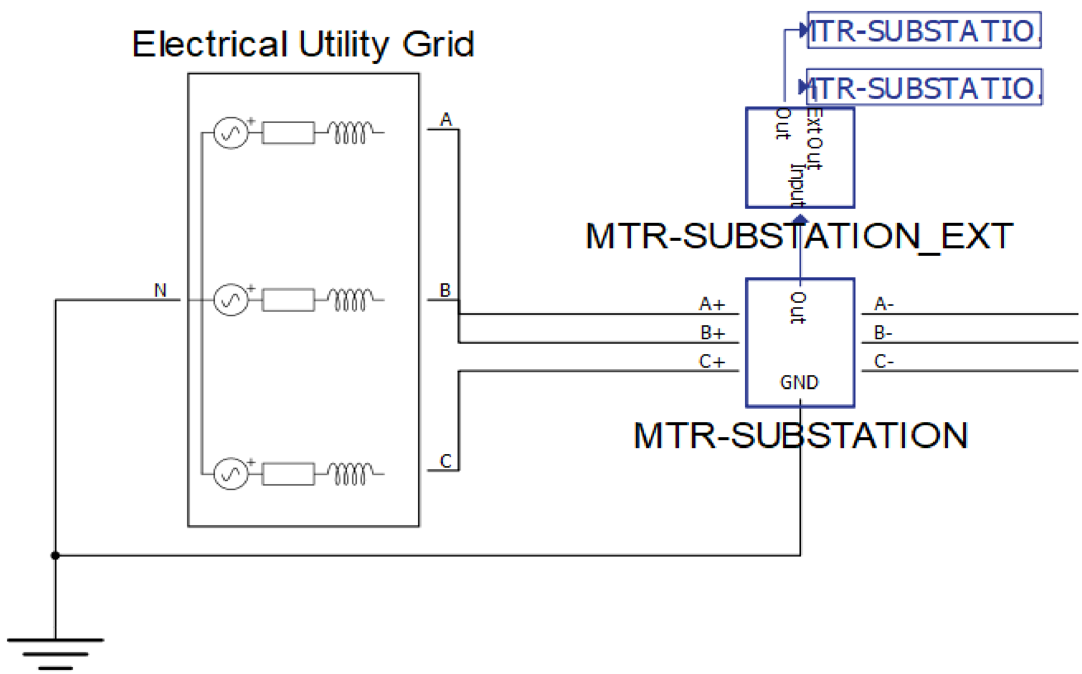

Figure 4.2: Simulation Diagram of Electrical Utility Grid

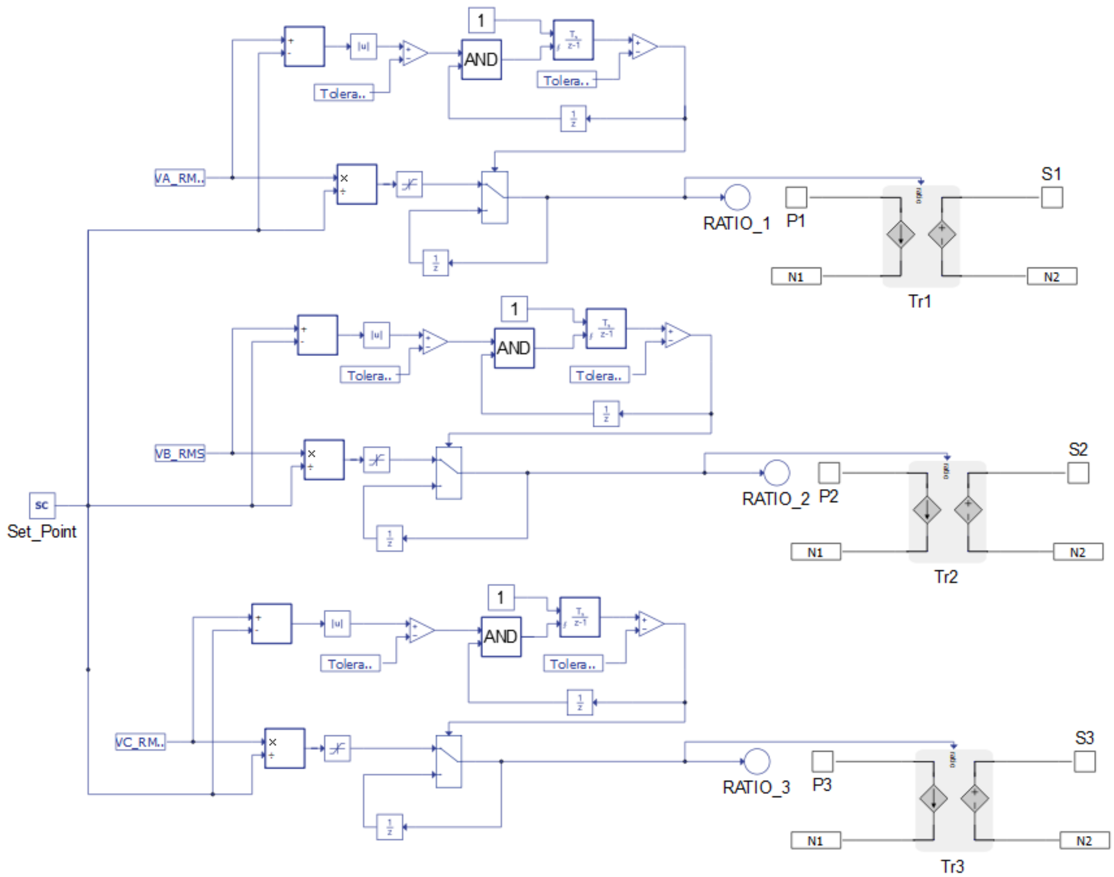

Figure 4.3: Simulation Diagram of Regulator

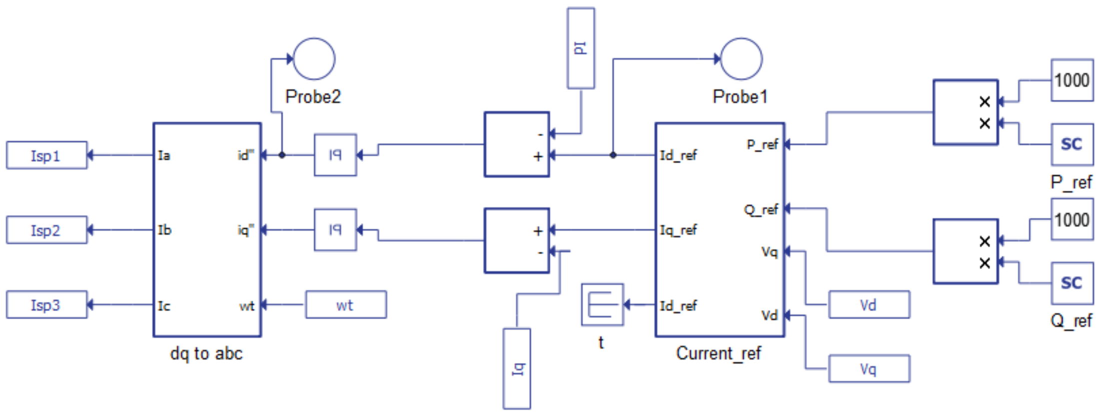

Figure 4.4: Block Diagram for Local PV Generation Source

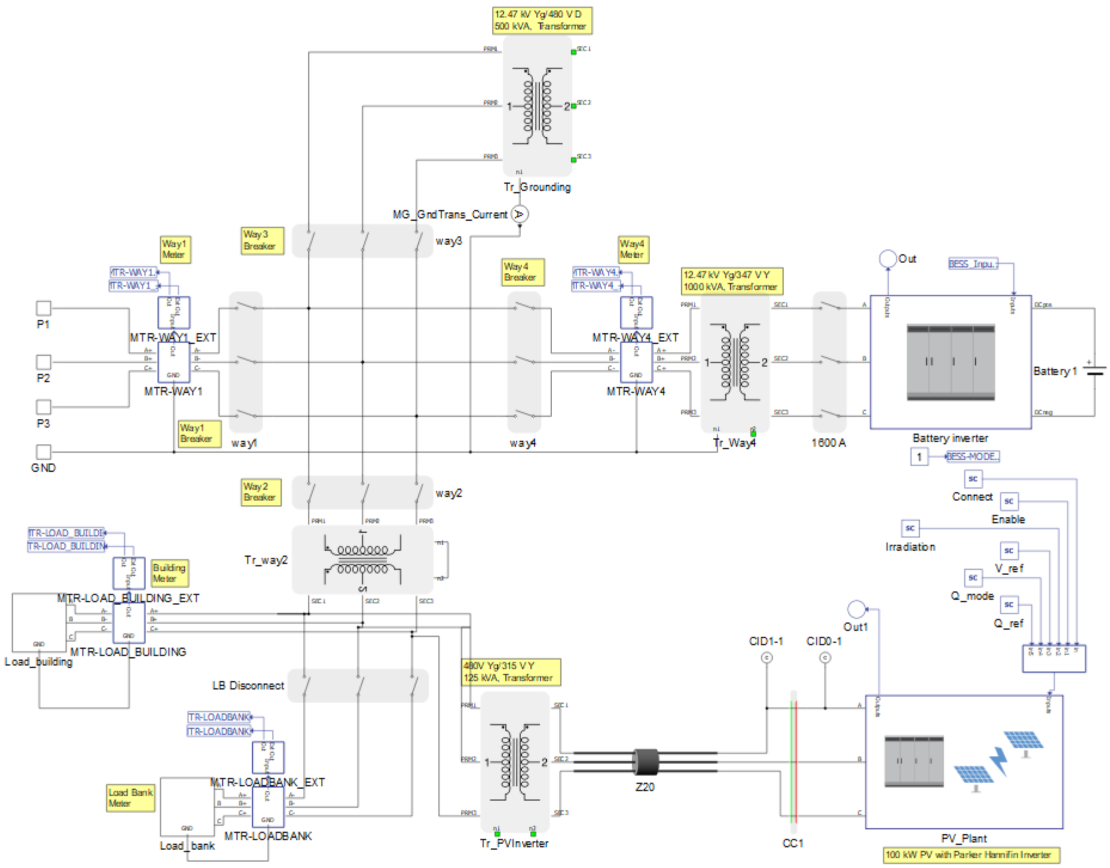

Figure 4.5: Simulation Diagram of Microgrid

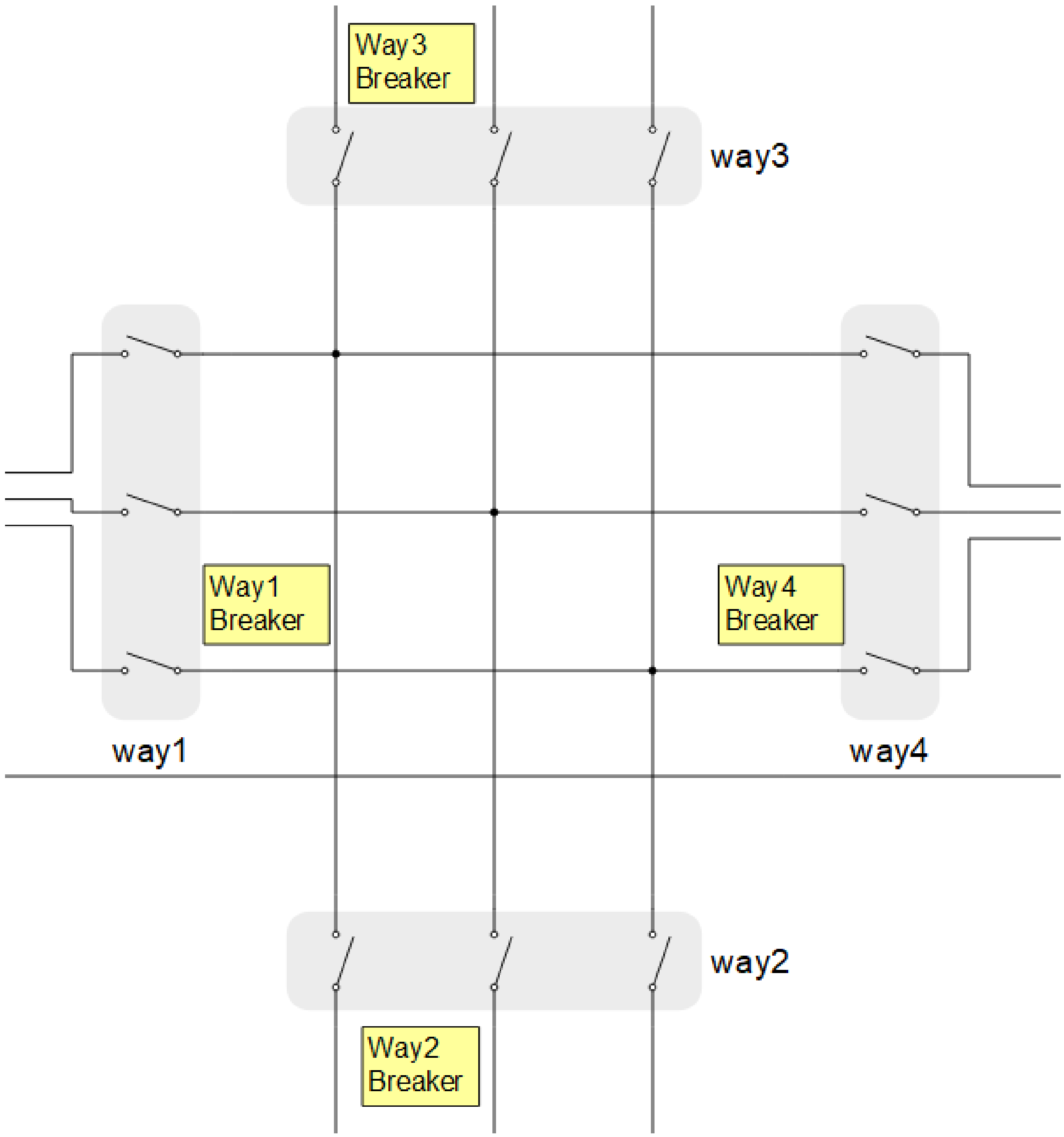

Figure 4.6: Simulation Diagram of 4-way switch

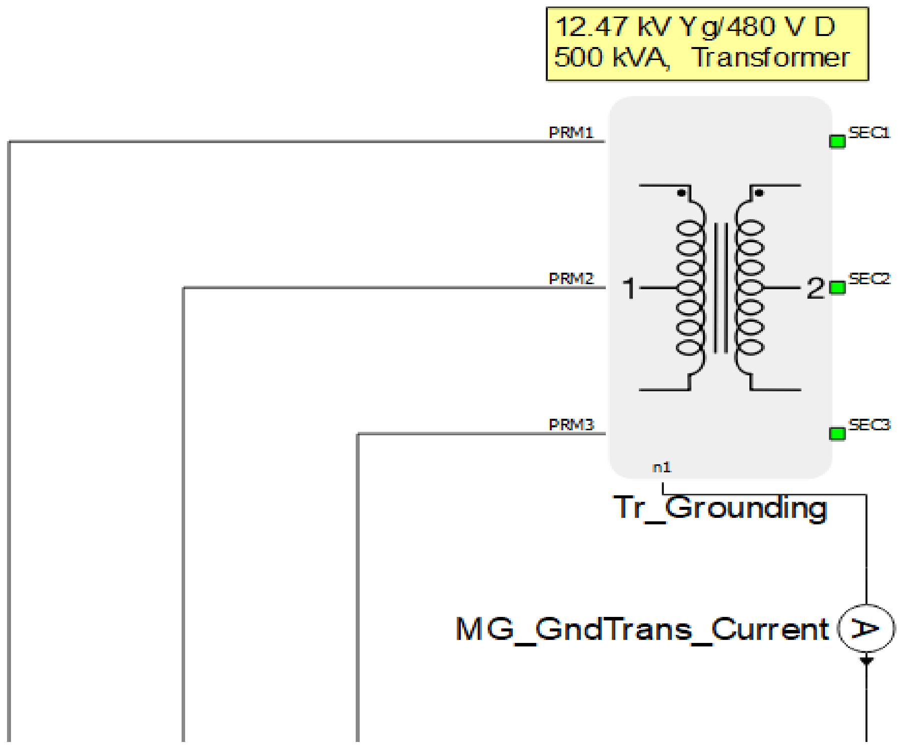

Figure 4.7: Simulation Diagram of Grounding Transformer

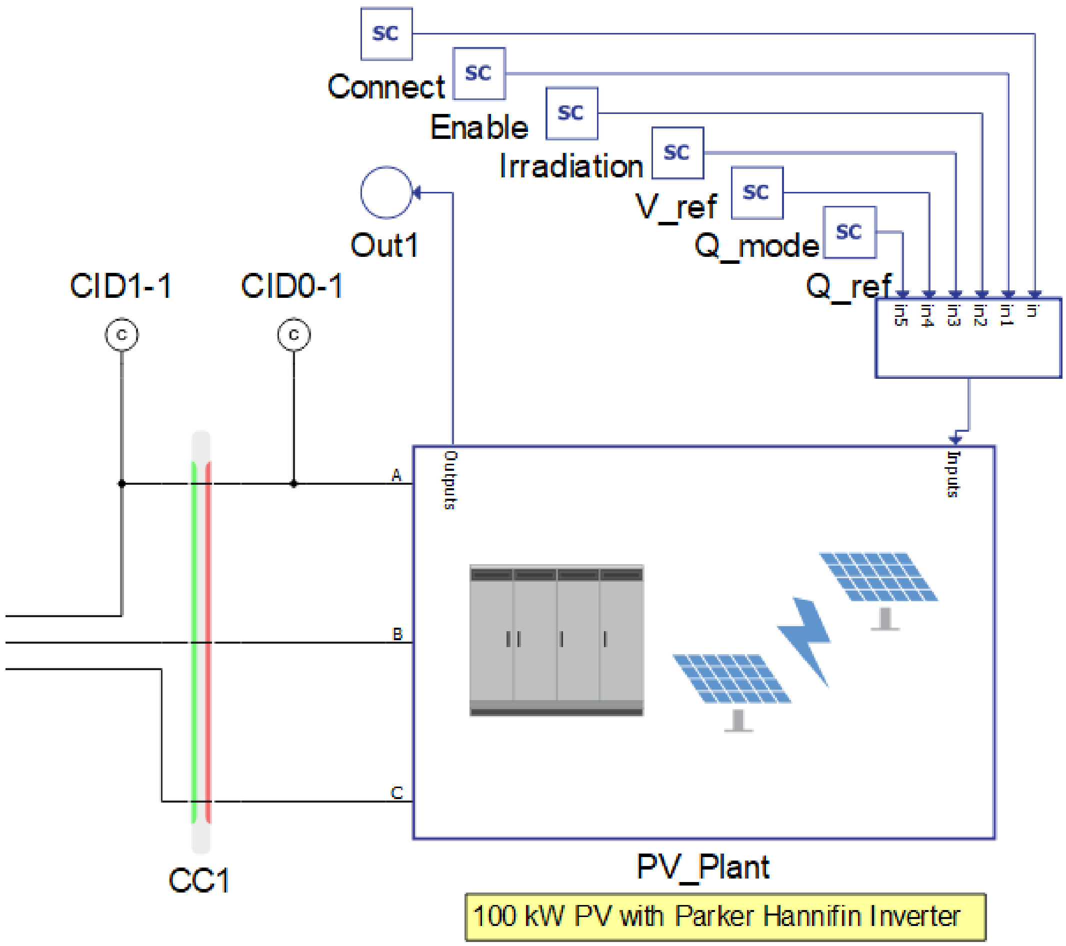

Figure 4.8: Simulation Diagram of Photovoltaic Farm

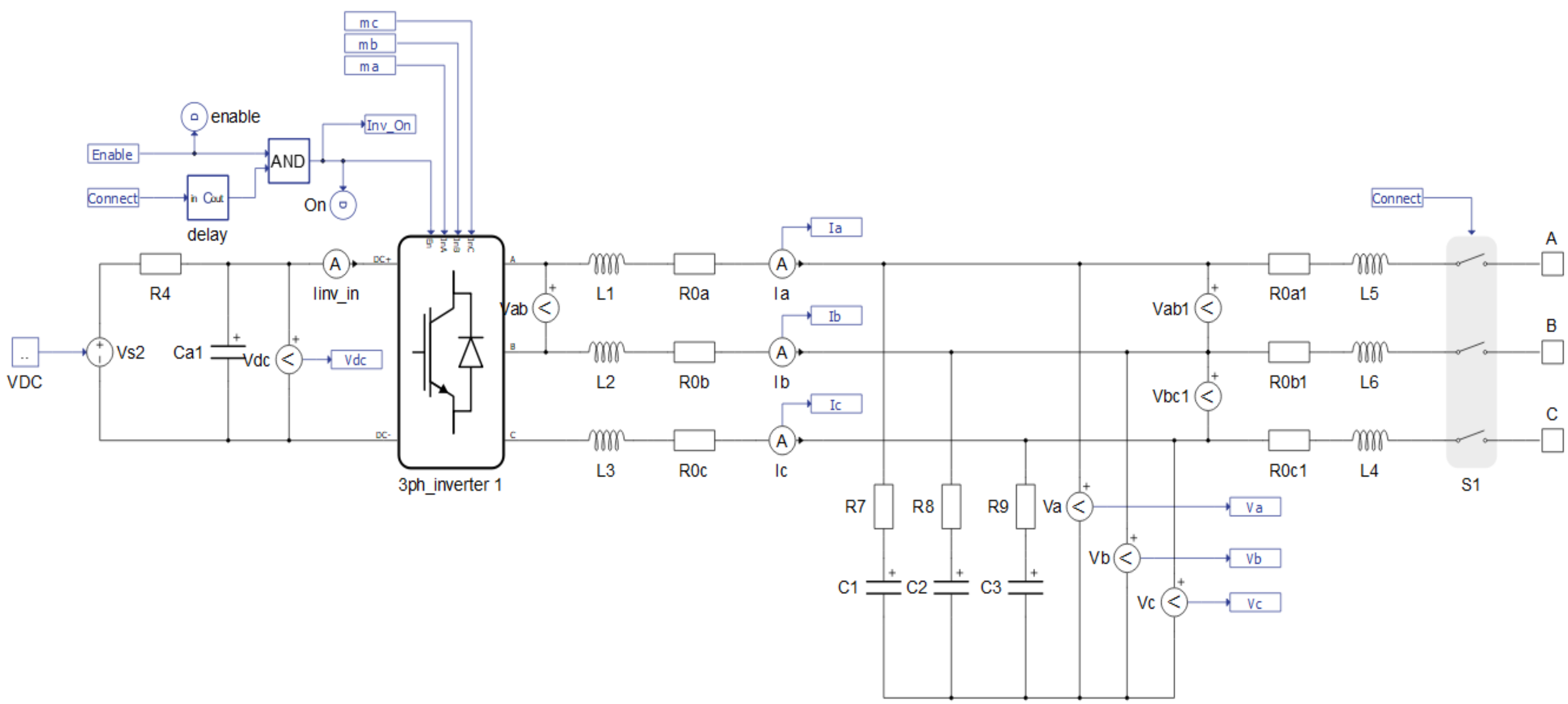

Figure 4.9: Simulation Diagram of PV inverter

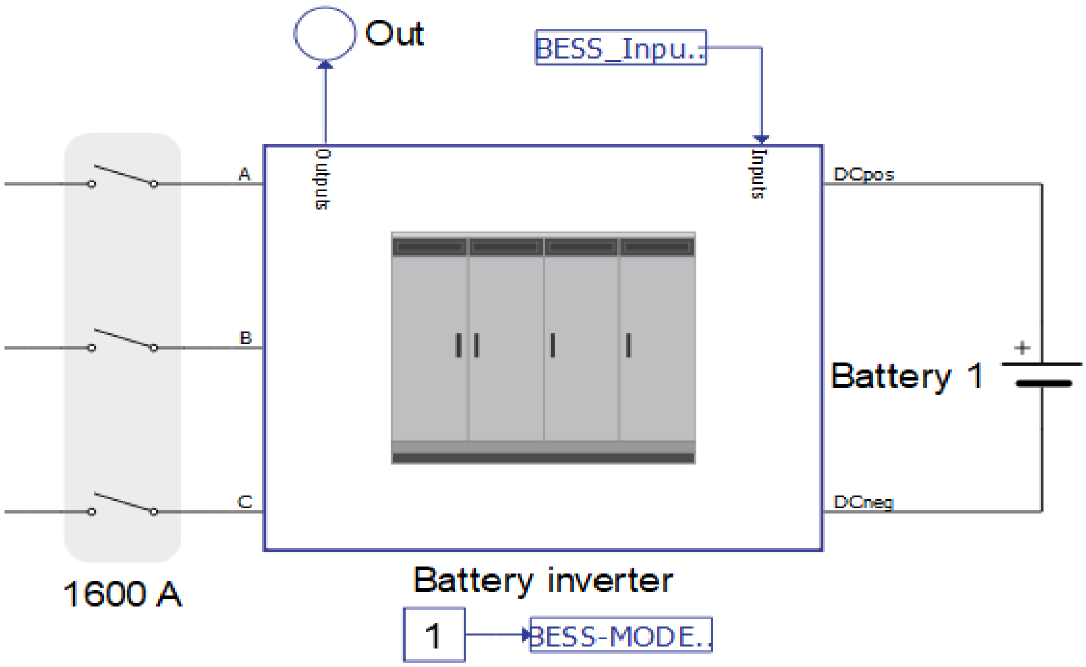

Figure 4.10: Simulation Diagram of Battery inverter

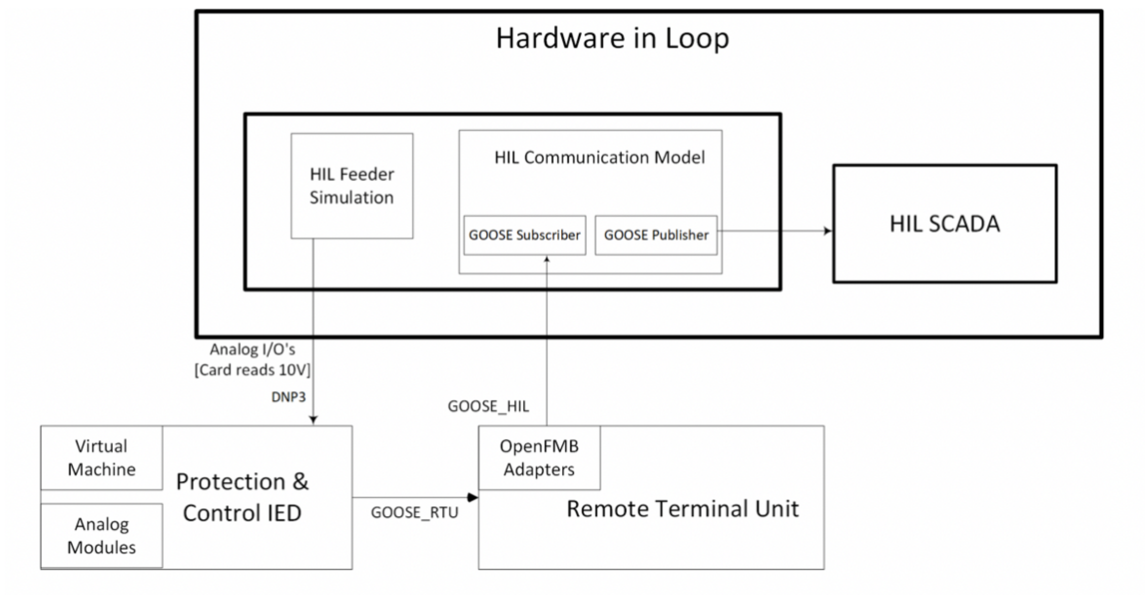

Figure 4.11: Architecture of Communication between Real-Time HIL Platform, P&C IED, RTU and HIL SCADA

CHAPTER 5: PROPOSED USE CASE

5.1 Introduction

This chapter describes the Classical Approach used in Traditional Centralized Systems to manage the process of grid following, grid islanding and grid-resynchronization. It also describes the Proposed Approach to manage the above three processes in a more efficient manner and the advantages of using OpenFMB adapter nodes.

5.2 Classical Approach used in Traditional Systems to manage Utility Grid-Microgrid inter-connections

A microgrid is a system which functions as an independent entity without any external power supply. It is capable of supplying the connected loads with the help of distributed energy resources connected in the system. The system usually contains distributed energy resources such as a combination of Photovoltaics (PV) and battery energy storage, natural gas generators, micro-turbines and wind-powered systems. The inclusion of battery energy source is mainly due to the intermittent nature of energy resources. So to meet the power conditioning requirement, the PV interconnect is taken by the DC-DC converter. In most cases, to meet the DC link voltage requirement, a boost converter [14]which converts (boosts) the input voltage to a higher required voltage. These type of DC-DC converters use proportional-integrator controllers to make voltage and current in sync and inject/draw power from the grid. In an automation based environment, the system also known as supervisory control and data acquisition (SCADA) system [17] is a must to have a safe and reliable operation of physical processes such as a microgrid itself. In recent years the benefits of sharing SCADA information with corporate networks has proven to be of utmost importance. However, the ability to access and control the functionality of isolated networks has displayed vulnerability to cyber-attacks.

During any event of fault occurrence due to storms, natural disasters or external attacks (physical or cyber), microgrid with flexible resources are designed such that they continue to supply electricity to customers in islanded operation/grid forming mode [22].

The objective remains the same for the system to seamlessly transition between Grid Connected (Grid Following) and Islanding (Grid Forming) mode. The inverter controllers operate in grid feeding, current source grid supporting, voltage source grid supporting and grid forming modes. The battery creates the voltage and frequency during the islanding operation mode and the two inverter operation include current source inverter (CSI) mode and voltage source inverter (VSI) mode. For grid following operation, VSI-P/Q control mode is opted for the main reason that the reference real and reactive power can be set by the user for the controller to reduce the error between reference power and produced power For grid forming operation, VSI-V/f control mode is opted so that the user can define the voltage and frequency droop setpoints and the battery makes sure that there is a seamless transition.

From Figure 5.3 it can be observed that during an event of fault, the centralized system in combination with supervisory control and data acquisition senses the fault and the message for the microgrid to disconnect from the main grid is sent to the switch. The switch receives the message and seamlessly tries to isolate the main grid from the microgrid to operate as a separate entity.

From the Figure 5.4 it can be observed that as soon as the fault is restored and the system is healthy, the message is sent for the microgrid to connect back to the main grid using the traditional centralized system.

5.3 Proposed Approach

The analog inputs and outputs of the simulation are configured in Protection and Control (P&C) Intelligent Electronic Device (IED). The data is communicated to RTU using DNP3 and IEC 61850 Generic Object-Oriented Substation Events (GOOSE). The RTU outputs data using communication protocol GOOSE_RTU. The data of RTU is converted into the respective understandable language. To perform this operation, a new North American Energy Standard interoperability framework known as Open Field Message Bus (OpenFMB) is used. Substation Configuration Files are given as input to the OpenFMB adapters. The publisher and subscriber controller blocks spew the values which validate and verify the operation of OpenFMB adapters.

From the fig 4.4 it can be observed that as soon as the fault is detected, the message is scaled and goes through the P&C device as well as a powerful, faster remote terminal unit. To obtain a faster response as the centralized site is far away, the OpenFMB adapters with their interoperable nature and distributed intelligence, maps the tags for different protocols and makes it a secure communication process. The controller subscribes the correct variable and then publishes out to the SCADA that a fault is detected and the switch should open for the microgrid to island.

From the fig 4.5 it can be observed that the fault is now restored the message is scaled and goes through the P&C device as well as a powerful, faster remote terminal unit. To obtain a faster response as the centralized site is far away, the openFMB adapters with their interoperable nature and distributed intelligence, maps the tags for different protocols and makes it a secure communication process. The controller subscribes the correct variable and then publishes out to the SCADA that a fault is restored and the switch should close back for the microgrid to synchronize back to the main grid.

The Open Field Message Bus (OpenFMB) provides distributed intelligence at the edge. The plug-n-play integration with the existing devices and systems using its adapter, makes it an interoperable medium to communicate throughout the system. Its unified semantics which are based on IEC 61850 and CIM enables advanced analytics. The adapters provide resiliency to the system when the main grid is segmented.

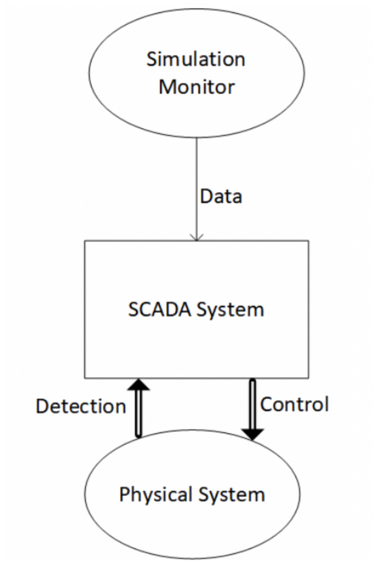

Figure 5.1: Data Flow in Classical SCADA System

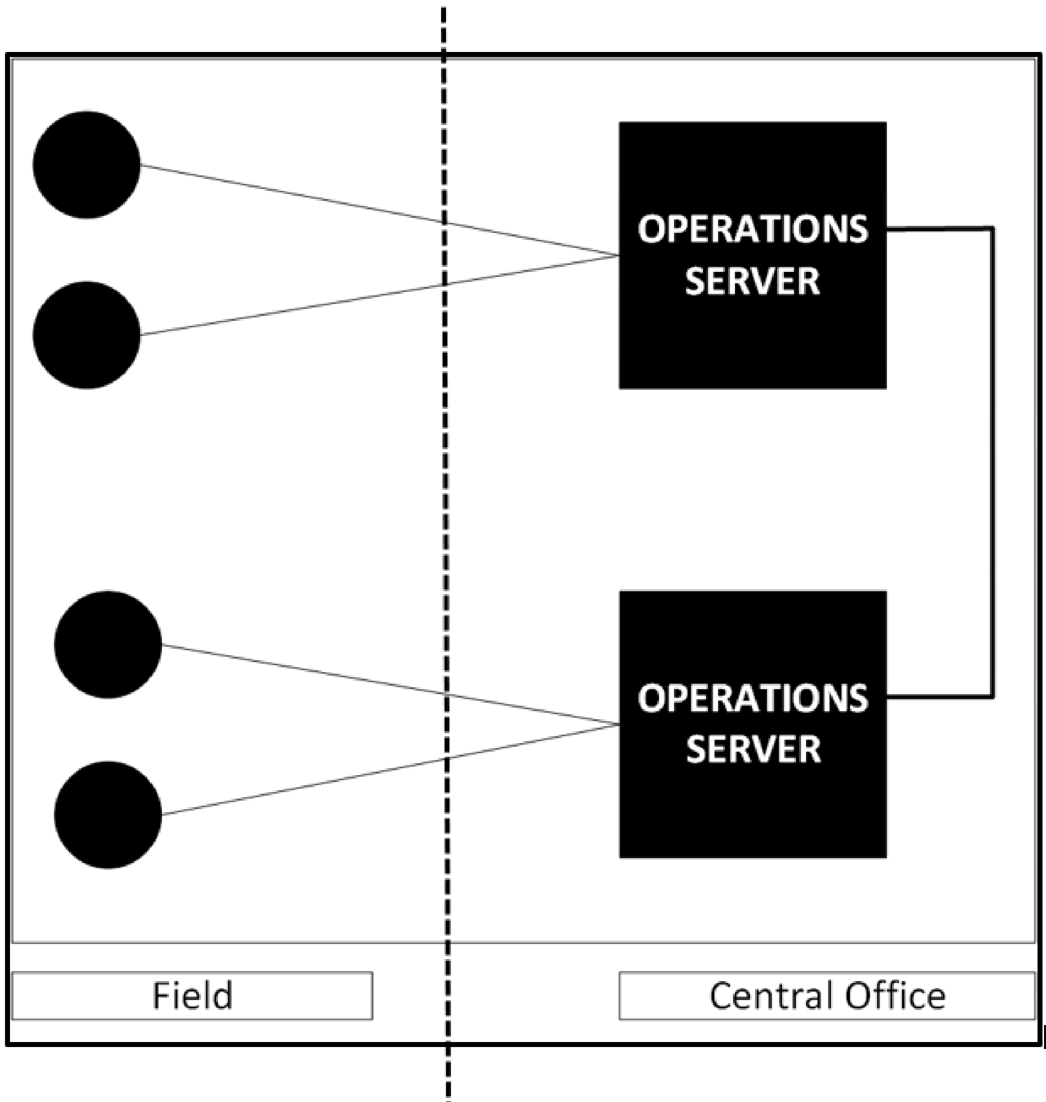

Figure 5.2: Classical Approach to manage the process of grid following, grid islanding and grid-resynchronization in microgrid

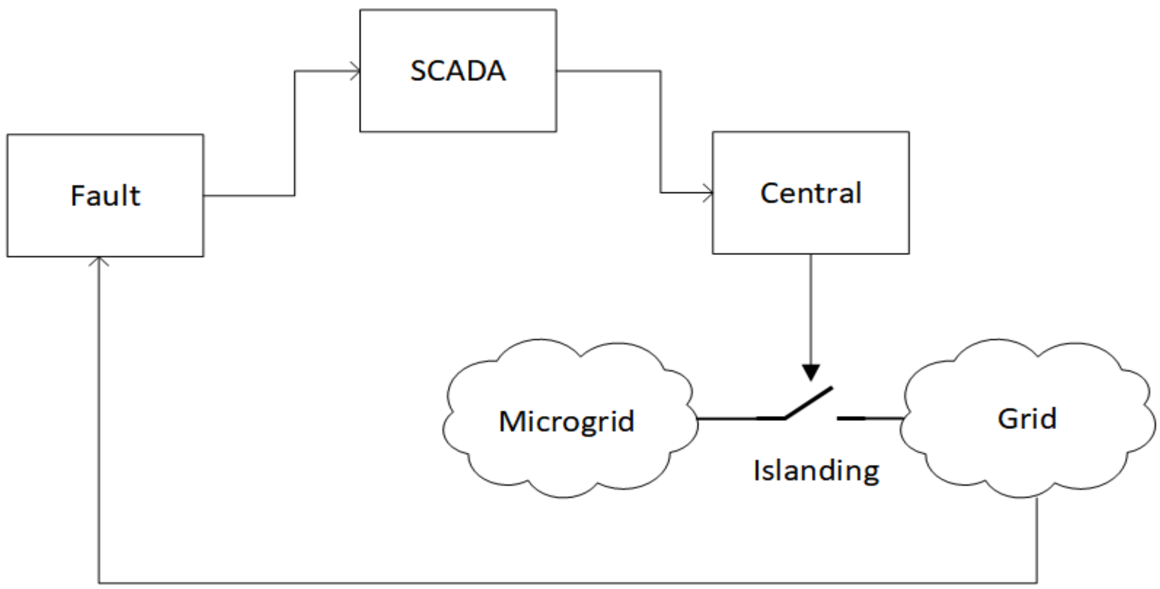

Figure 5.3: Islanding of microgrid in Classical Approach

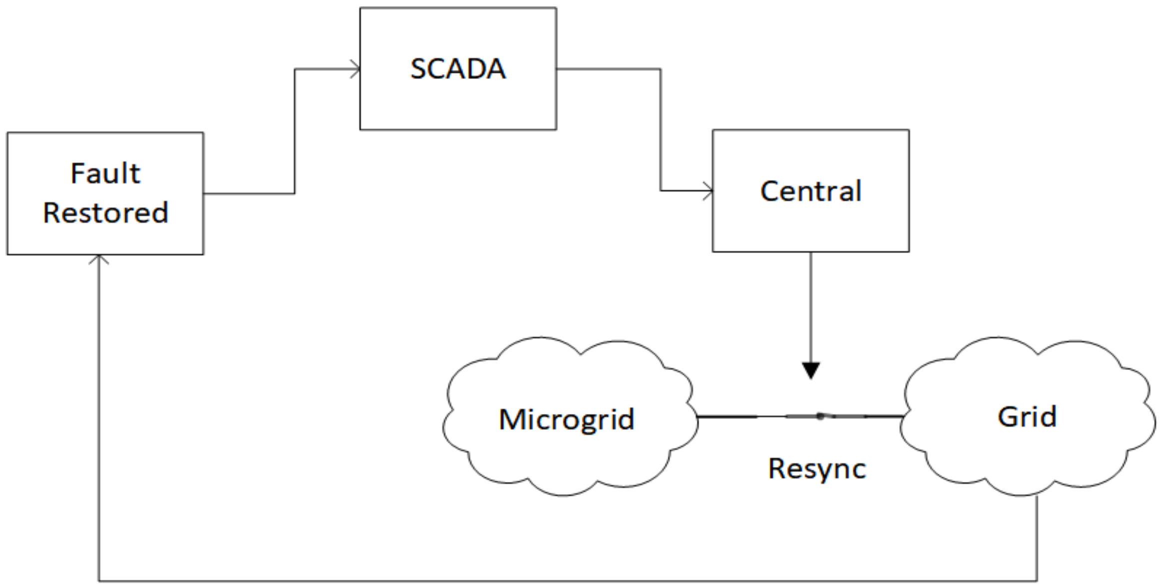

Figure 5.4: Resynchronization Operation of microgrid in Classical Approach

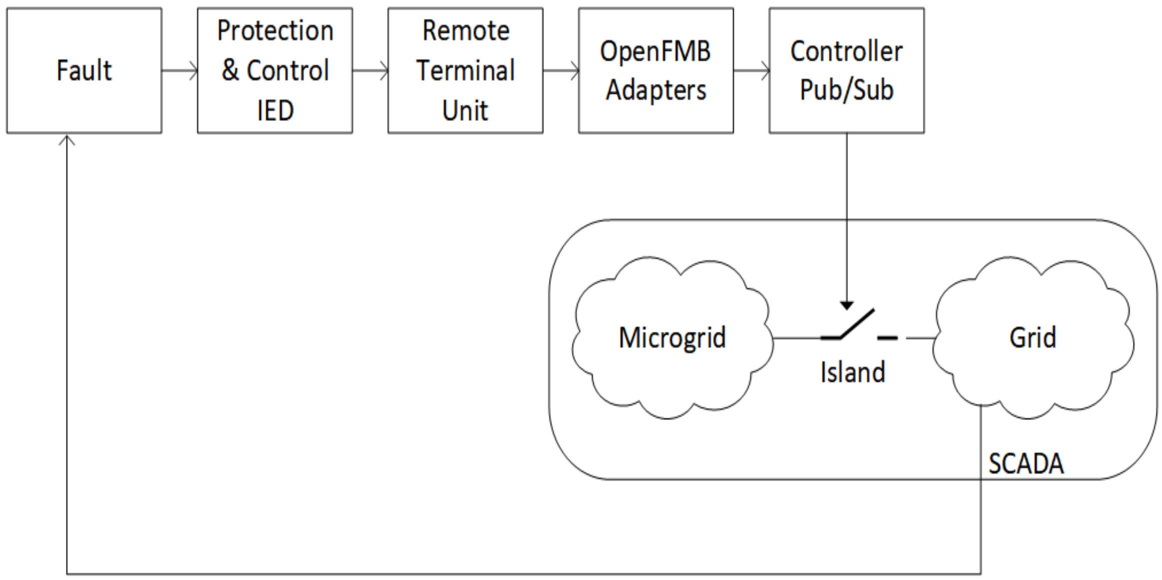

Figure 5.5: Islanding Operation of microgrid in Proposed Approach

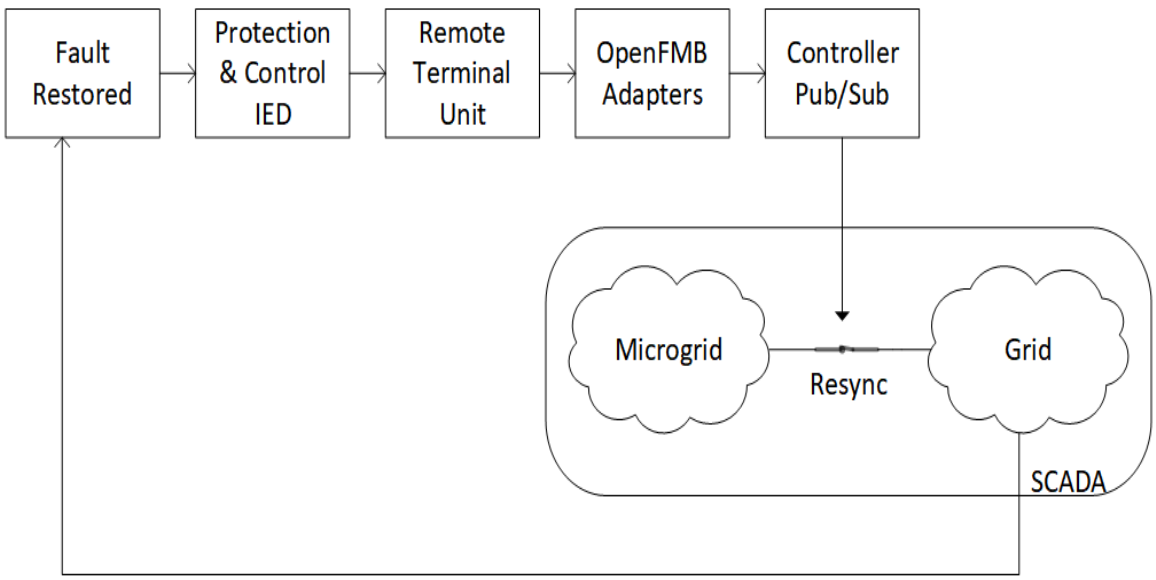

Figure 5.6: Resynchronization Operation of microgrid in Proposed Approach

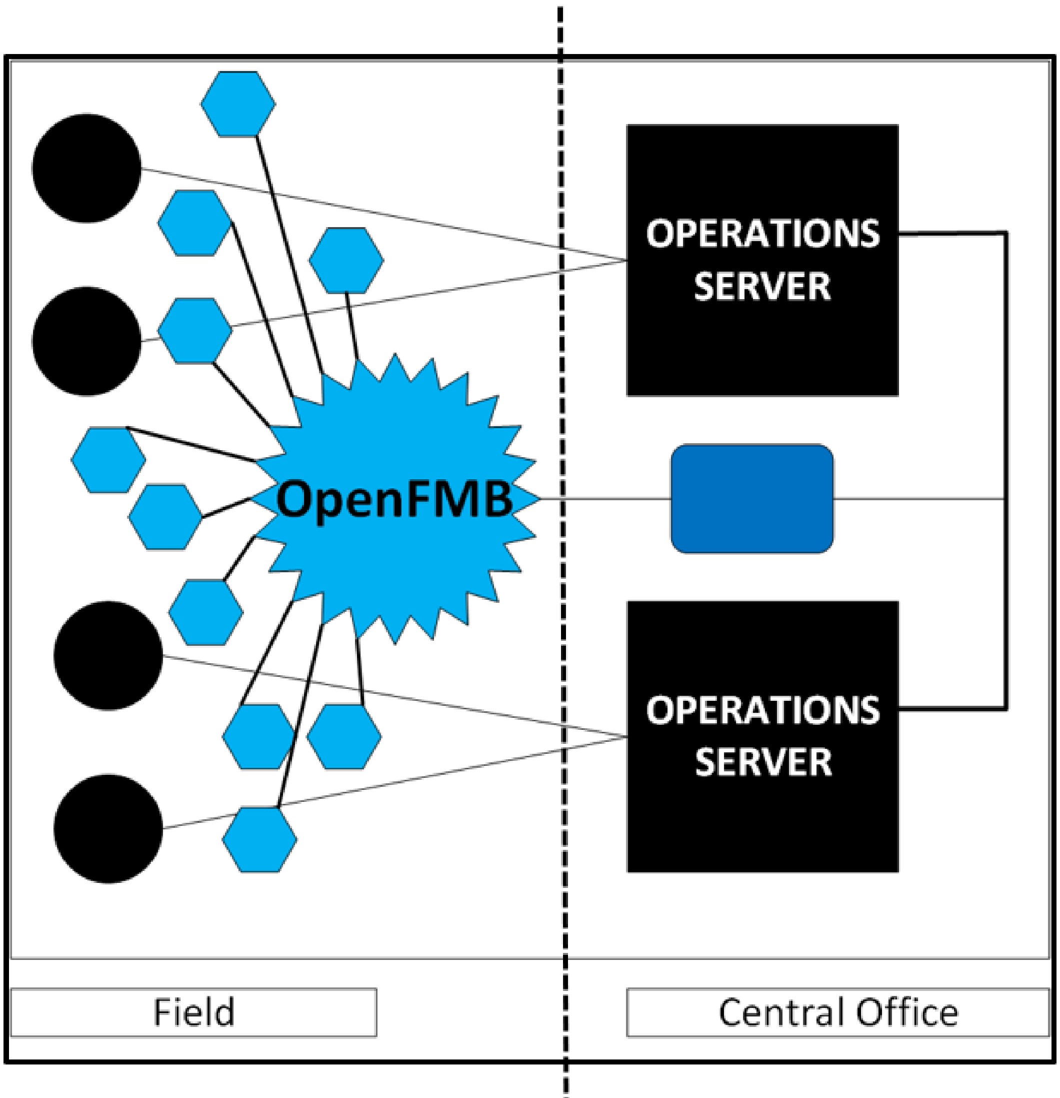

Figure 5.7: Proposed OpenFMB System [33]

CHAPTER 6: HARDWARE CONFIGURATIONS

6.1 Introduction

The chapter demonstrates the detailed configuration of the proposed approach. It describes the configuration of RTU and P&C and defines the configuration of Substation Configuration Description (.scd file). It demonstrates the use cases of proposed approach and the process flow of events. It also explains the importance of having OpenFMB and provides a detailed comparative analysis between classical and proposed approach.

6.2 Demonstration of Proposed Approach

Communication between vendor specific devices is the key for collaborative operation inside a substation. The devices under consideration include the inverter controller, i.e., Power Conversion System (PCS) which consists of inverter modules operated using pulse width modulation, Typhoon Hardware in-loop (HIL) 604 modules, Protection & Control device, Remote Terminal Unit (RTU), which contains analog cards and the Virtual Machine (VM) for HIL Typhoon system, Managed switch, 2.1 Ghz Quad core computer. The communication can either be done using ethernet switches or various protocols including MODBUS, IEC-61850 Generic Object-Oriented Substation Event (GOOSE) and DNP. Each of these devices have a unique Internet Protocol (IP) and MAC (∗) Address which acts as a pointer to the reference of the device.

Distributed Network Protocol (DNP)

Distributed Network Protocol (DNP) is a communication protocol which is mainly used as a tool for system integration and SCADA purposes. DNP is used to process and send data as well as control variables while implementing limited bandwidth communications. DNP is known for broadcasting a single unit message to multiple available devices, timestamping data, quality flags to show the essence of data, and provides the option of select-before-operate for reliable device control. DNP uses master-slave communications.[29] The user enters the client and server IP address along with integrity poll period and number of polls retries. A DNP master polls slave device for data, and broadcasts control commands to slave devices.[31] Data is stored in an allotted location in available device. There are types of data to be stored in the location, and a specific format for the data. Easy implementation, low bandwidth requirements for data communications, are some advantages of DNP. The mapping and remapping of data to each device containing the DNP configuration is one of the major drawbacks of this protocol. IEC 61850−GOOSE IEC 61850−GOOSE stands for Generic Object−Oriented Substation Events. It is used to implement communications for all data in a substation. The advantage of having a 61850 based communication is that the data is shared between the devices in peer to peer trend. After inputting data, according to the standard, the data is sent to every 61850 based devices. The aim of 61850 is to develop a group of data objects. Each Intelligent Electronic Device consist of a logical device made up of logical nodes. Each logical node consists of different type of classes and instances. The data objects (in-built) are inherent to every class. Depending on the class and logical node, these data objects are the means to mapping in the peer to peer translation. GOOSE is published only when a dataset item changes value.

6.3 Configuration of RTU & P&C

There are seven points from where the meters are sccumulating data and these points will be mapped in the Remote Terminal Unit (RTU) as follows:

Table 6.1: RTU Node-1 Setup

RTU	Power Coupler	V1	I1	V2	I2	V3	I3	Digital I/O Card
AXION RTU-2241	RTU-2243	RTU-2243	RTU-2245-22 AI	RTU-2245-22 AI	RTU-2245-22 AI	RTU-2245-22 AI	RTU-2245-22 AI	RTU-2244-3 AI

Table 6.2: RTU Node-2 Setup

Power Coupler	V4	I4	V5	I5	V6	I6	V7	I7
RTU- 2243	RTU-2245-22 AI	RTU-2245-22 AI	RTU-2245-22 AI	RTU-2245-22 AI	RTU-2245-22 AI	RTU-2245-22 AI	RTU-2245-22 AI	RTU-2245-22 AI

Following are the steps used for making a new project in SEL AcSELerator

Click New SEL RTAC Project

Adding modules in the project

Adding power coupler in node-1

Modules are added as the actual hardware and the model can be read from modules. Go to Insert tab and click “Fieldbus I/O”. Select 2243XXXX, Power Coupler and the appropriate model. Devices “22431100, Coupler, RJ45 Cu, Power 125/250Vdc or 120/240 Vac and EtherCAT Protocol4” module are used.

Rename device name. Click Insert.

Adding analog input modules in node-1

Select the Insert tab and go to Fieldbus I/O. Select “22452200000, 4AI-ER, AC(LEA), EtherCAT Protocol”.

Add the following modules

1. AI_Node1_CB_I
2. AI_Node1_HPOI_V
3. AI_Node1_HPOI_I
4. AI_Node1_UPOI_V
5. AI_Node1_UPOI_I

Adding another power coupler and connecting them.

Select Insert tab and go to 2243xxxx, Power Coupler and select “22431100, Coupler, RJ45 Cu, Power 125/150 Vdc or 120/240 Vac, EtherCAT Protocol”.

Inside the EtherCAT I/O Network, right click and select ”Attach Devices”.

Select all the devices that need to be attached in node-1 and click Attach.

Right click and select “Add Node”.

Right click and select “Attach Devices” in Node2.

Select and click “Attach”

Select PC_Node1_ECAT [Coupler′s] Port1 options.

If there are only two power couplers, then changing option for one will be enough. Other one will automatically change.

Adding analog input modules in node 2

Add the following modules:

1. AI_Node2_GPOI_V

2. AI_Node2_GPOI_I
3. AI_Node2_HPOI_V
4. AI_Node2_HPOI_I
5. AI_Node2_PCC12_V
6. AI_Node2_PCC12_I

Attach the modules in node2 as previously did in node 1.

6.4 Configuration of Substation Configuration Desciption(.scd file)

Development of Substation Configuration Description (.scd file)

Step1: Download and Open SEL Architect

Step2: Right Click on the Projector and add the IED's for respective data communication

Step3: Enter IP Address, Subnet Mask and Gateway for the IED

Step4: Click on the server model tab. Add all the Logical Devices (data metering points). Create logical nodes with class MMXU. Tick all the physical quantities read and measured by the meters

Step5: Create data set points for each logical device on the DataSet tab.

Step6: Choose MX (Measurands) as Functional Constraint and all the physical quantities measured for that data point using drag and drop.

Step7: Under the GOOSE Transmit tab, import the dataset, specify MAC Address, APP ID, VLAN ID and VLAN PRIORITY

Step8: Repeat Steps 3-8 for the second IED.

Step9: Under GOOSE Receive tab, drag and drop all the data (for both IED's) with their respective datatype until the LED turns green.

6.5 Process Flow

The analog inputs and outputs of the simulation as well as the digital inputs are configured in the Protection and Control (P&C) Intelligent Electronic Device (IED)

.The Remote Terminal Unit (RTU) houses a virtual machine (VM) which makes it a major part in the communication process. To increase the response time, data is being communicated using DNP3 and IEC 61850 Generic Object-Oriented Substation Events (GOOSE) to RTU. This device outputs data using communication protocol GOOSE_RTU. For the subscriber and publisher block inside the HIL model to speak GOOSE, the data coming out of RTU needs to be converted into a respective understandable language. To perform this operation, a new North American Energy Standard interoperability framework known as Open Field Message Bus (OpenFMB) is used. The OpenFMB adapters are used to input different Substation Configuration Description (scd) files which are used to map respective I/O for the given devices. To validate and verify the operation of OpenFMB adapters, GOOSE publisher and subscriber blocks are configured with their respective scd file. The scd file allows the development and mapping of a server model on to the dataset which can be used to communicate between the IED and RTU using IEC 61850-GOOSE [28]. The subscriber requests data from the RTU, which sends out data GOOSE_RTU. The data goes through the OpenFMB adapters which translates the data for the Goose publisher block inside Typhoon HIL schematic. This data is received by GOOSE subscriber block which is termed as GOOSE_HIL. This ensures, verifies and validates the whole architecture if the data coming from the simulation and GOOSE publisher are identical or with minimal error.

6.6 Importance of Open Field Message Bus in the Proposed Approach

Open Field Message Bus (OpenFMB) is a framework for distributed intelligence and grid edge interoperability. The OpenFMB Users Group was created in 2018 after a transition to the Utility Communications Architecture International Users Group (UCAIug) from a Priority Action Plan previously organized by the Smart Grid interoperability Panel (SGIP). The goal of the framework is to use the existing standards for communication between different vendor-based devices in the field and synchronize them with the utility standards.

The key feature of OpenFMB is that it consists of open and observable interfaces at different scales for interoperability. It consists of a detailed block-wise semantics, based on standards, one of them being IEC 61850, which makes it a great tool for enhanced analysis. Different vendor-based devices have various output communication standards which OpenFMB can harmonize using plug-n-play integration through adapters.

The framework allows the use of Industrial Internet of Things (IIoT) publish/subscribe protocols such as OASIS's MQTT: Message Queue Telemetry Transport (MQTT), Data Distribution Service (DDS) and Cloud Native Computing Foundation's NATS (nats.io). It provides the ability to flexibly integrate renewable energy sources and storage with the existing grid.

OpenFMB Approach is totally independent of the platform. It syncs the IEC CIM and 61850 reference standards and comes up with an OpenFMB unified modeling language (UML)IEC CIM is a standard for exchanging information between systems whereas IEC 61850 defines communication protocols for IEDs From figures 6.38 and 6.39 it can be safely conveyed that the adapters successfully interpret one protocol and maps the tag from another protocol to that of the former. Since the vendors of RTU and HIL devices are different, the GOOSE protocol communicated between both the devices need not be same leading to unsuccessful mapping of tags from both the devices. The OpenFMB adapters help in mapping the correct tags from different vendor devices irrespective of the protocol. Hence the adapters are embedded inside the RTU which help in successfully communicating to the Hardware in loop testbed.

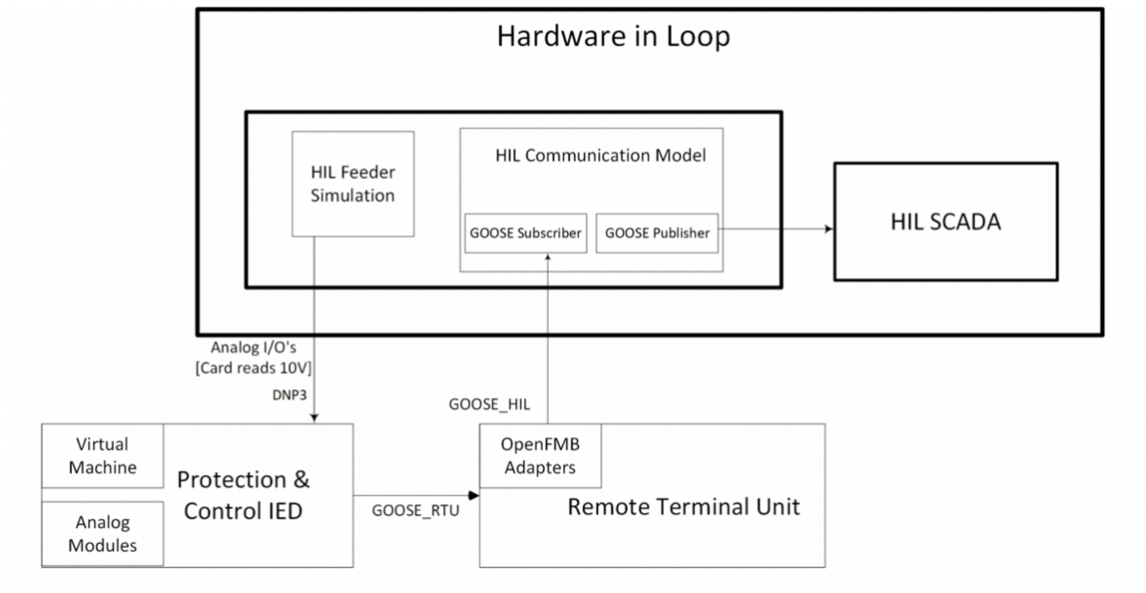

Figure 6.1: Demonstration of Proposed Approach

Figure 6.2: Making new project step-1

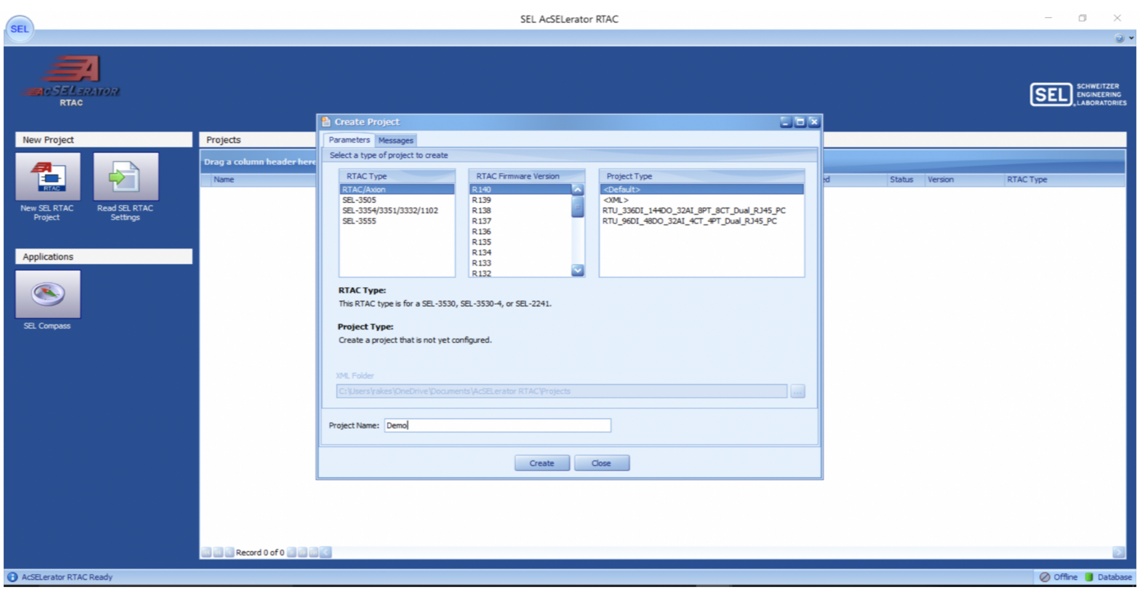

Figure 6.3: Making new project step-2

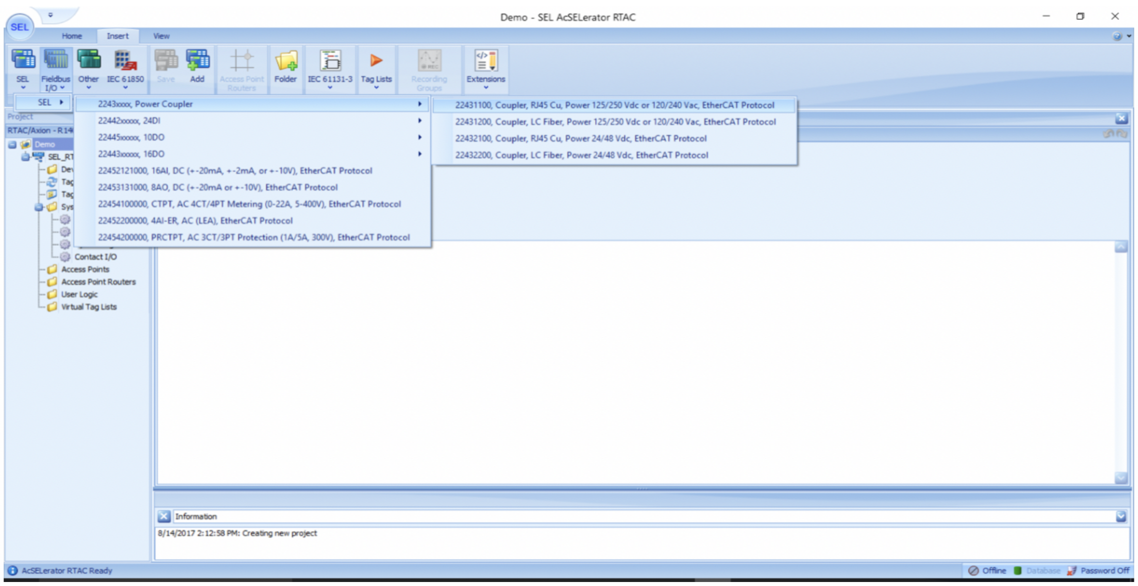

Figure 6.4: Adding power coupler step-1

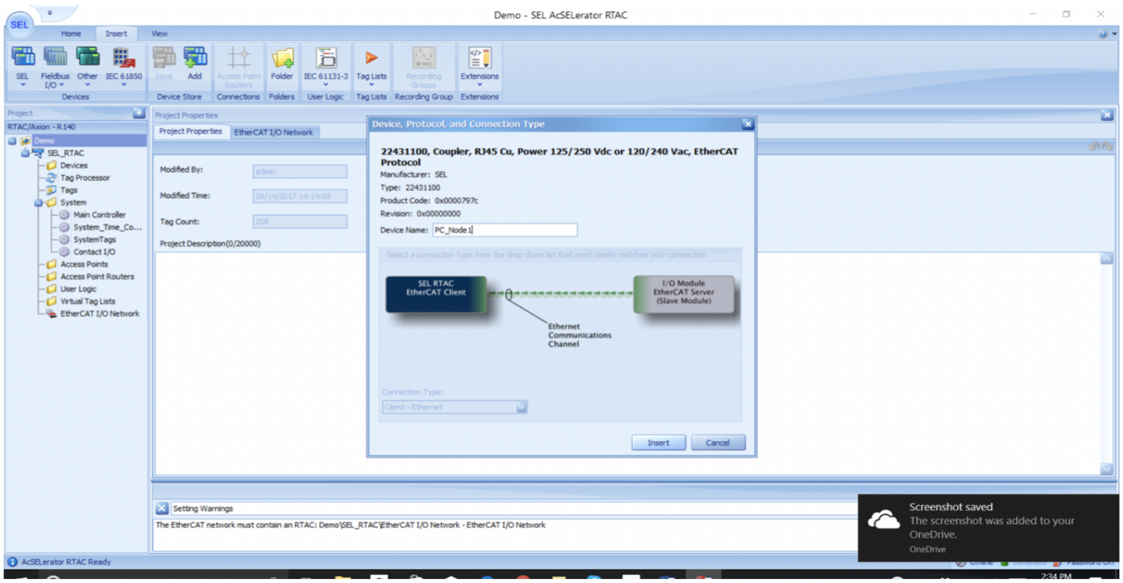

Figure 6.5: Adding power coupler step-2

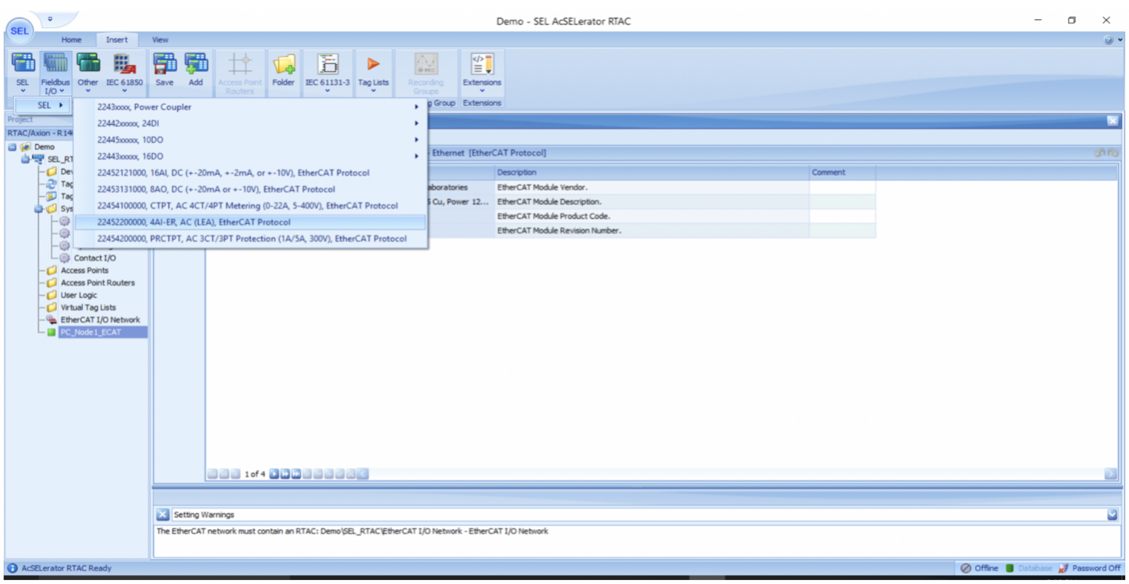

Figure 6.6: Adding analog input modules step-1

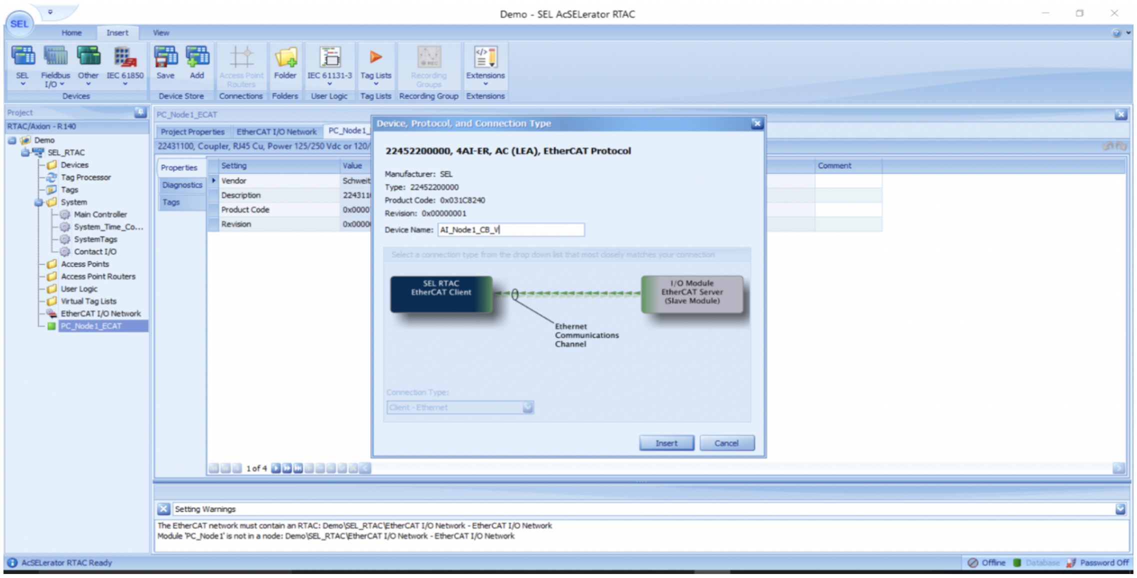

Figure 6.7: Adding analog input module step-2

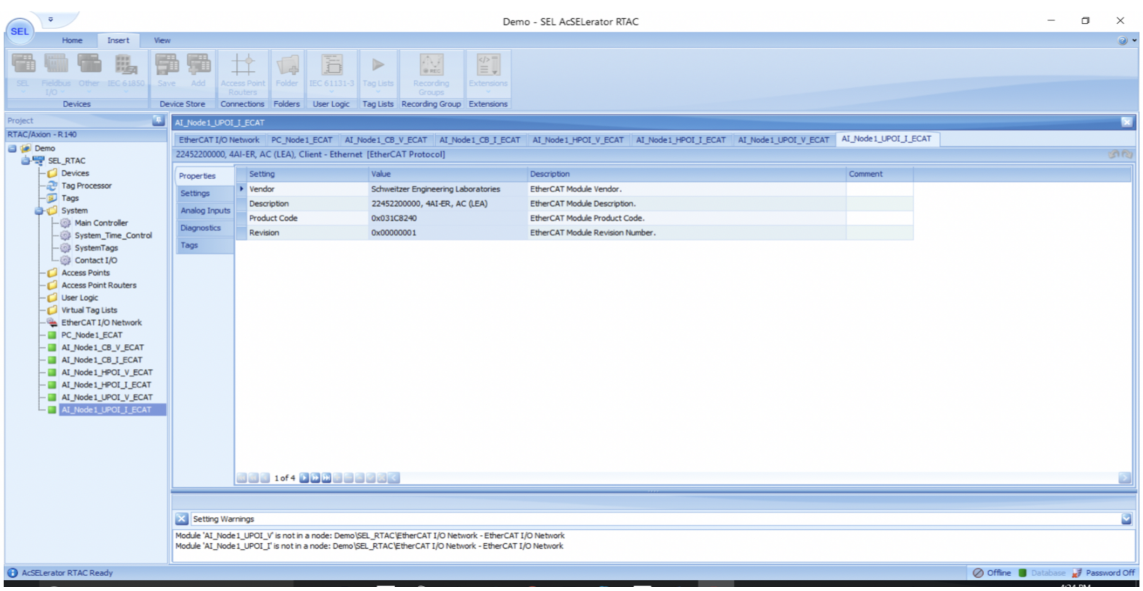

Figure 6.8: Project visualization after adding all analog input modules at node-1

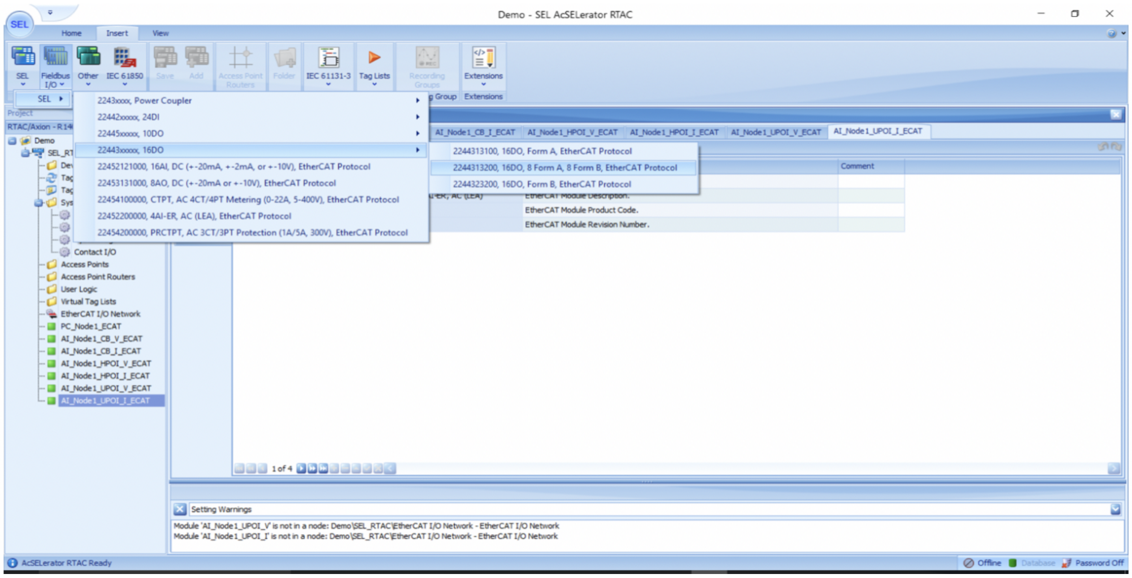

Figure 6.9: Adding DO module step-1

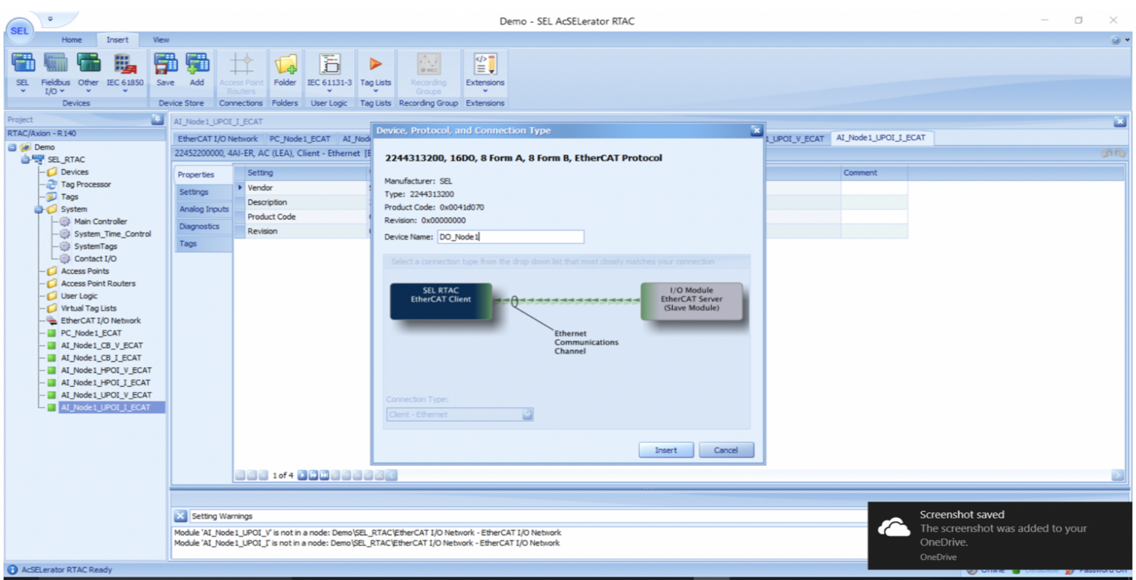

Figure 6.10: Adding DO module step-2

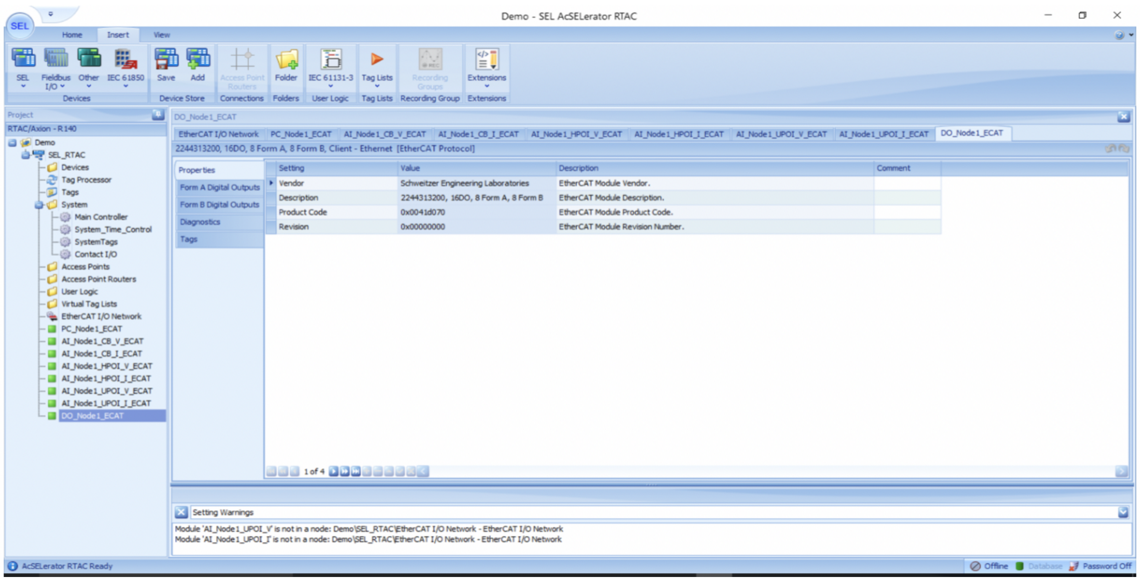

Figure 6.11: Project visualization after adding DO at node-1

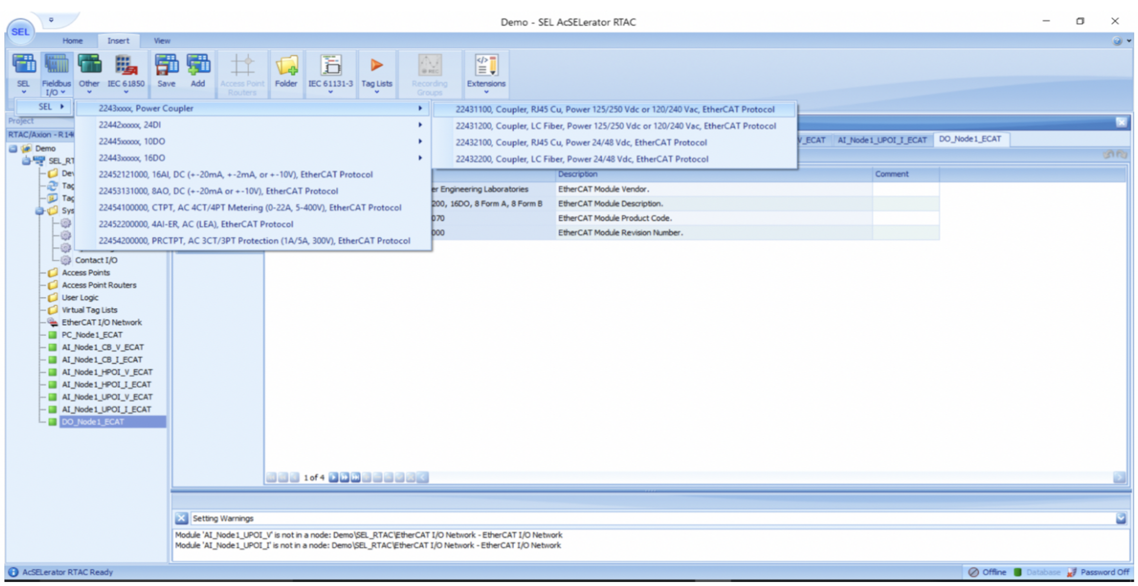

Figure 6.12: Adding power coupler at node-2 step-1

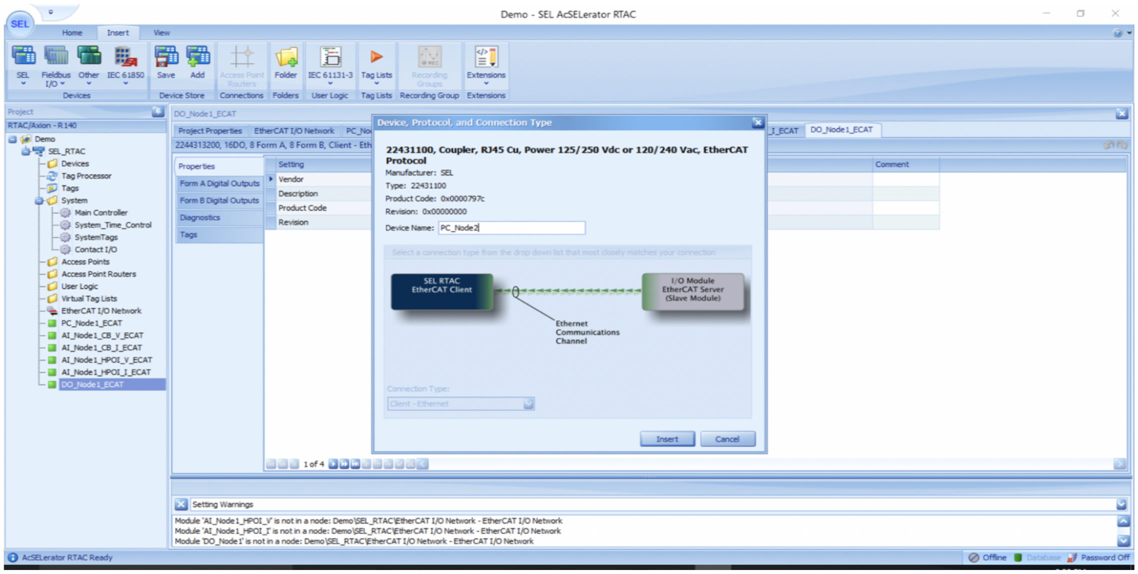

Figure 6.13: Adding power coupler at node-2 step-2

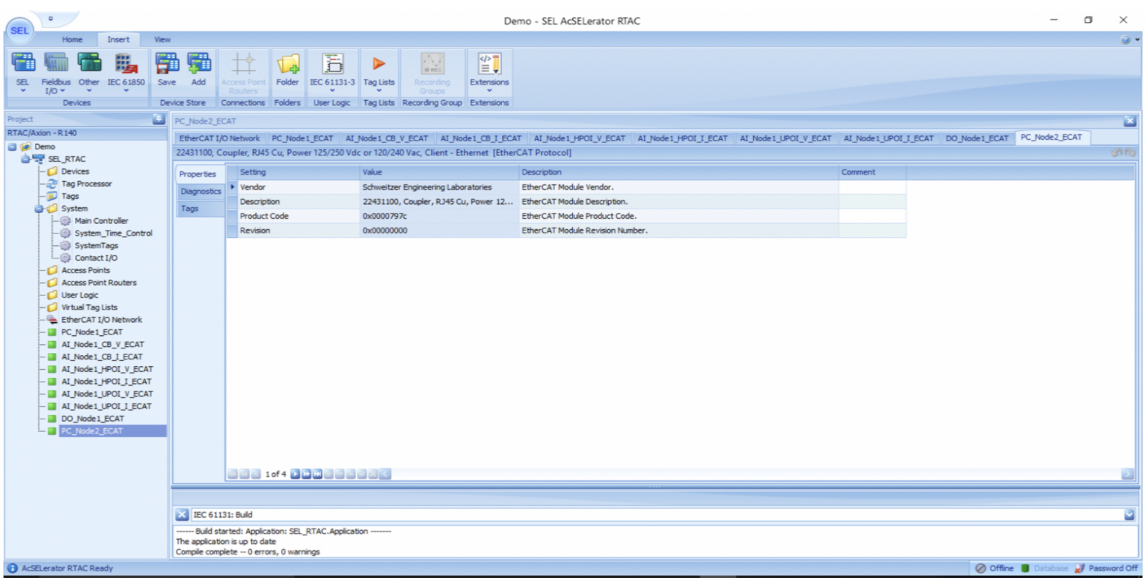

Figure 6.14: Project visualization after adding power coupler at node-2

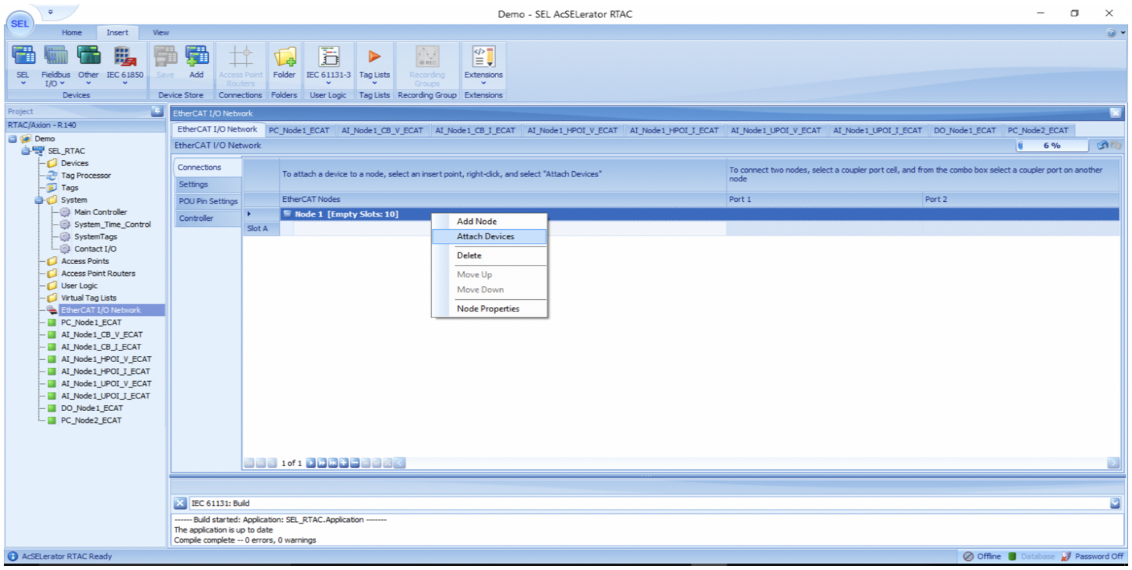

Figure 6.15: Selecting node-1 modules

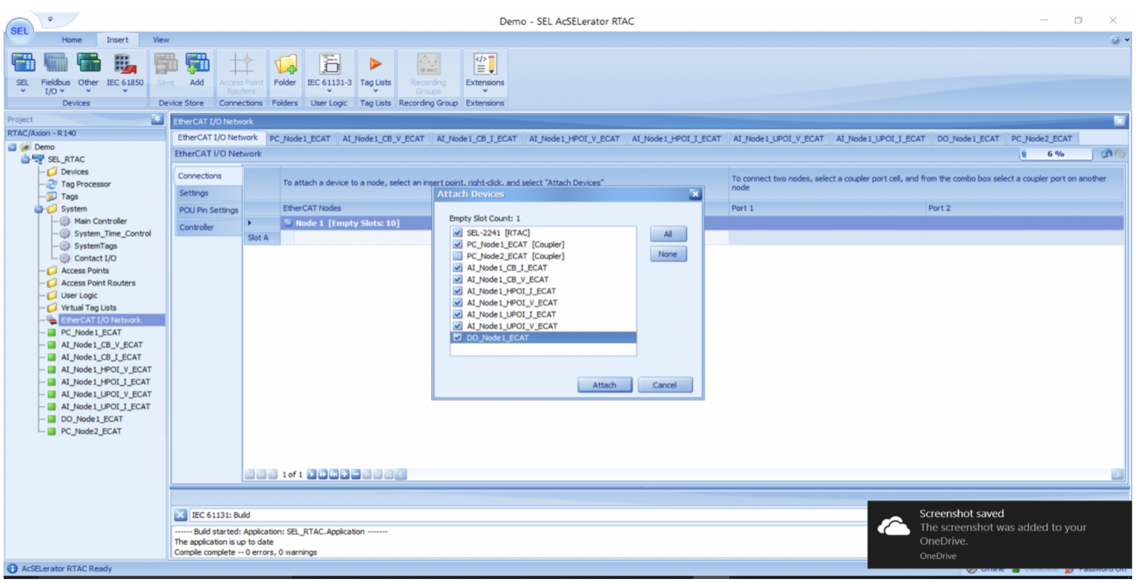

Figure 6.16: Selecting devices to be connected at node-1

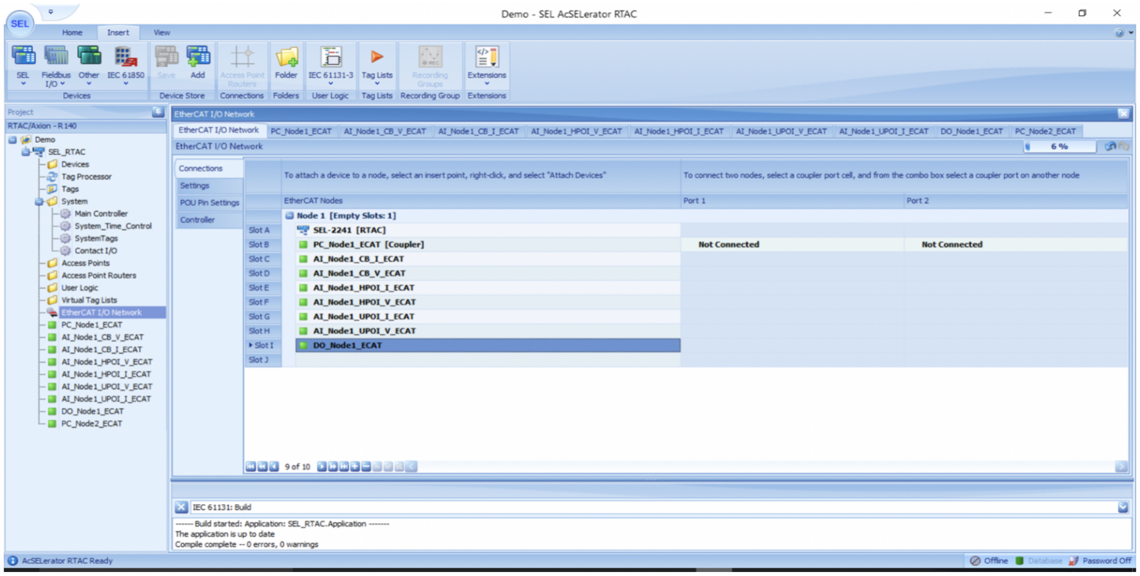

Figure 6.17: Project visualization after attaching node-1 modules

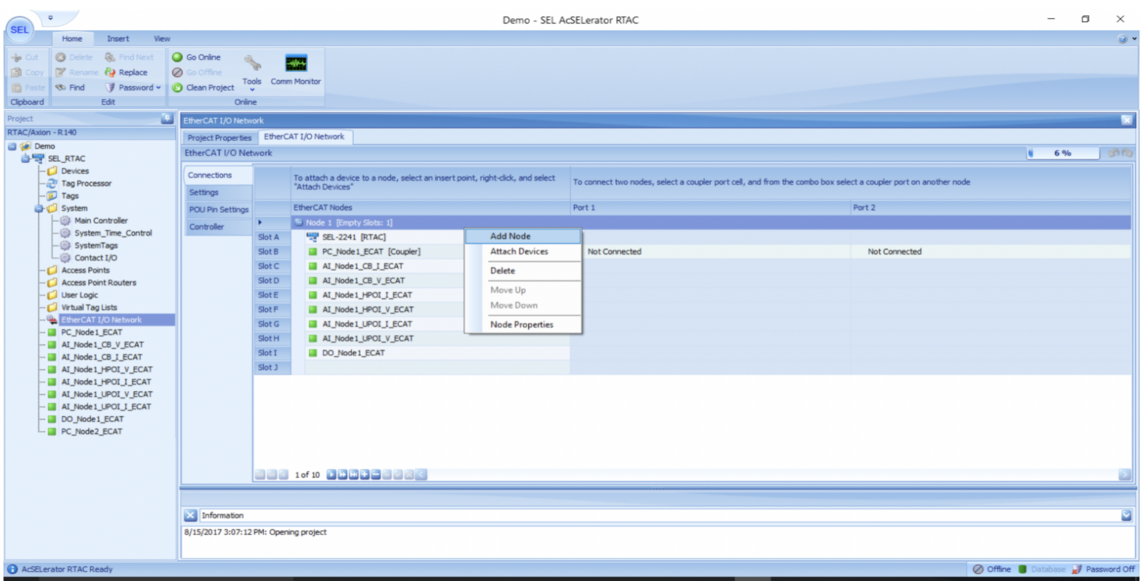

Figure 6.18: Adding another node: step-1

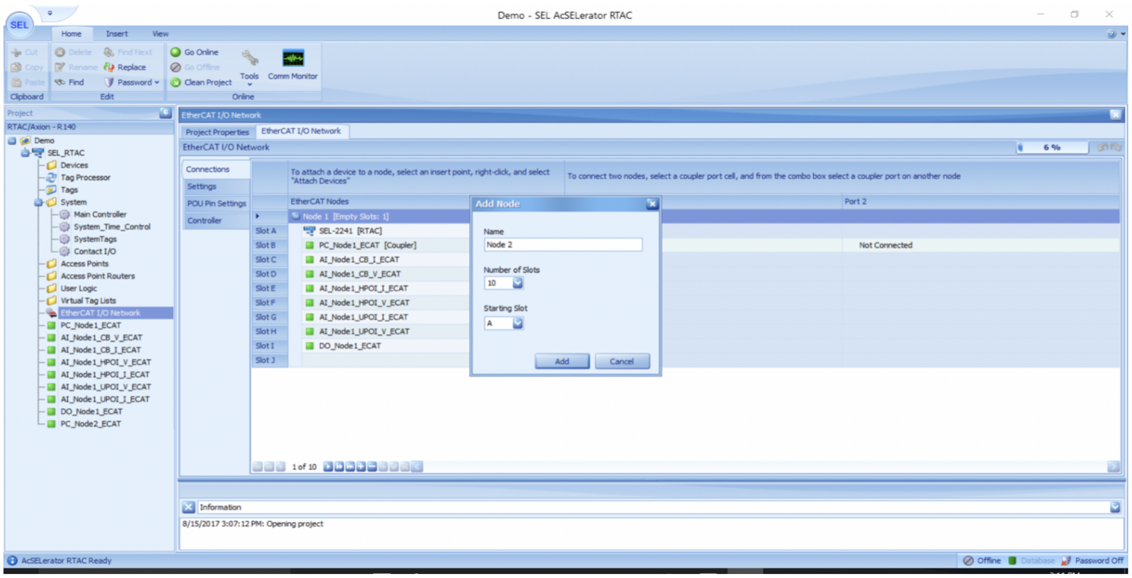

Figure 6.19: Adding another node step-2

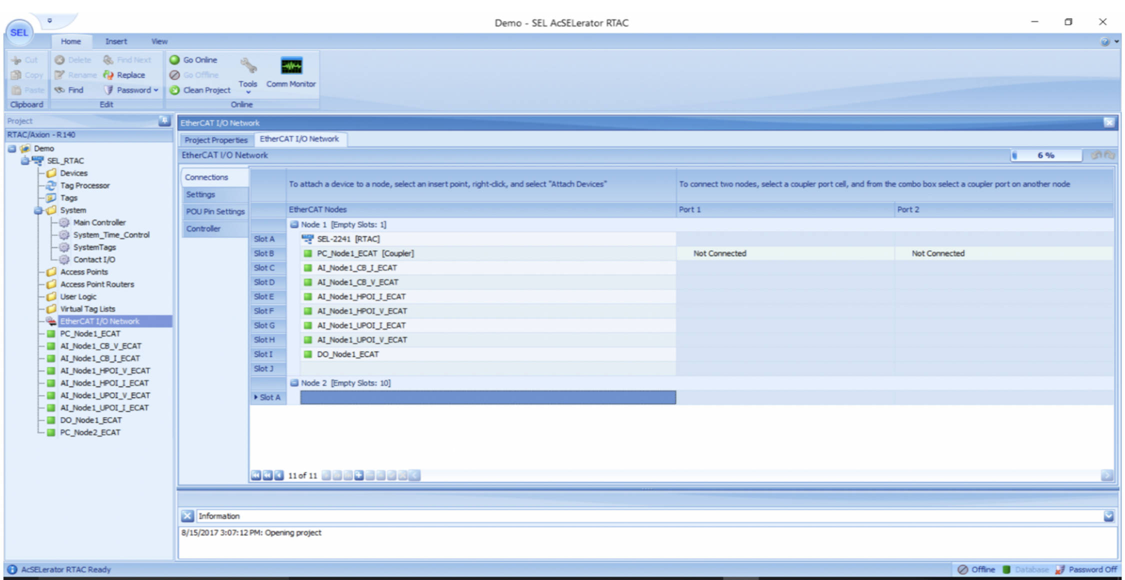

Figure 6.20: Project after adding node

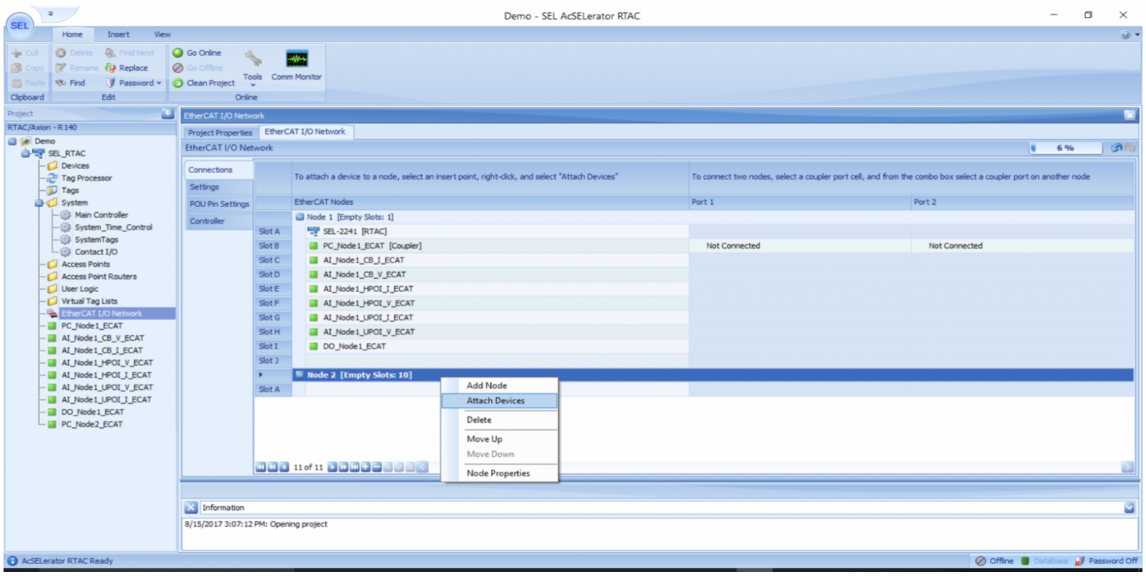

Figure 6.21: Adding power coupler in node-2 step-1

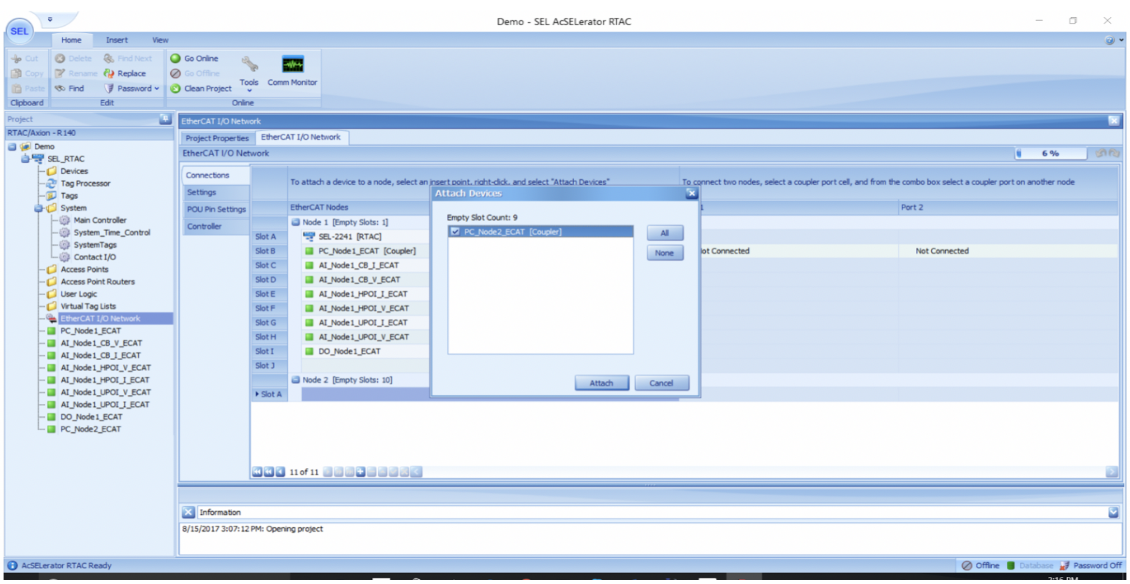

Figure 6.22: Adding power coupler in node-2 step-2

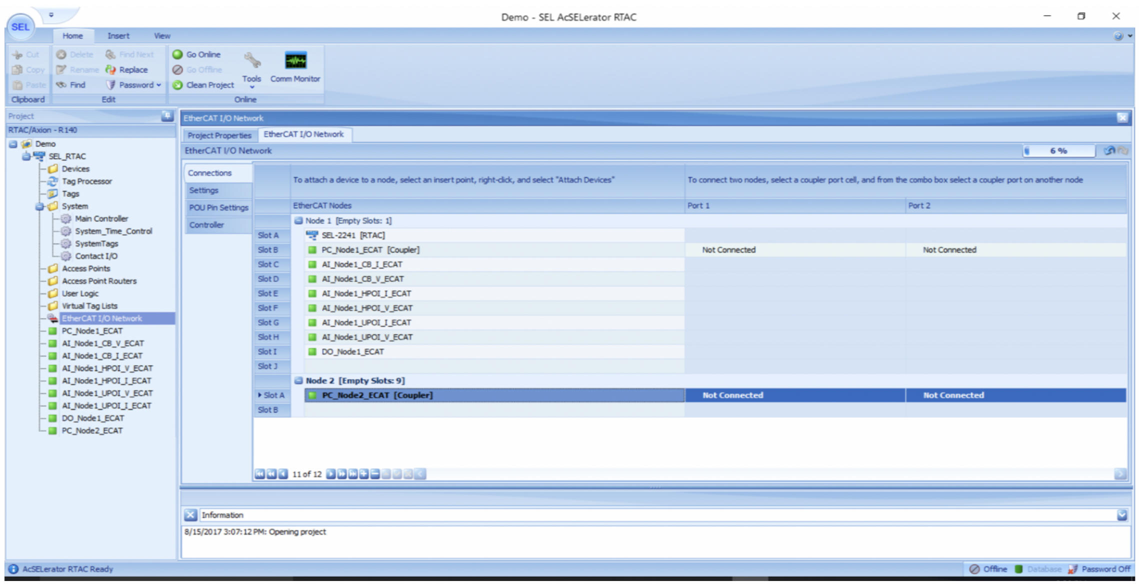

Figure 6.23: Project visualization after adding power coupler in node-2

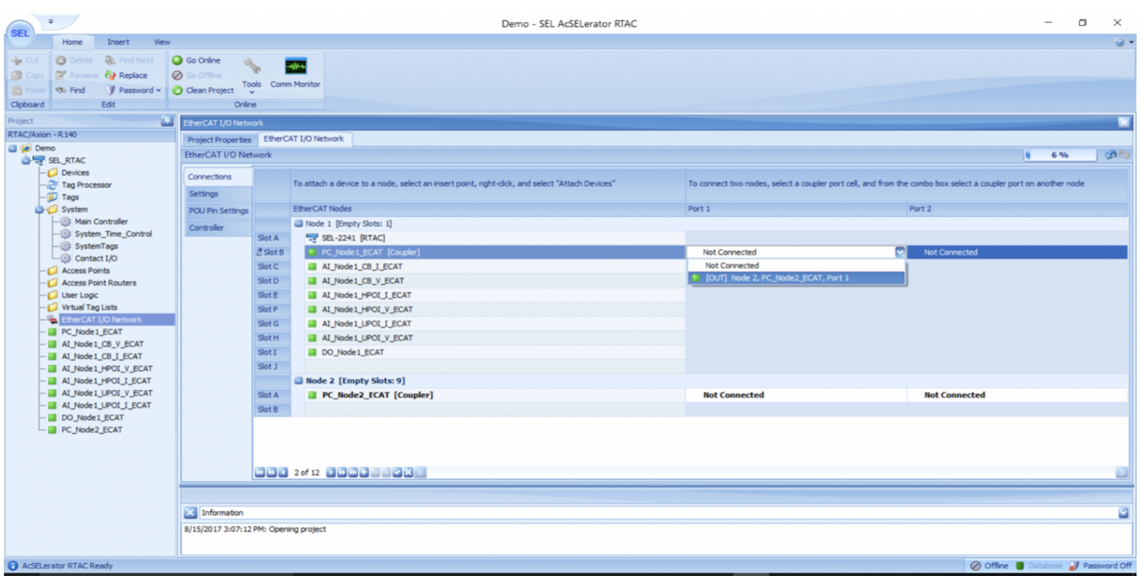

Figure 6.24: Selecting the options in pop-up menu to connect power couplers

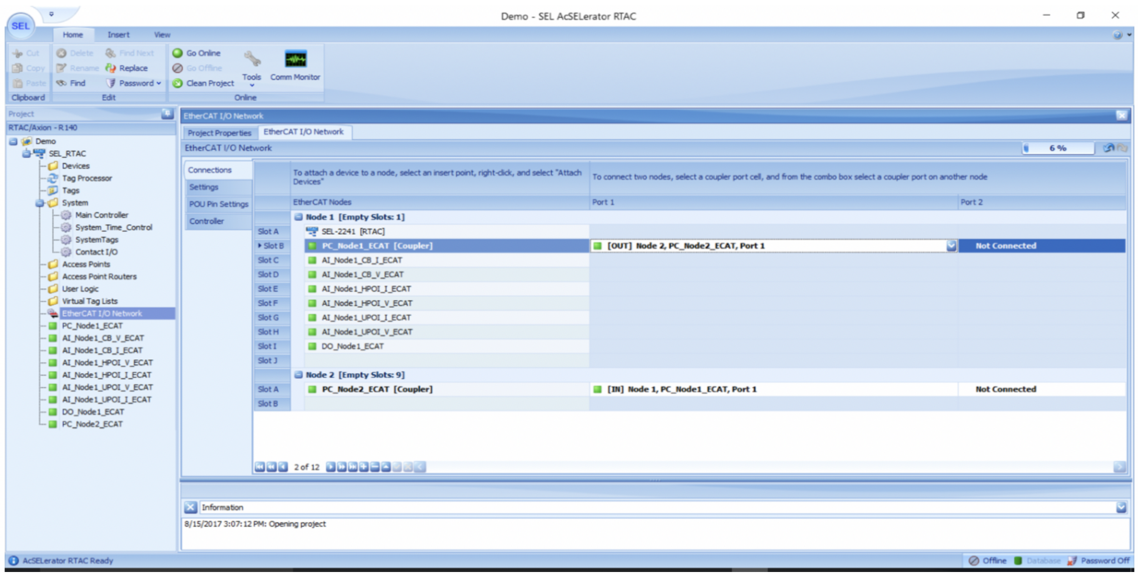

Figure 6.25: Project visualization after linking power couplers

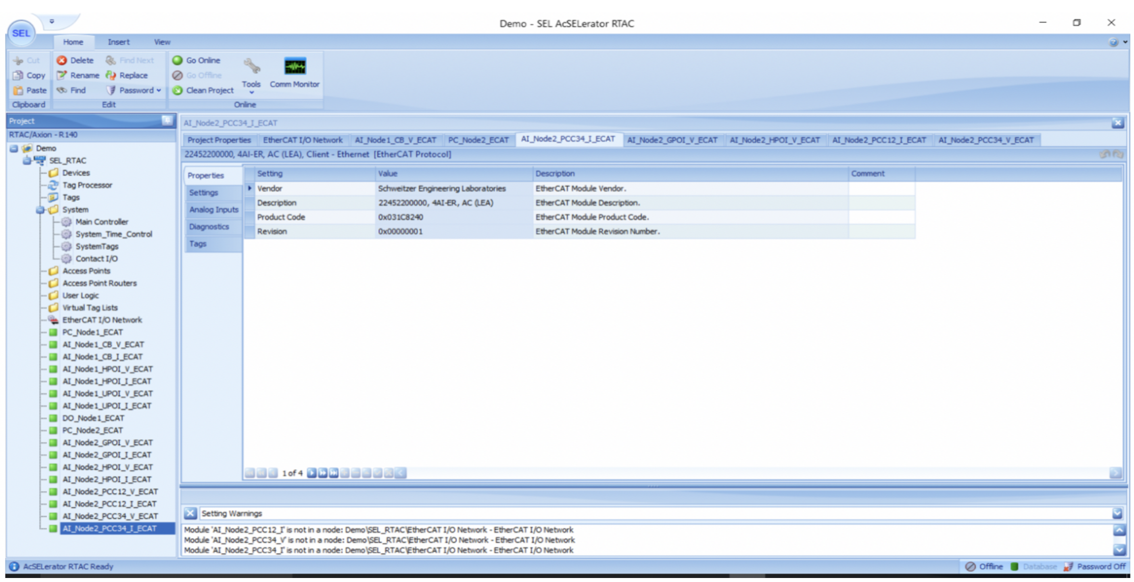

Figure 6.26: Project visualization after adding all analog modules in node-2

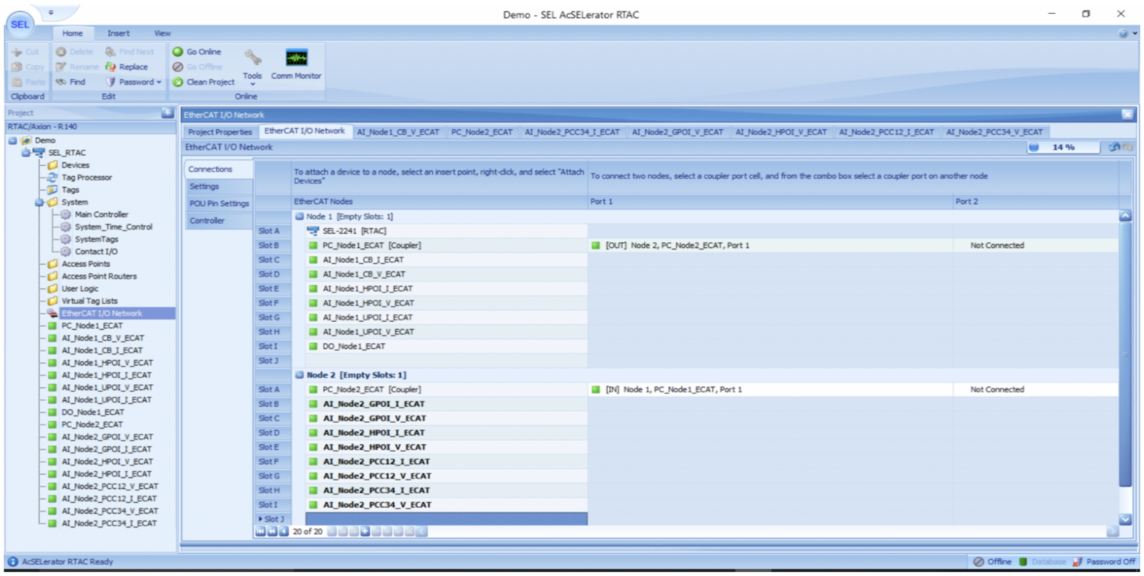

Figure 6.27: Attaching modules in node-2

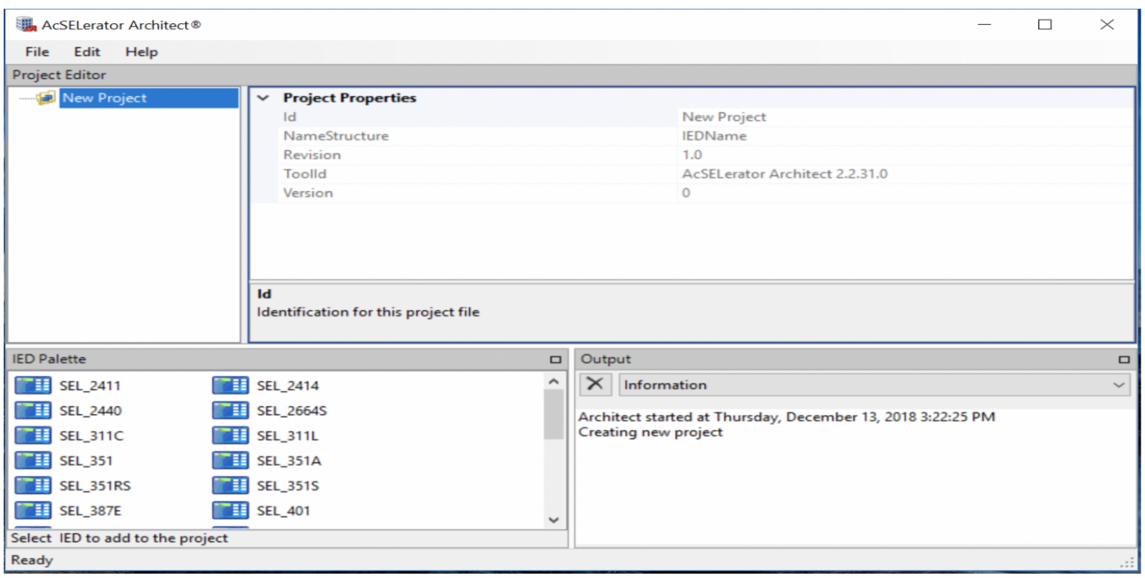

Figure 6.28: Opening SEL Architect

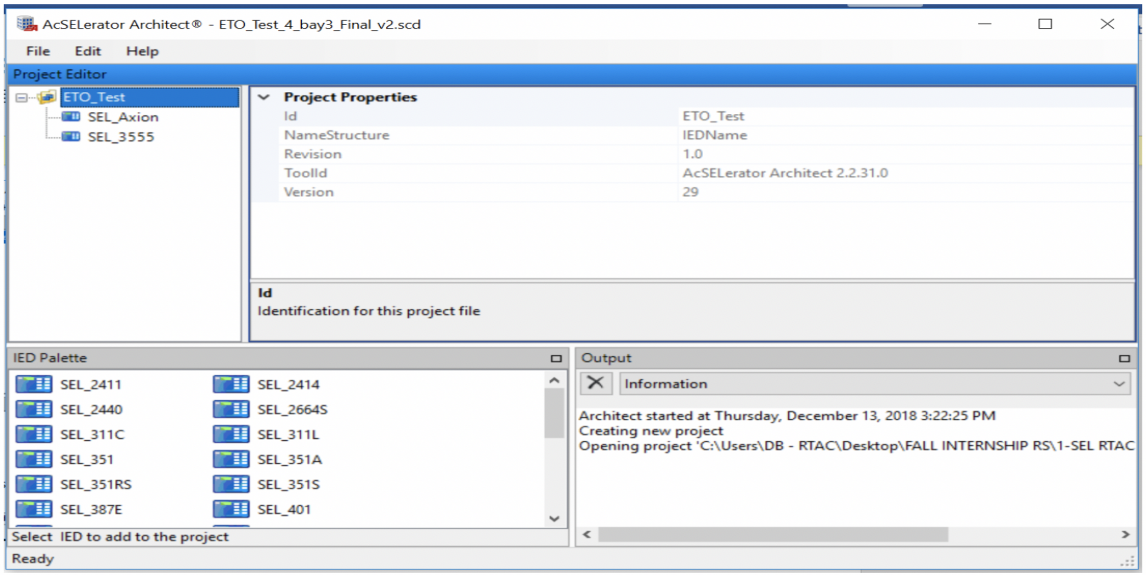

Figure 6.29: Adding IED's for respective data communication

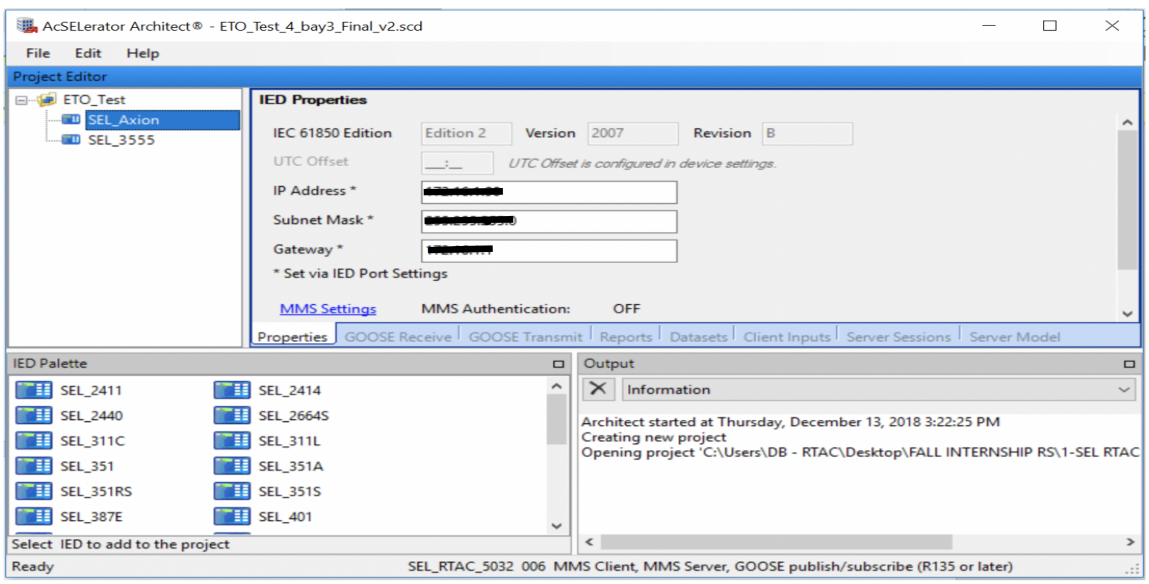

Figure 6.30: Entering data for IED's

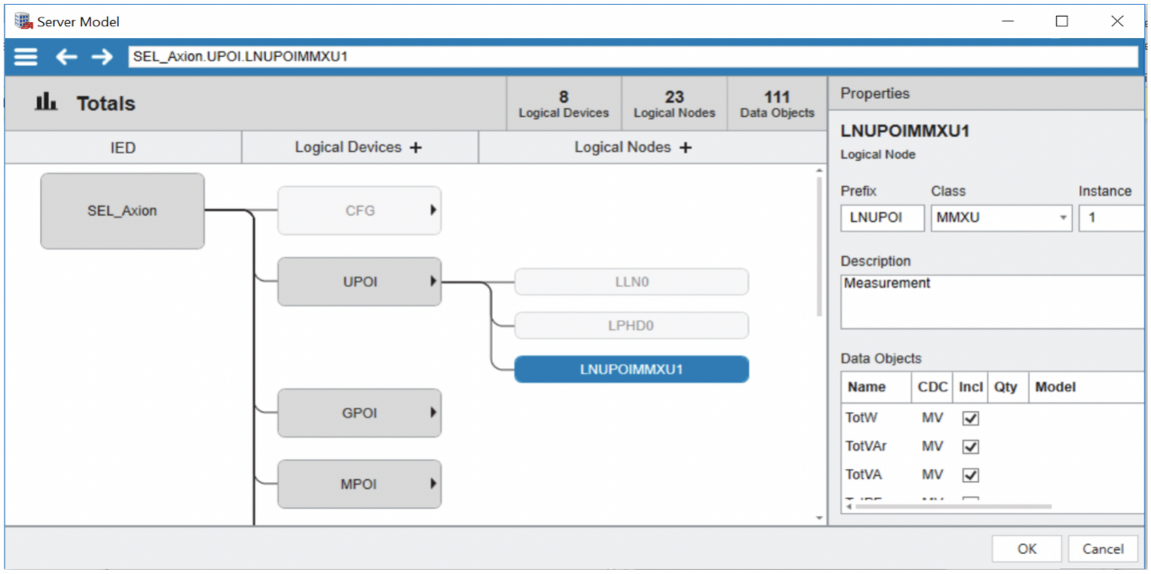

Figure 6.31: Creating Logical Nodes with MMXU

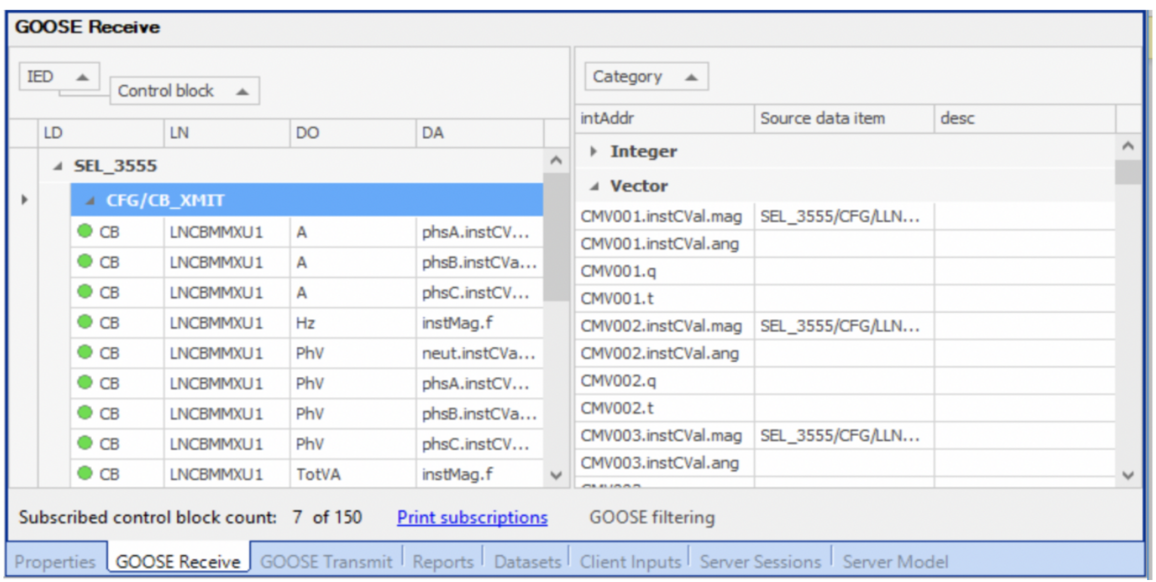

Figure 6.32: Receiving Dataset

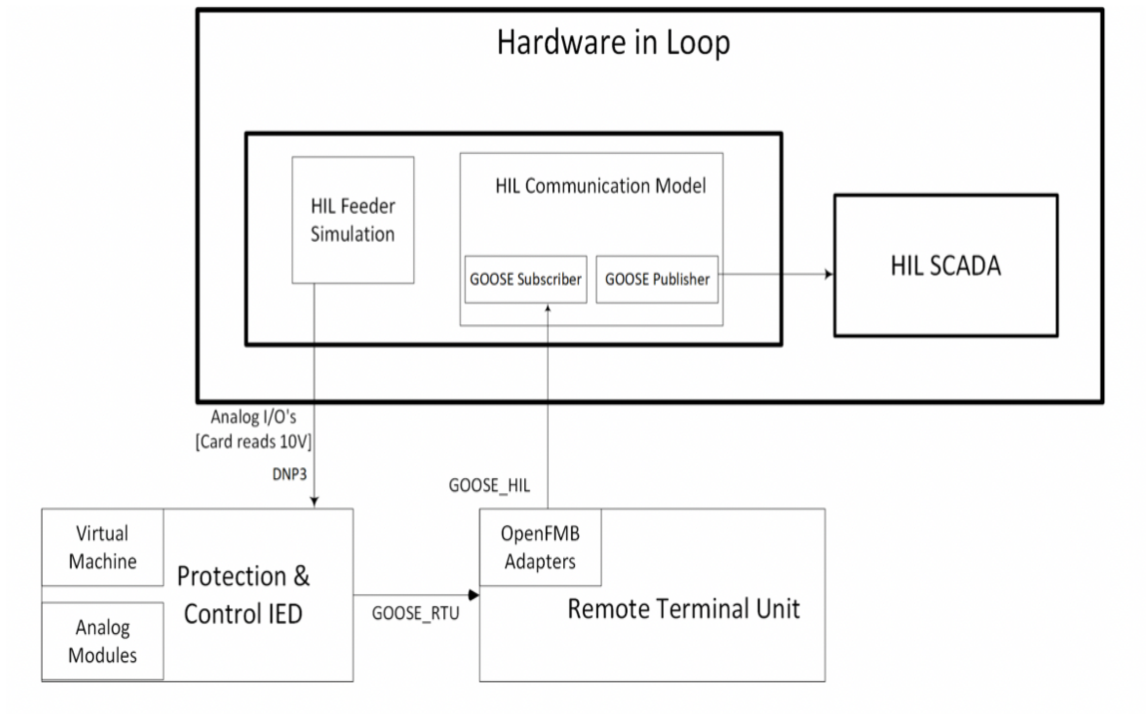

Figure 6.33: Proposed Process Flow

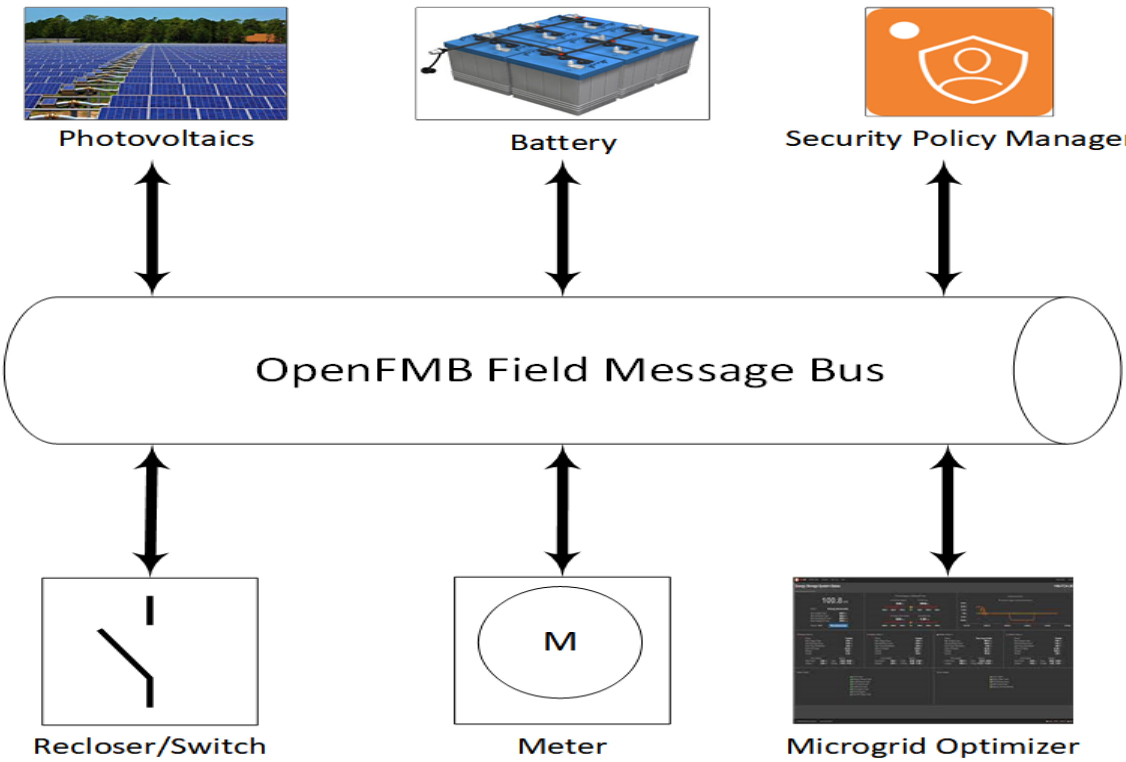

Figure 6.34: OpenFMB Federated Deterministic Exchanges[32]

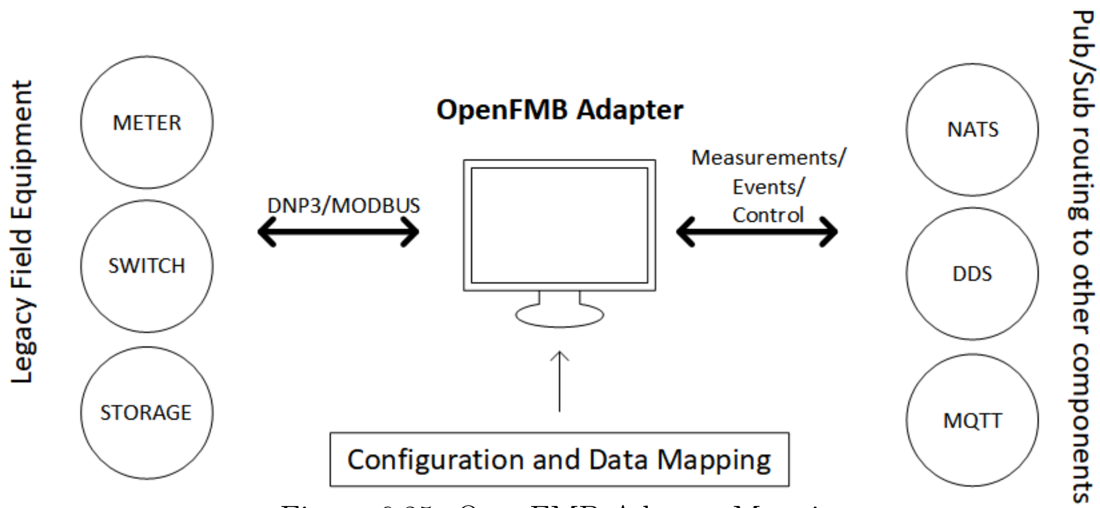

Figure 6.35: OpenFMB Adapter Mapping

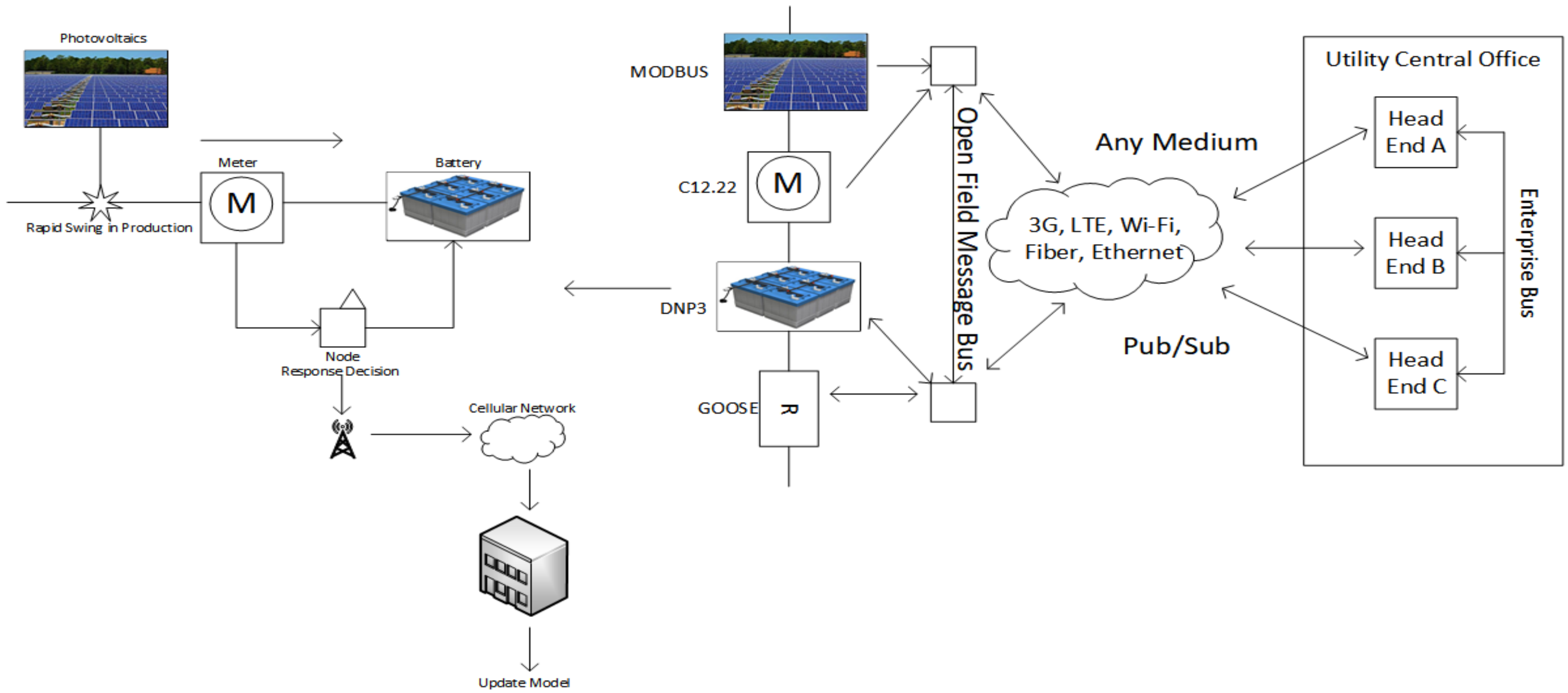

Figure 6.36: Unlocking Data with OpenFMB

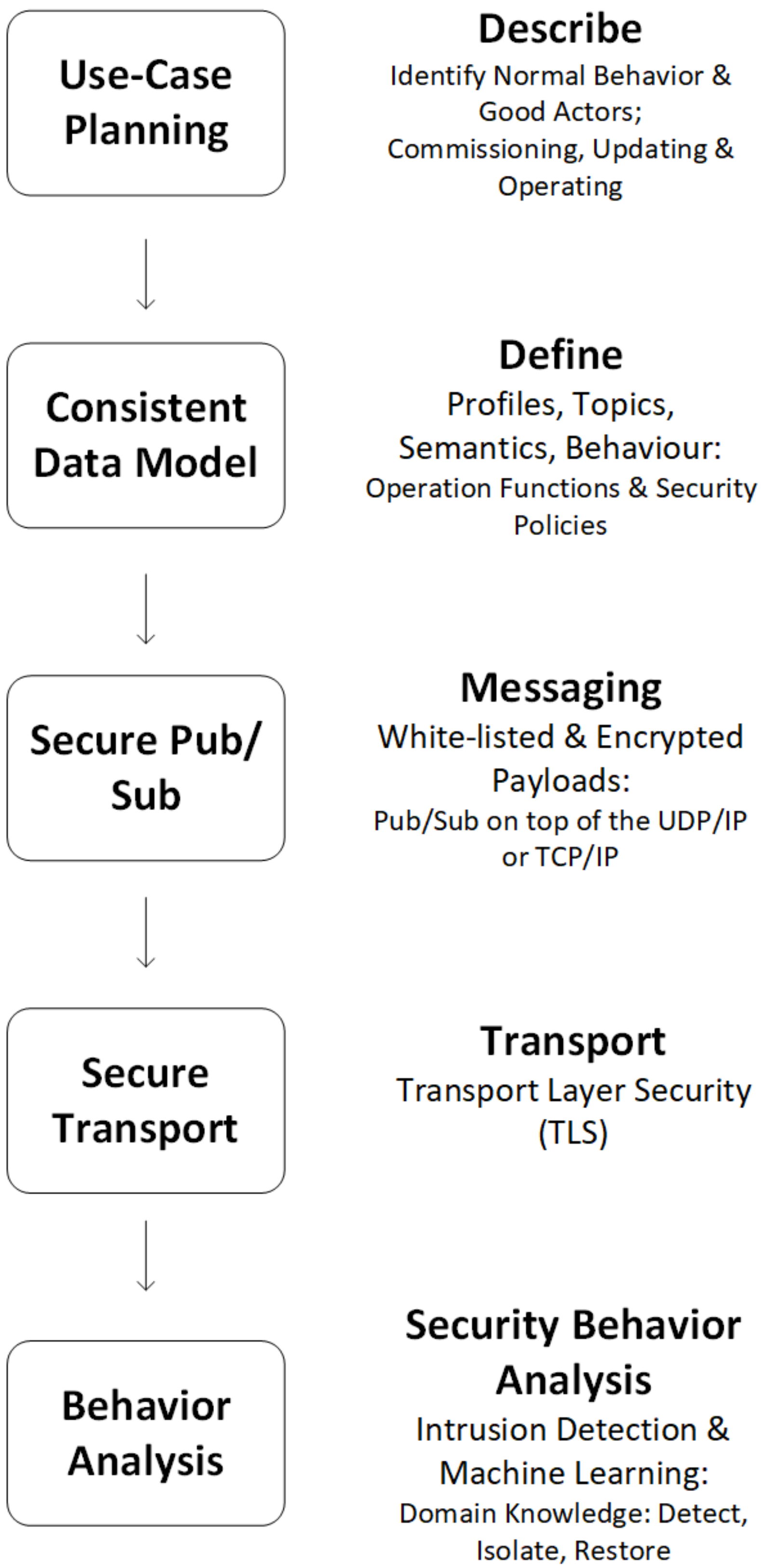

Figure 6.37: OpenFMB Security Analytic Framework

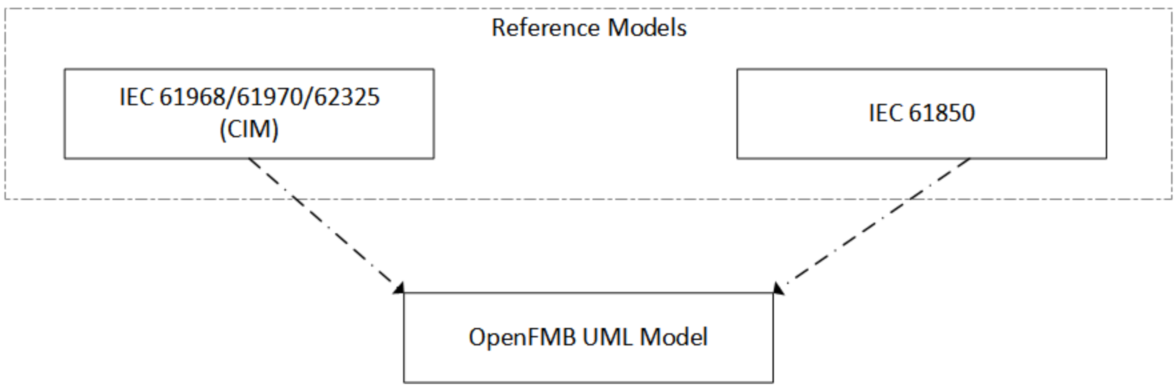

Figure 6.38: Harmonization amongst reference models

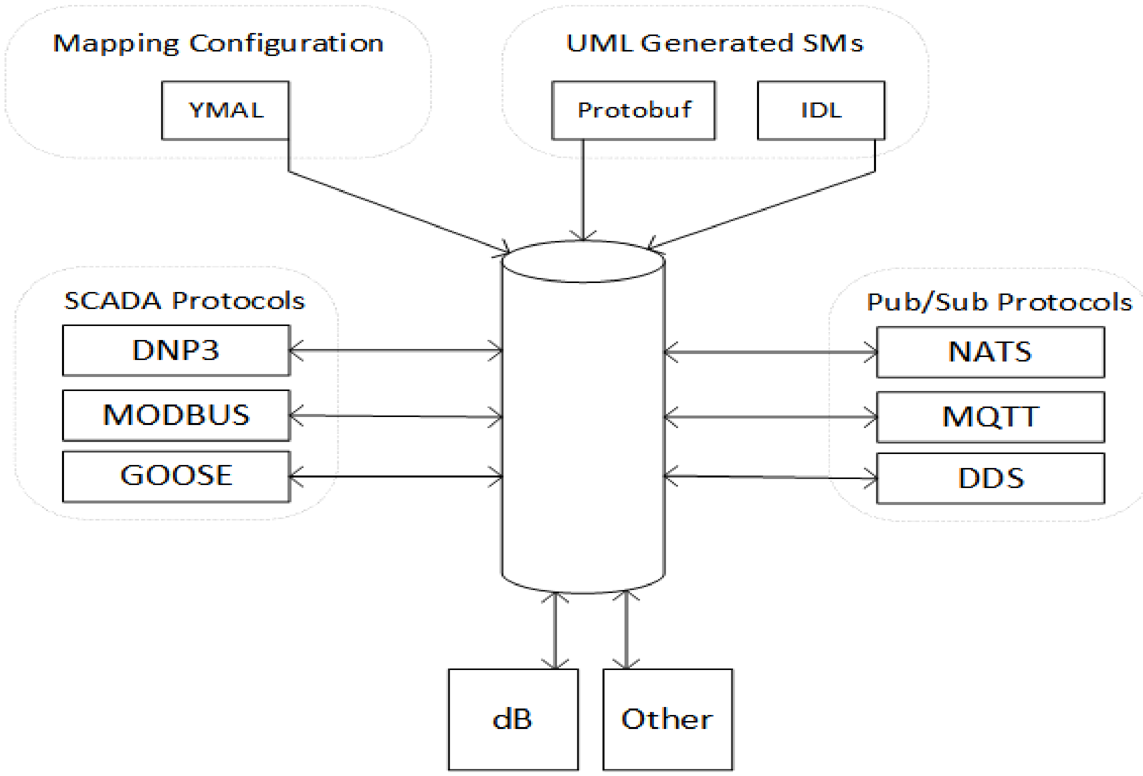

Figure 6.39: Protocol Transition: OpenFMB Adapters

CHAPTER 7: SIMULATION RESULTS

7.1 Introduction

This chapter discusses the various results obtained from simulating the microgrid connected distribution feeder in Typhoon HIL. The simulation is made to run for 256 seconds and is switched between three different modes, namely: Grid Following (connected), Grid Forming (islanded) and Grid-Re synchronization. This chapter will discuss the validation of the simulation model by verifying the power balance between generation and load. The important fundamentals of various converters will be discussed in detail using the help of observed simulation results. The chapter will demonstrate the latency observed by using the proposed approach and compare it with that of the classical approach.

7.2 Simulation Results - Power Flow Analysis

7.2.1 Battery State of Charge (SOC)

The normal operation of the Battery State of Charge ranges between 20% and 80%. The initial Battery State of Charge (SOC) is kept as 80%. During grid following mode, the SOC operates at approximately 82%. It can be deduced that after reaching 82% SOC, the battery is not much used for serving the loads and hence operated near around 82% SOC.

During the grid forming mode, i.e., when the microgrid acts as a separate unit, the two loads connected to the microgrid are served by the battery and the PV. There are a lot of disturbances in Battery SOC observed during the islanded mode. PV and battery provide power to the two loads connected in the microgrid. Since these two loads are not constant, the result of charging/discharging of the battery produces the spikes in the SOC as observed.

7.2.2 Load Power observed during the three modes of microgrid

There are nine loads connected on the distribution feeder. Each load is dynamically varying, i.e., the value of the load power is given through csv file.

The figure shows the power consumed by a single load. To obtain the aggregated value of power consumed by the load, this power is multiplied by 9. The values of these load power are taken from validated CYME model of the electrical utility distribution feeder system.

7.2.3 Substation Power observed during the three modes of microgrid

As expected, the substation at the distribution feeder provides the power to the loads. It can be observed that the substation power follows the same trend as that of the loads. This happens because the substation provides the amount of power required by the connected loads.

7.2.4 Photovoltaic Power observed during the three modes of microgrid

Throughout the simulation, the power output of the PV is controlled at 100 kW. The transition from grid following mode to grid forming mode and then from grid forming to grid Re-synch is observed with increase and decrease in PV power. This is observed because the loads connected on the microgrid are only served during the islanded mode. The sudden demand and loss of these loads affect the PV power. PV inverter act as voltage controlled current sources and cannot form the grid just by themselves.

In order for PV system to be able to be operational, it needs a source of voltage and frequency, which is provided by the power grid. So, the PV system is paired with a suitable DER that can provide the source of voltage/frequency. The PV inverter allow bi-directional power flow. If a battery is integrated on the DC bus of the PV system, then it has the ability to capture the excess of kWh lost throughout the day due to the clipping and early morning/late evening times, and then discharge it later when the feeder is experiencing the peak power consumption, thus effectively enabling the peak-shaving. PV farm acts as a current source inverter and output of the PV inverter is active (P) and reactive power (Q). This control mode does not change regardless of the microgrid's operating mode.

7.2.5 Battery Energy Storage System Power observed during the three modes of microgrid

It can be observed that the Battery Energy Storage System power is tracking the reference power. The battery inverter is a three-phase inverter connected to the battery for power conversion from DC-AC and vice-versa. The power command reference dictates whether the batter is charging or discharging (depending on the direction in which the measuring devices are connected).

If current is entering the Battery then it is charging, and it is discharging if the current is leaving the battery. The battery inverter can operate in two modes: current source inverter (CSI) mode and voltage source inverter (VSI) mode. The inverter has four modes:

1. CSI: Represented as voltage controlled current source with high current impedance source to the grid. To get a quick current output response, the user inputs active power (P) and reactive power (Q) reference points.

2. VSI-PQ: Similar to CSI mode, represented by high current impedance but low voltage impedance, this mode is also a voltage controlled current source but outputs relatively slower current response than CSI mode.

3. VSI-V/f: This mode regulates the voltage and frequency at the inverter AC terminals based on the voltage and frequency user defined set-points. The inverter response is defined based on the droop control for both voltage and frequency. This mode is typically used in islanded operation when the DER

with the inverter is not the largest unit used for forming the grid and is rather used for operation in parallel with other DERs.

4. VSI-ISO: This mode regulates both voltage and frequency at the inverter AC terminals. The set-points do not include any droop levels i.e. both voltage and frequency droops are zero.

The BESS inverter provides or absorbs the real power in order to support the grid frequency and also provides the reactive power to support the grid voltage. BESS maintains the power at Point of Common Coupling.

7.2.6 Power Flow Analysis

It can be deduced from Figure 7.2, 7.3, 7.4, 7.5 that the grid, PV and BESS are generating the amount of power that is required by the loads connected on the distribution feeder. The table shows the exact kW generated by the grid, PV and BESS and demonstrates the power sharing between generation and load. Mathematically, to serve a load of 1544.4kW, At t = 30.5sec the photovoltaic system in combination

Table 7.1: Test Case-1

Component	Substation	PV	BESS	Load
Power (kW)	1452.35	100.0016	1.519	171.6 X 9 = 1544.4

with Battery Energy Storage System can provide an approximate power of 102kW and remaining power is provided by the main utility grid. The PV and BESS are designed such that it can provide required power to the loads inside the microgrid. Throughout the simulation, the power output of the PV is controlled at 100kW and the profile of substation power and load varies almost proportionally with little input from the battery energy storage system.

7.2.7 Current through Way 1

Before simulating the model, the status of switches is as follows: Way 1= Close, Way 2 = Close, Way 3 = Open and Way 4 = Close. As soon as the microgrid controller detects that the frequency and voltage between battery inverter and the grid is out of the range: 59.3Hz$<$f$<$60.5 Hz and 0.88$<$Vpu$<$1.1 respectively, the switchgear operates by opening Way 1 and closing Way 3. During grid forming mode, the Way1 switch of the 4-way switch opens and this can be verified by observing the zero current verifying that microgrid is islanded from the distribution feeder.

7.2.8 Frequency (pu) observed during the three modes of microgrid

Frequency is one of the most important factors for the switch from grid connected to grid forming mode. As observed from the figure, as soon as the frequency goes out of the set limits, the microgrid islands itself. The instant when the frequency is no longer under frequency lock, i.e., (Δf $>$ 0.15), where Δf is the difference in the inverter frequency and the frequency.

7.2.9 Virtual HIL vs Controller HIL

It may be observed from the Figure 7.8 that virtual-HIL (vHIL) lacks the intrinsic details that controller-HIL (cHIL) is able to provide.

7.3 Simulatin Results: Classical vs Proposed Approach

The figure represents the voltage at the substation from proposed approach when compared to the traditional centralized system. The voltage at the substation obtained using proposed approach result is 7198V and voltage at the substation obtained using classical approach result is 7193V.

7.4 Latency

HIL SCADA Time Manager offers three time slots: 250ms, 500ms and 1000ms for updating the SCADA system. The Supervisory Control and Data Acquisition (SCADA) system in the simulations is updated every 250ms and can be observed from Figure 7.10.

The substation voltage obtained using classical approach is received in 960us. This can be observed from Figure 7.11 which shows the execution rates for proposed approach (ER0=240us), classical approach (ER1=960us) and the power meters (ER2=120us).

Hence it takes 250ms + 960us = 250.96ms to obtain the result through classical approach. The substation voltage obtained using proposed approach is received in 240us. Hence it takes 250ms + 240us = 250.24ms to obtain the result through proposed approach which is faster than the classical approach.

The latency observed during the simulations demonstrate the faster response and distributed intelligence at the edge provided by Open Field Message Bus.

The above figure demonstrates the OpenFMB message structure pinged when the simulation value transitions from the Protection and Control device to Remote Terminal Unit, passed through the OpenFMB adapters. The values are subscribed from the adapters and then published on to the HIL SCADA. The message highlighted in the above figure verifies that the OpenFMB adapters successfully map the tags from both vendor devices.

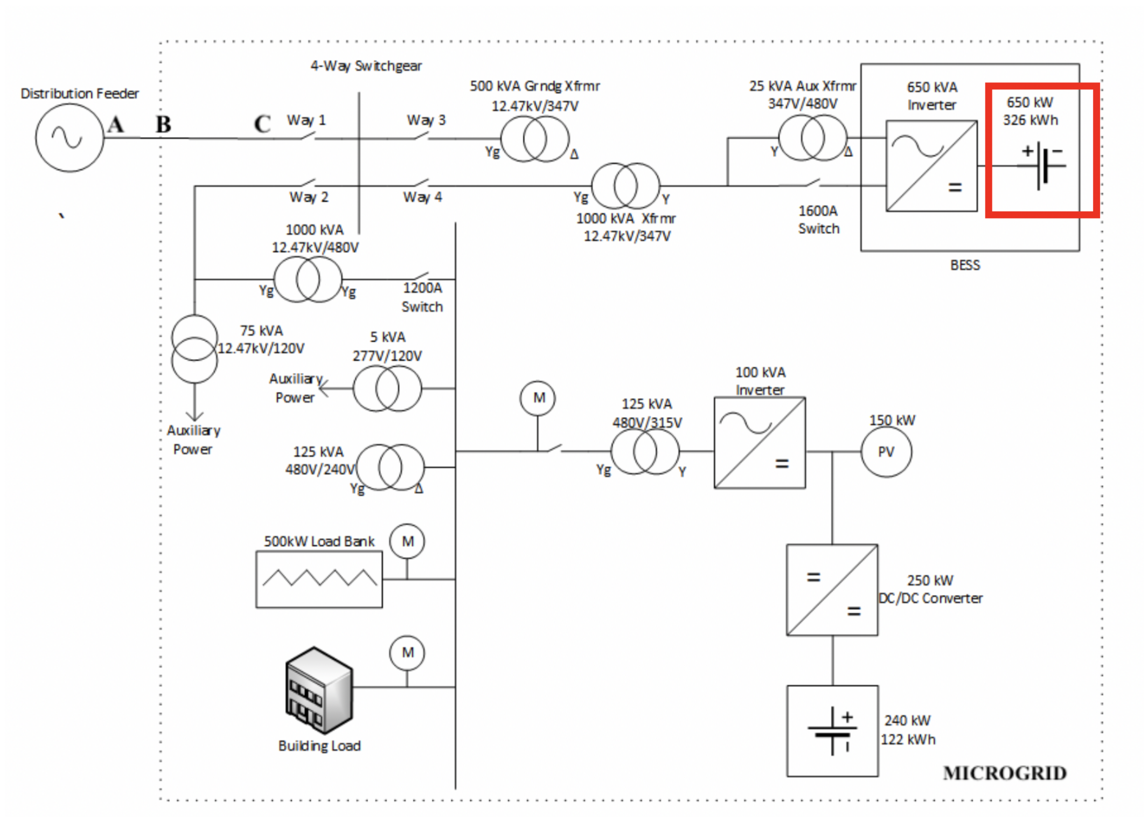

Figure 7.1: Simulation Diagram of Microgrid highlighting the battery

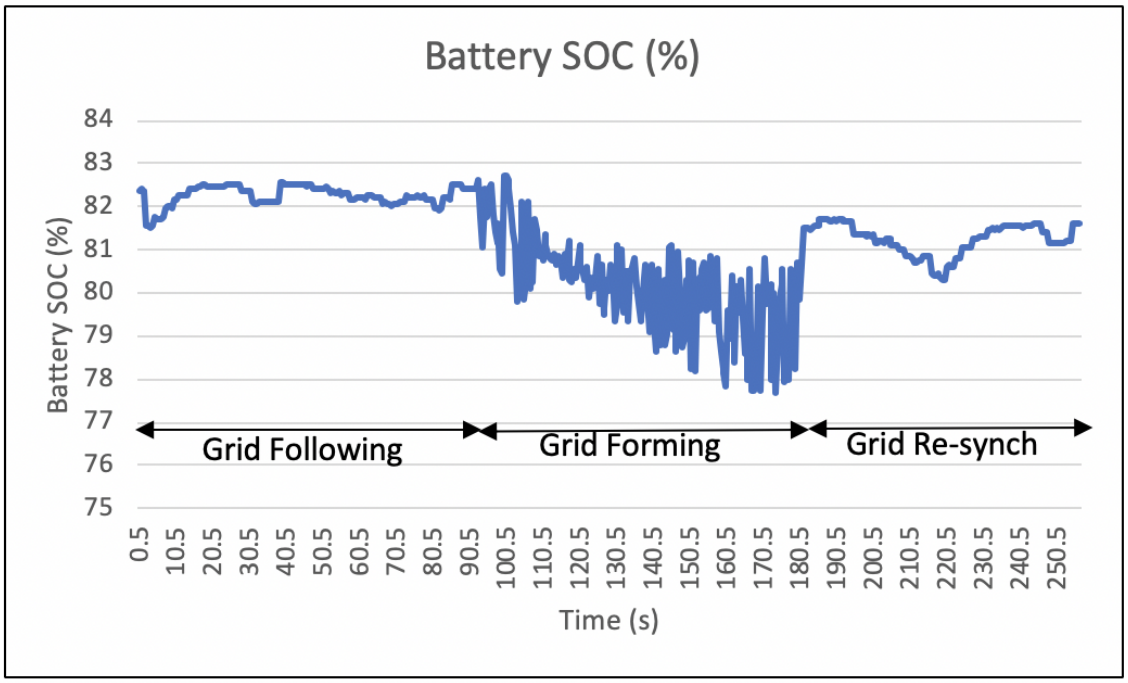

Figure 7.2: Battery State of Charge

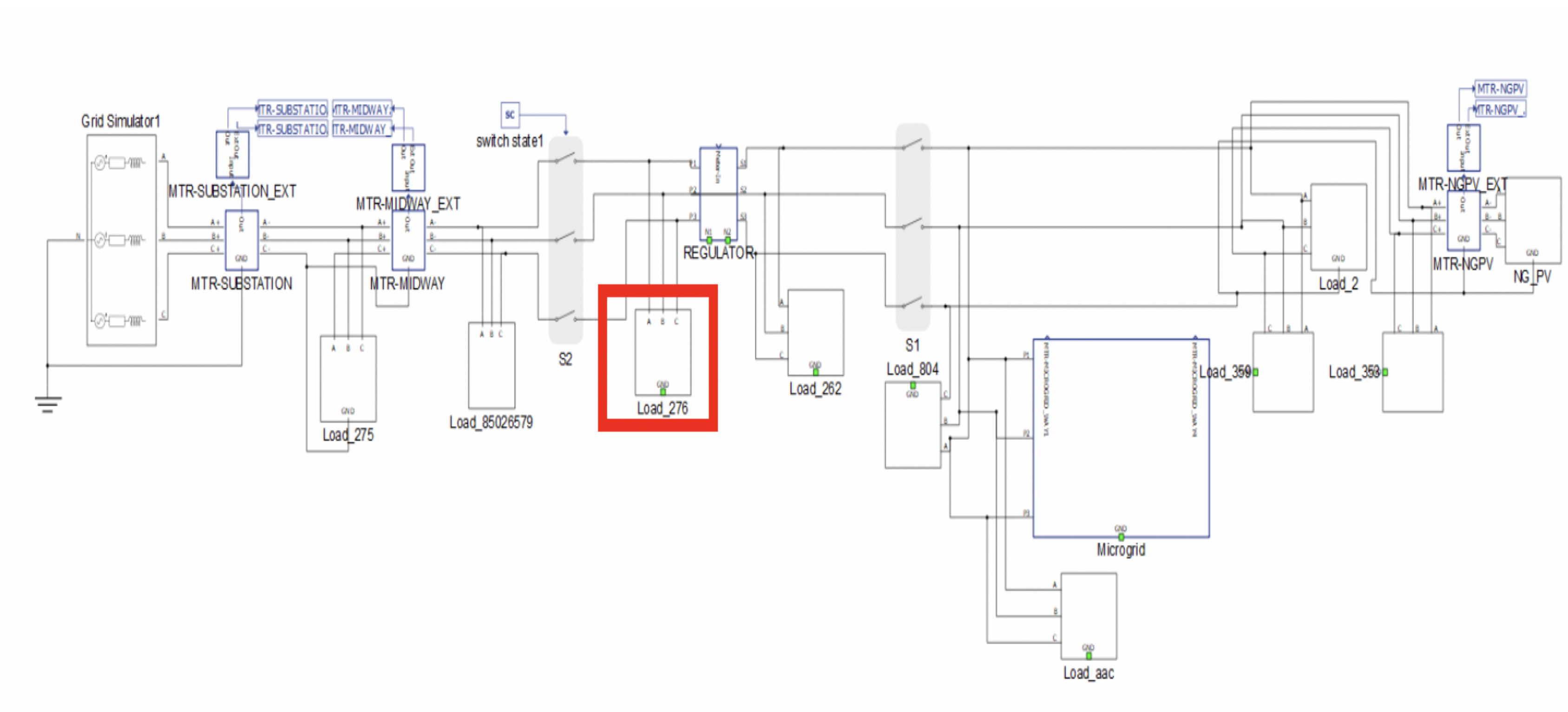

Figure 7.3: Simulation Diagram of feeder model highlighting the load

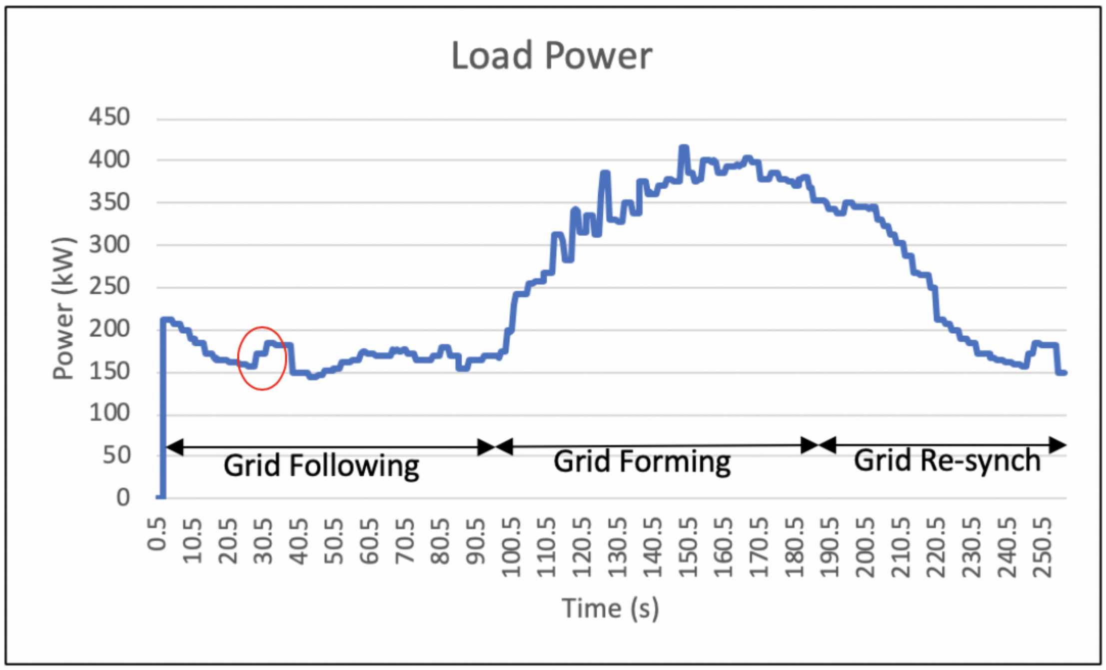

Figure 7.4: Load Power observed during the three modes of microgrid

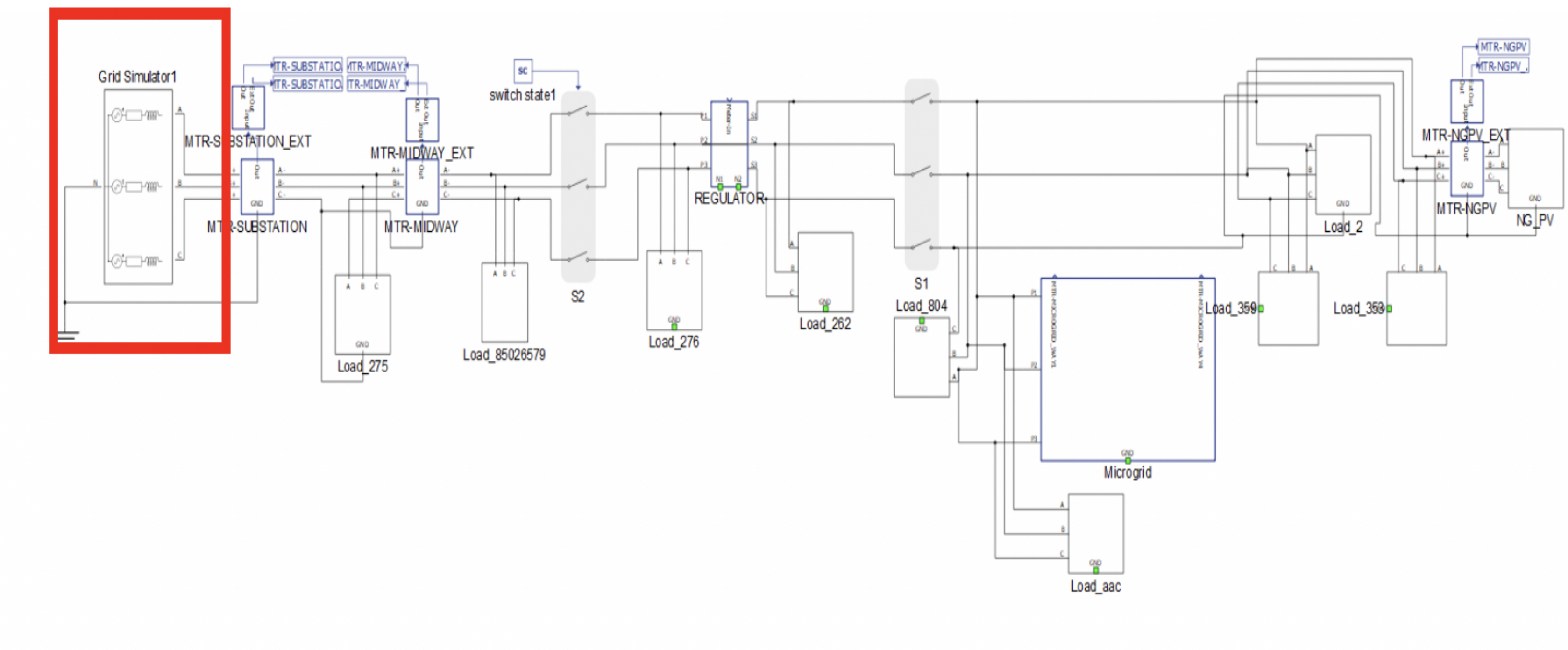

Figure 7.5: Simulation Diagram of feeder model highlighting the electrical utility grid

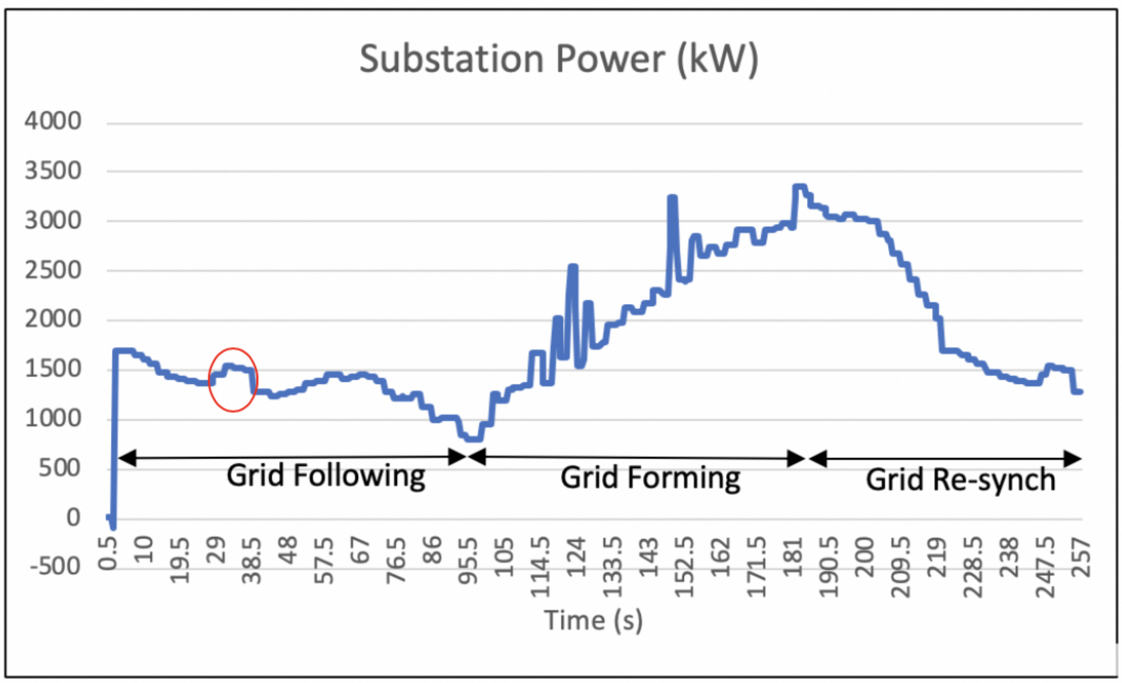

Figure 7.6: Substation Power observed during the three modes of microgrid

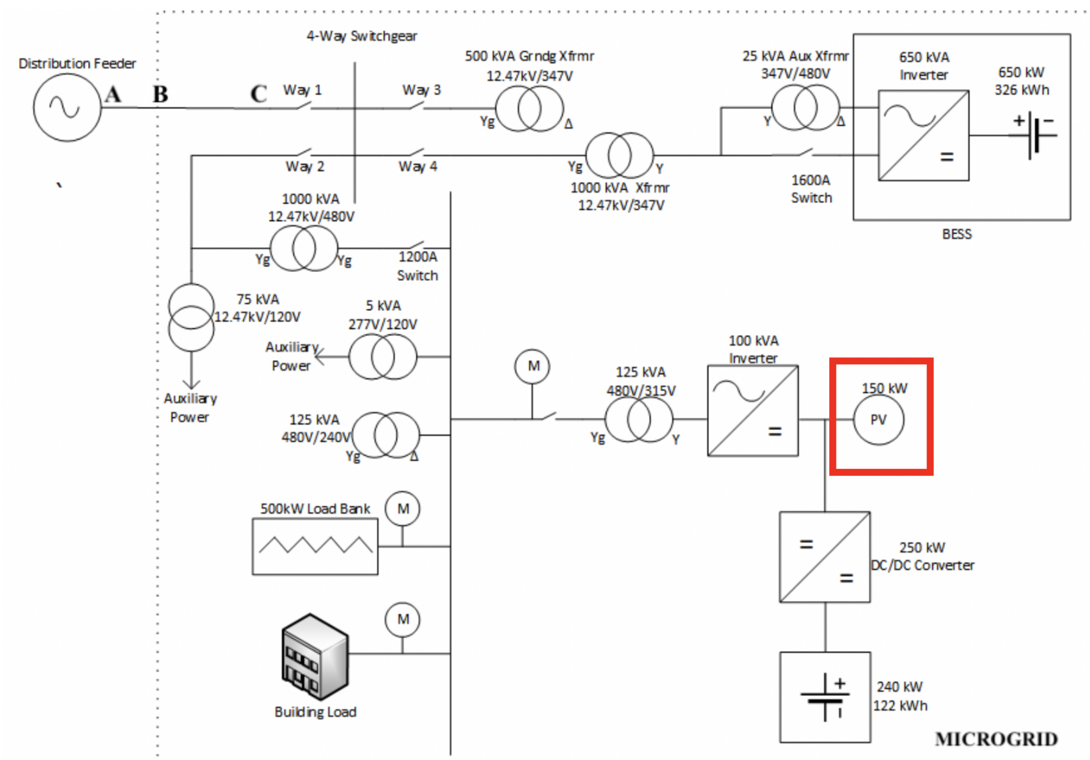

Figure 7.7: Simulation Diagram of Microgrid highlighting the Photovoltaic Source

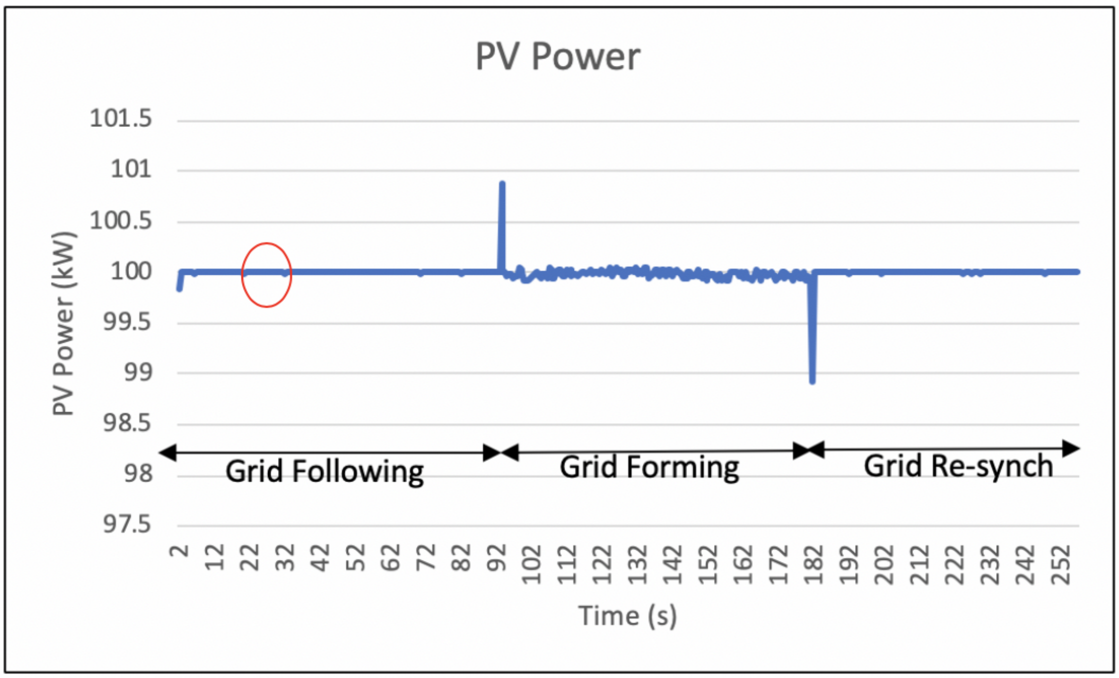

Figure 7.8: Photovoltaic Power observed during the three modes of microgrid

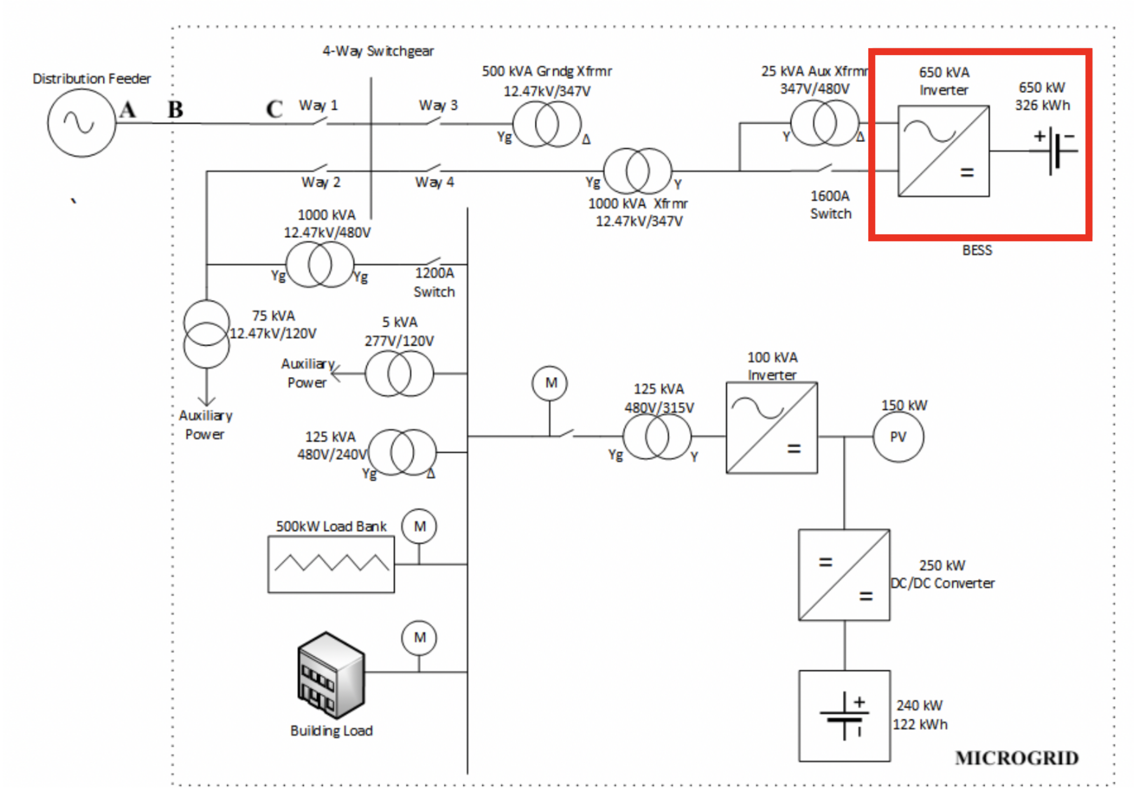

Figure 7.9: Simulation Diagram of Microgrid highlighting the Battery Energy Storage System

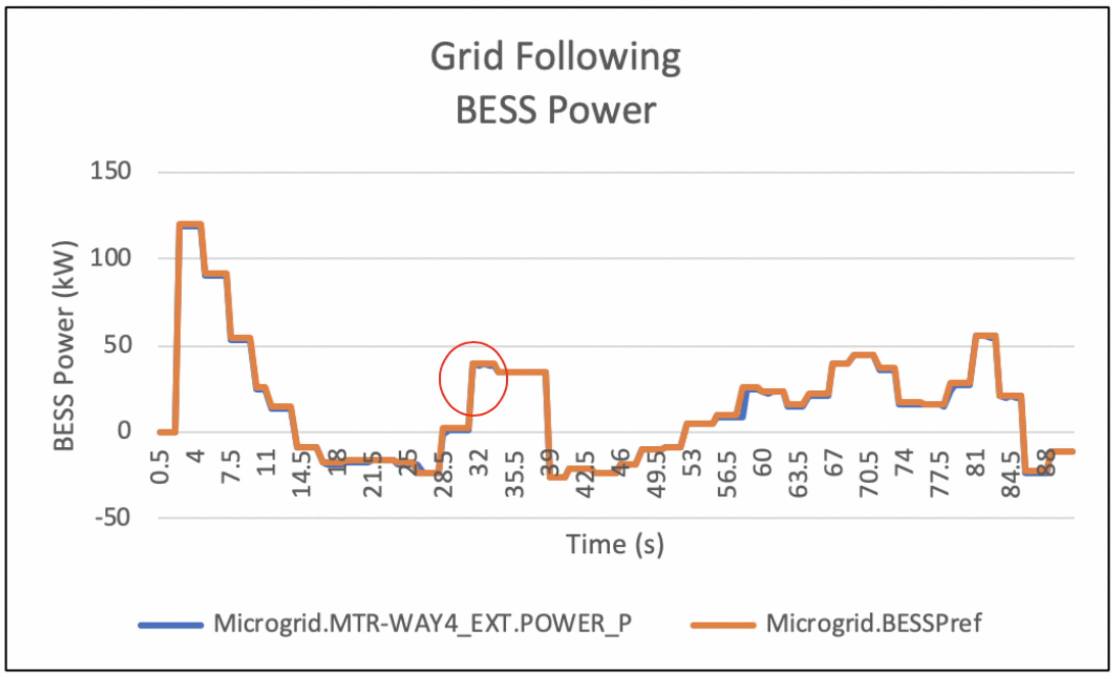

Figure 7.10: Battery Energy Storage System Power observed during the three modes of microgrid

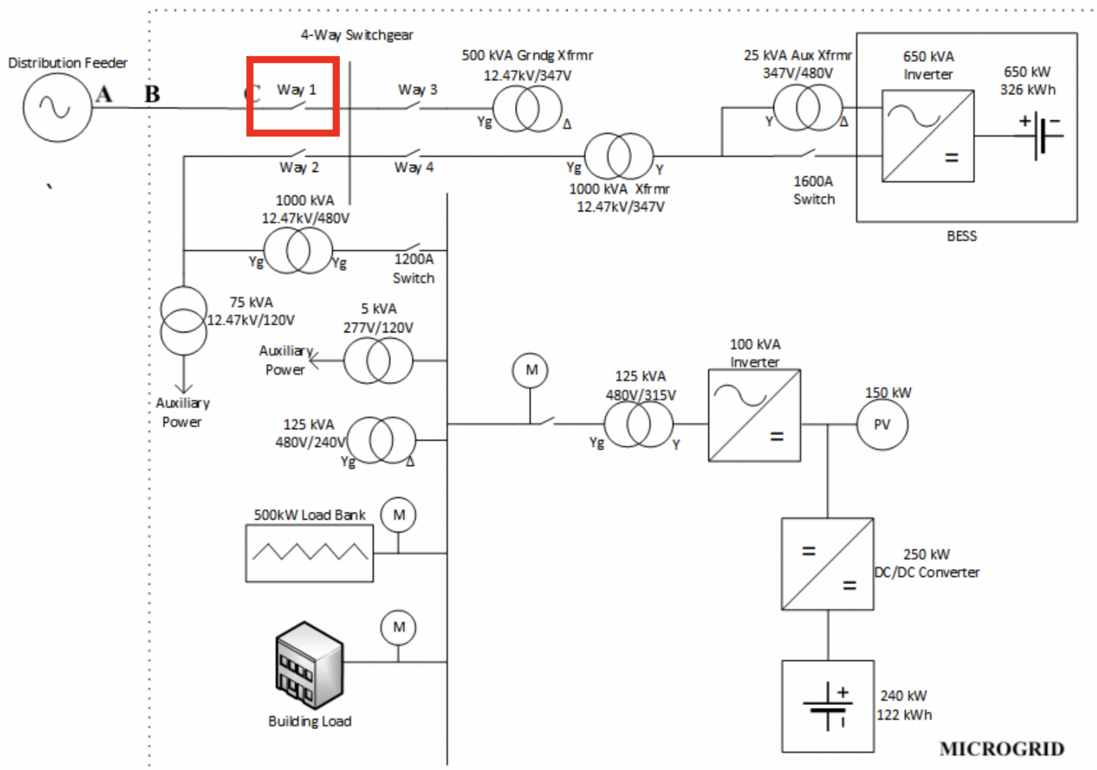

1.png

Figure 7.11: Simulation Diagram of Microgrid highlighting the Battery Energy Storage System

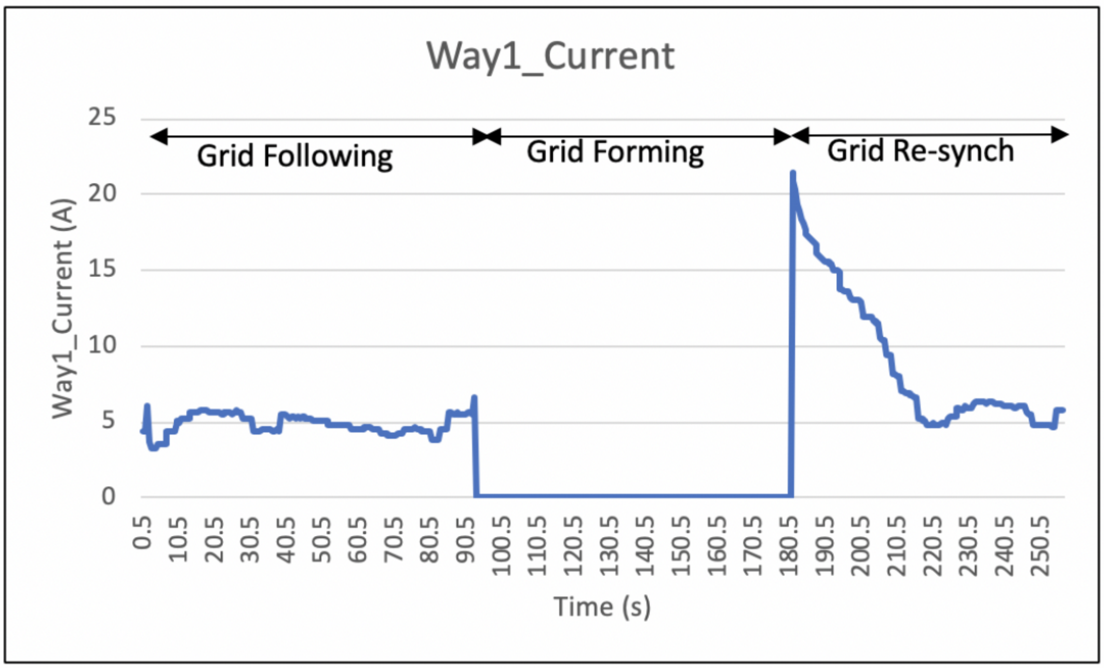

Figure 7.12: Current through Way 1

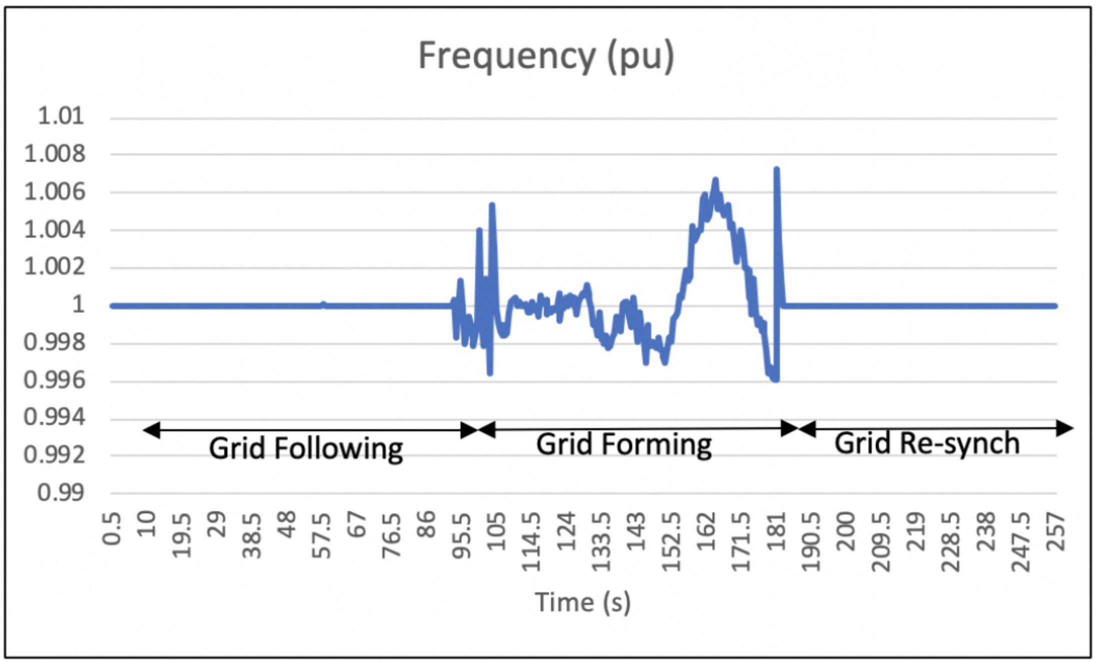

Figure 7.13: Frequency (pu) observed during the three modes of microgrid

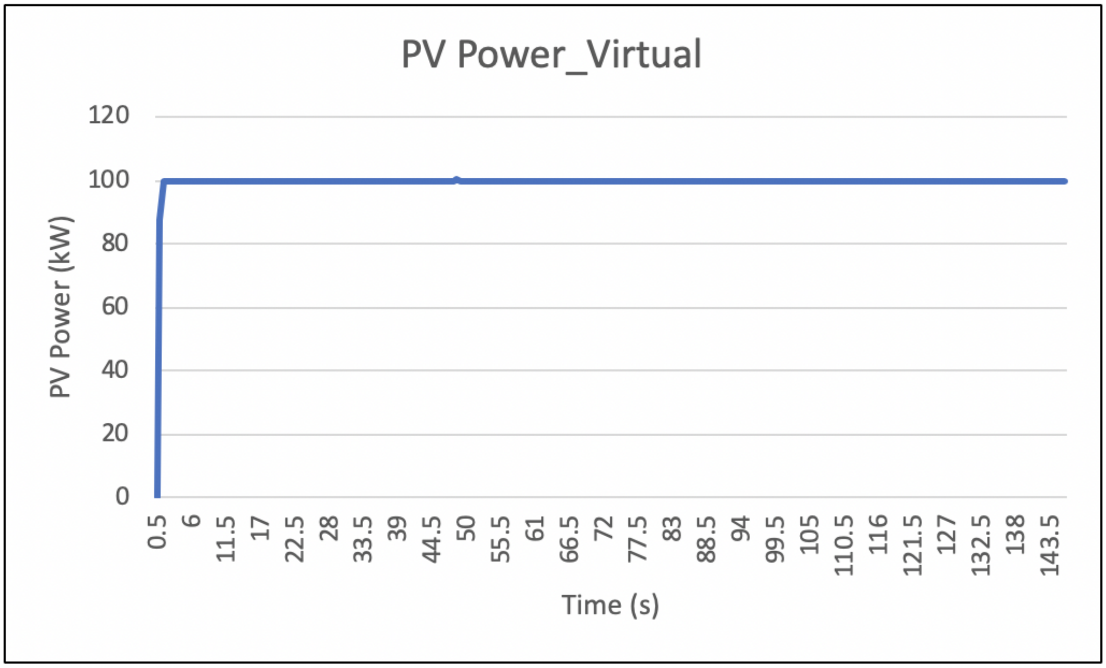

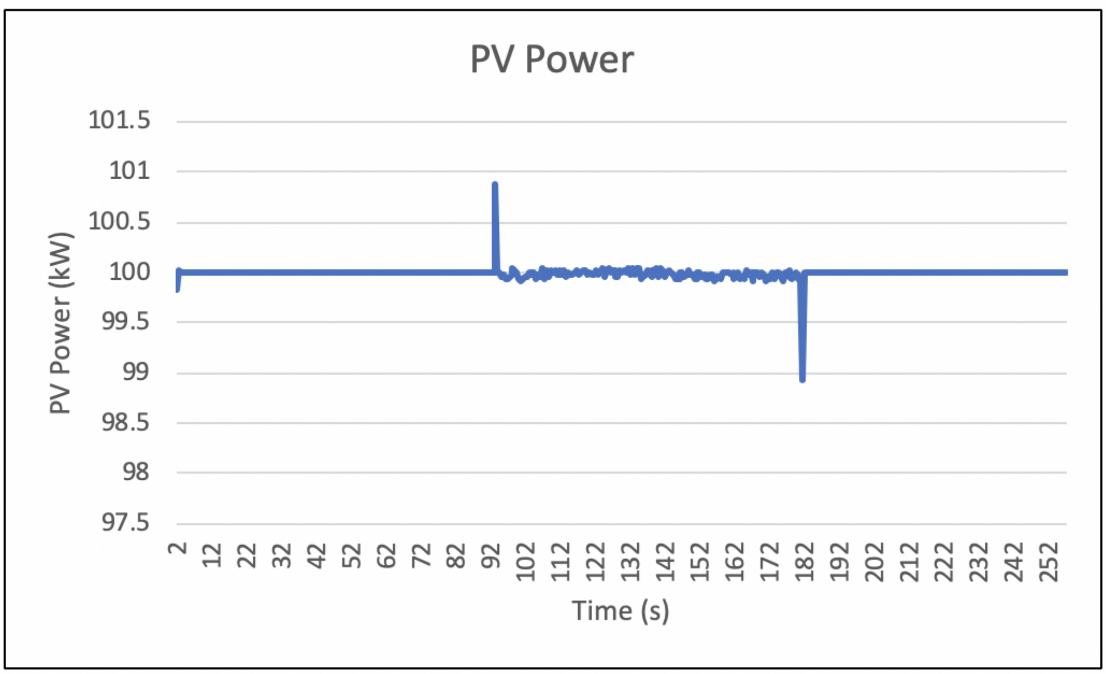

Figure 7.14: Photovoltaic Power - vHIL vs cHIL

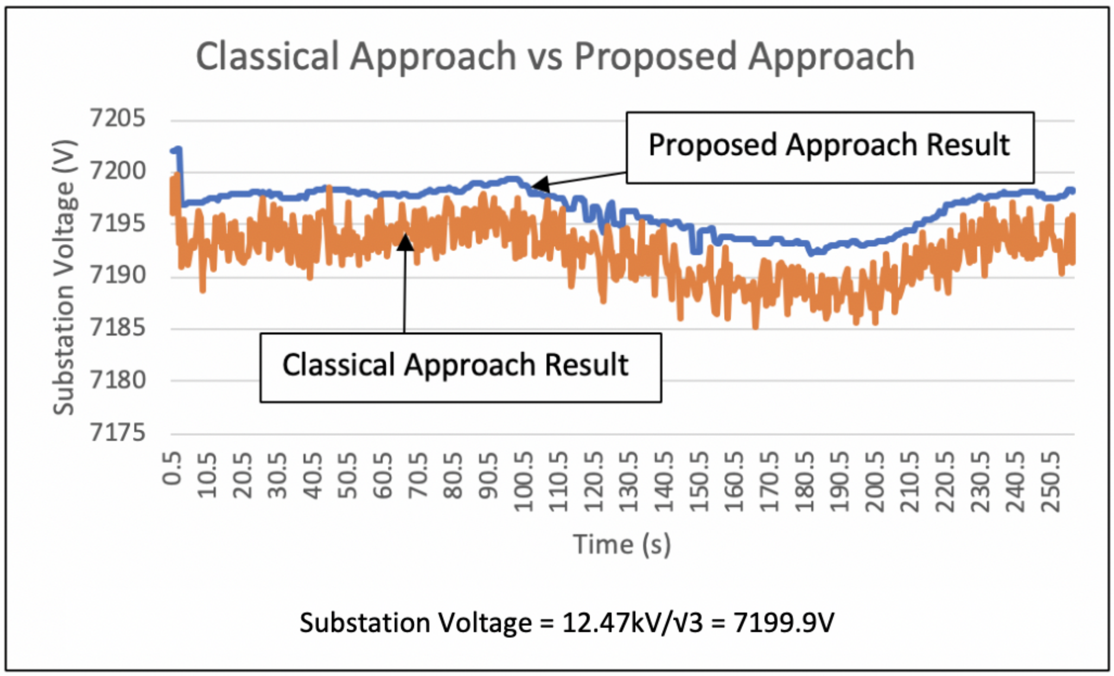

Figure 7.15: Proposed vs Classical Approach Result

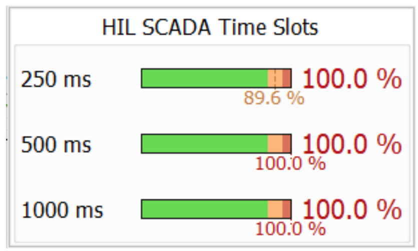

Figure 7.16: HIL SCADA Update Rate

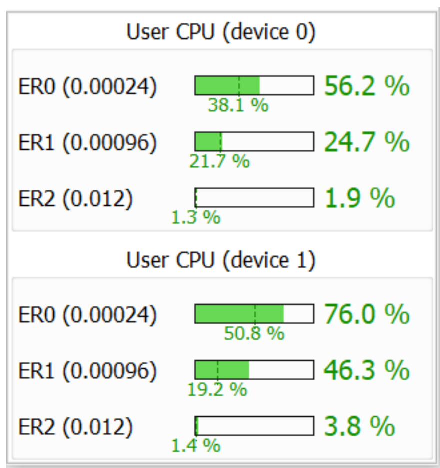

Figure 7.17: Execution Rates of signals coming through Proposed (ER0), Classical Approach (ER1) and Meters(ER2)

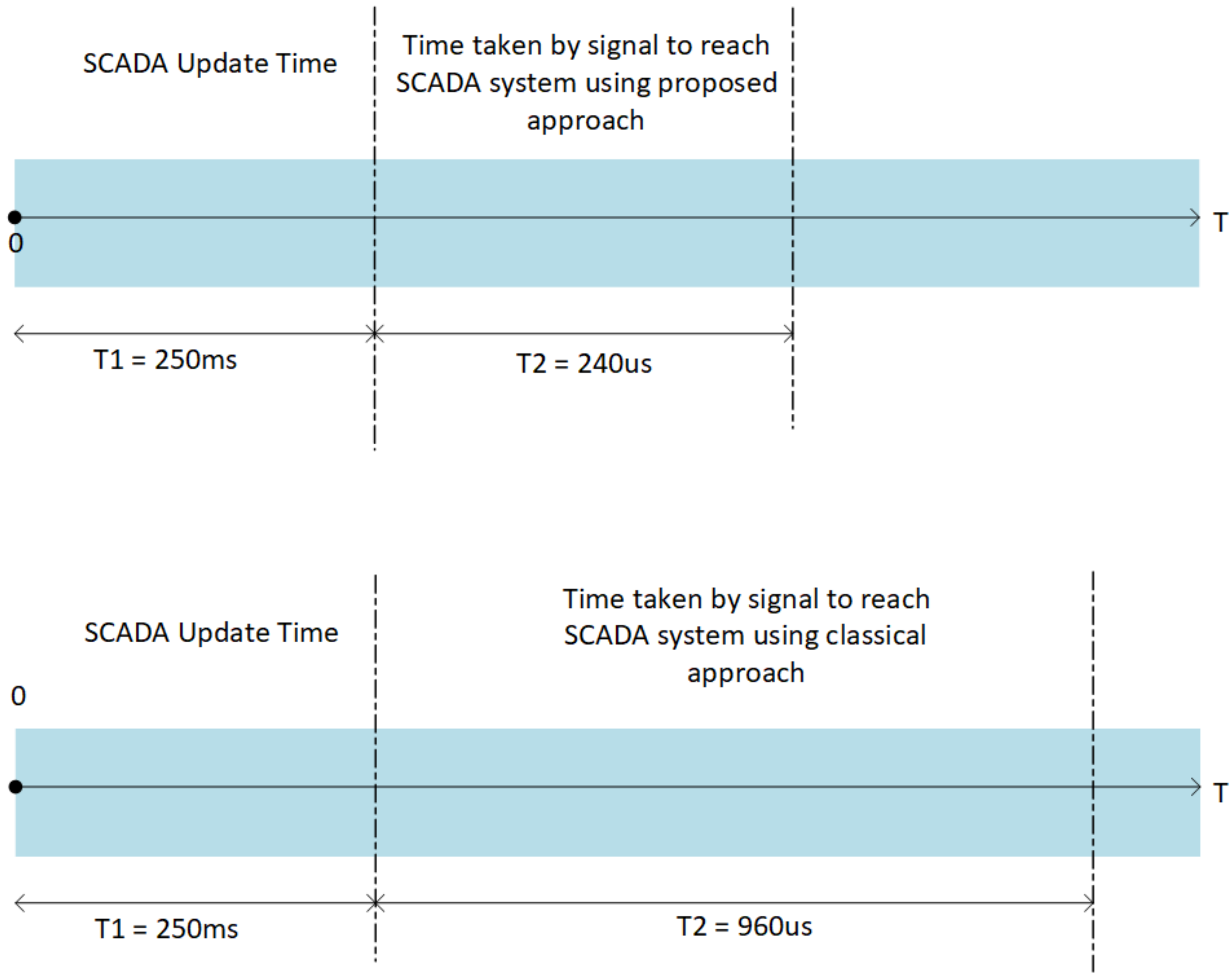

Figure 7.18: Time taken by signal to reach SCADA system using classical and proposed approach

```
dVArh":{"q":{"detailQual":{}},"t":{"tq":{}},"units":{}},"DmdWh":{"q":{"detailQual":{}},"t":{"tq":{}}
"detailQual":{}},"t":{"tq":{}},"units":{}}},"phsB":{"logicalNode":{"identifiedObject":{"description"
SupWh":{"q":{"detailQual":{}},"t":{"tq":{}},"units":{}},"TotVAh":{"q":{"detailQual":{}},"t":{"tq":{}
"units":{}},"DmdWh":{"q":{"detailQual":{}},"t":{"tq":{}},"units":{}},"SupVAh":{"q":{"detailQual":{}}
":{}}},"readingMMXU":{"logicalNode":{"identifiedObject":{"description":"","mRID":"","name":""}},"A":
},"mag":{"f":0,"i":0}},"q":{"detailQual":{}},"t":{"tq":{}},"units":{"multiplier":{}}},"neut":{"cVal"
"t":{"tq":{}},"units":{"multiplier":{}}},"phsC":{"cVal":{"ang":{"f":0,"i":0},"mag":{"f":0,"i":0}},"q"
:{"cVal":{"ang":{"f":0,"i":0},"mag":{"f":0,"i":0}},"q":{"detailQual":{}},"t":{"tq":{}},"units":{"mul
q":{"detailQual":{}},"t":{"tq":{}},"units":{"multiplier":{}}},"phsB":{"cVal":{"ang":{"f":0,"i":0},"ma
```


Figure 7.19: OpenFMB Data

CHAPTER 8: CONCLUSIONS & FUTURE SCOPE

8.1 Conclusions

The practical implementation of a new North American Energy Standard interoperability framework: Open Field Message Bus (OpenFMB) in a real-time hardware-in-loop testbed is performed in this work.

An electrical substation feeding a utility's microgrid is considered for a test simulation. A number of test cases are performed to validate the functionalities of the microgrid. The microgrid is made to island from the main grid considering the fact that there is a fault on the system. The microgrid is able to supply the required amount of power to the load with the help of 800kW worth of distributed energy resources. The microgrid is made to synchronize back to the main grid under the set limits of voltage and frequency. The analog and digital inputs from the simulation are configured to the P&C and RTU devices. The OpenFMB adapters are embedded inside the RTU which helps in mapping the tags of two different speaking protocol devices. The values are subscribed from the Remote Terminal Unit and then published on to the Supervisory Control and Data Acquisition (SCADA). The values from the traditional centralized system (classical approach) are compared to the proposed approach. It can be concluded that proposed approach yields similar result as that of classical approach with negligible error. The main difference that needs to be highlighted here is that the results observed from the proposed approach are from a secure environment. The process is as simple as plug-n-play integration between different vendor devices and interoperable. The key to distributed intelligence at the edge when compared to the traditional centralized system is the OpenFMB node which yields a faster and resilient response.

8.2 Future Work

The work done as a part of this masters thesis is purely based on Controller Hardware-in-loop (c-HIL) simulations. To get better real-time results, the next steps to perform Power Hardware-in-loop (p-HIL) simulations with Real Hardware including inverters/batteries can be implemented.

A better Human Machine Interface (HMI) between the OpenFMB adapters and the user can be created for this particular testbed.

A secure node can be created to improve cyber-security of the system.

REFERENCES

[1] A. Ahmed, Mohamed & Kang, Y.C. & Kim, Young-Chon. (2015).Communication Network Architectures for Smart-House with Renewable Energy Resources. Energies. 8. 8716-8735. 10.3390/en8088716

[2] X. Fang, S. Misra, G. Xue and D. Yang, "Smart Grid - The New and Improved Power Grid: A Survey," in IEEE Communications Surveys & Tutorials, vol. 14, no. 4, pp. 944-980, Fourth Quarter 2012

[3] K. M. Son, K. Lee, D. Lee, E. Nho, T. Chun and H. Kim, "Grid interfacing storage system for implementing microgrid," 2009 Transmission & Distribution Conference & Exposition: Asia and Pacific, Seoul, 2009, pp. 1-4

[4] M. M. Rana and L. Li, "Controlling the Distributed Energy Resources Using Smart Grid Communications," 2015 12th International Conference on Information Technology - New Generations, Las Vegas, NV, 2015, pp. 490-495

[5] Kritigya, A. Bhattacharya, R. L. Meena and D. K. Khatod, "Control and operation of grid-connected solar photovoltaic for DC microgrid application," 2016 IEEE 7th Power India International Conference (PIICON), Bikaner, 2016, pp. 1-5

[6] H. K. Vidyashree, H. B. Jagadamba and T. Yuvaraja, "Photovoltaic incorporated in microgrid system," 2017 International Conference on Electrical, Electronics, Communication, Computer, and Optimization Techniques (ICEECCOT), Mysuru, 2017, pp. 220-222

[7] S. Augustine, N. Lakshminarasamma, M. K. Mishra and T. Sreekanth, "MPP tracking of PV based low voltage DC microgrid system with adaptive droop algorithm," 2015 IEEE 42nd Photovoltaic Specialist Conference (PVSC), New Orleans, LA, 2015, pp. 1-4

[8] B. M. Omar, H. Samir, Z. S. Ahmed and D. K. Y. Islam, "A Comparative investigation of maximum power point tracking techniques for grid connected PV system under various weather conditions," 2017 5th International Conference on Electrical Engineering - Boumerdes (ICEE-B), Boumerdes, 2017, pp. 1-5

[9] H. Suyanto and R. Irawati, "Study trends and challenges of the development of microgrids," 2017 15th International Conference on Quality in Research (QiR) : International Symposium on Electrical and Computer Engineering, Nusa Dua, 2017, pp. 383-387

[10] Radhakrishnan, Rohikaa & Lakshmi, R & Sunitha, R & Ashok, Sharmila. (2016). Assessment of voltage stability in microgrid. 1268-1273. 10.1109/ICEEOT

[11] H. Kakigano, Y. Miura, T. Ise and R. Uchida, "DC Voltage Control of the DC Micro-grid for Super High Quality Distribution," 2007 Power Conversion Conference - Nagoya, Nagoya, 2007, pp. 518-525

[12] J.J.Justo,F.Mwasilu,J.Lee,J-W Jung, "AC-microgrids versus DC-microgrids with distributed energy resources: A review," 2013 Elsevier Renewable and Sustainable Energy Reviews

[13] B. A. Karuppaswamy, S. Gulur and V. John, "A grid simulator to evaluate control performance of grid-connected inverters," 2014 IEEE International Conference on Power Electronics, Drives and Energy Systems (PEDES), Mumbai, 2014, pp. 1-6

[14] H. F. Jamahori and H. A. Rahman, "Hybrid energy storage system for life cycle improvement," 2017 IEEE Conference on Energy Conversion (CENCON), Kuala Lumpur, 2017, pp. 196-200

[15] A. Mamen and U. Supatti, "A survey of hybrid energy storage systems applied for intermittent renewable energy systems," 2017 14th International Conference on Electrical Engineering/Electronics, Computer, Telecommunications and Information Technology (ECTI-CON), Phuket, 2017, pp. 729-732

[16] S. Lin, C. Yang, W. Song and Z. Feng, "Analysis of Capacity and Control Strategy for Distributed Energy System with Hybrid Energy Storage System," 2018 International Conference on Smart Grid and Clean Energy Technologies (ICSGCE), Kajang, 2018, pp. 84-88

[17] F. Li, L. Shen, Y. Si and J. Niu, "A Method to Enhance SCADA Systems Survivability through Simulation Technology," 2009 International Conference on Measuring Technology and Mechatronics Automation, Hunan, 2009, pp. 175-178

[18] H. Lotfi and A. Khodaei, "AC Versus DC Microgrid Planning," in IEEE Transactions on Smart Grid, vol. 8, no. 1, pp. 296-304, Jan. 2017

[19] H. Niu, M. Jiang, D. Zhang and J. Fletcher, "Autonomous micro-grid operation by employing weak droop control and PQ control," 2014 Australasian Universities Power Engineering Conference (AUPEC), Perth, WA, 2014, pp. 1-5

[20] K. G. Jayanth, V. Boddapati and R. S. Geetha, "Comparative study between three-leg and four-leg current-source inverter for solar PV application," 2018 International Conference on Power, Instrumentation, Control and Computing (PICC), Thrissur, 2018, pp. 1-6

[21] M. A. Salam and S. Sethulakshmi, "Control for grid connected and intentional islanded operation of distributed generation," 2017 Innovations in Power and Advanced Computing Technologies (i-PACT), Vellore, 2017, pp. 1-6

[22] R. Hunt and B. Popescu, "SCADA communications for protection engineers," 2015 68th Annual Conference for Protective Relay Engineers, College Station, TX, 2015, pp. 881-891

[23] S. Datta and S. De, "Study of 230/11 kV Substation Under Different Type of Faults," 2017 International Conference on Computer, Electrical & Communication Engineering (ICCECE), Kolkata, 2017, pp. 1-4

[24] H. Kunlun, C. Zexiang and L. Yang, "Study on protective performance of HVDC transmission line protection with different types of line fault," 2011 4th International Conference on Electric Utility Deregulation and Restructuring and Power Technologies (DRPT), Weihai, Shandong, 2011, pp. 358-361

[25] M. D. Borkar and K. D. Thakur, "Analysis of unsymmetrical fault using symmetrical component for improvement of overcurrent protection scheme," 2013 International Conference on Computer Communication and Informatics, Coimbatore, 2013, pp. 1-5

[26] V. N. Ogar, D. N. Abara and E. J. Akpama, "Symmetrical and unsymmetrical faults analysis: Using Nigeria 330-KV grid as case study," 2017 IEEE 3rd International Conference on Electro-Technology for National Development (NIGERCON), Owerri, 2017, pp. 1-7

[27] M. A. Hasan, S. Sourabh and S. K. Parida, "Impact of a microgrid on utility grid under symmetrical and unsymmetrical fault conditions," 2016 IEEE 7th Power India International Conference (PIICON), Bikaner, 2016, pp. 1-6

[28] M. Hosny Tawfeek Essa and P. Crossley, "GOOSE performance assessment on an IEC 61850 redundant network," in The Journal of Engineering, vol. 2018, no. 15, pp. 841-845, 10 2018

[29] R. Amoah, S. Camtepe and E. Foo, "Securing DNP3 Broadcast Communications in SCADA Systems," in IEEE Transactions on Industrial Informatics, vol. 12, no. 4, pp. 1474-1485, Aug. 2016

[30] L. Cheng, "Study and application of DNP3.0 in SCADA system," Proceedings of 2011 International Conference on Electronic & Mechanical Engineering and Information Technology, Harbin, 2011, pp. 4563-4566

[31] M. Aamir, M. A. Uqaili, J. Poncela, N. A. Khan and B. S. Chowdhry, "Implementation and testing of optimal design of RTU hardware for Wireless SCADA," 2014 4th International Conference on Wireless Communications, Vehicular Technology, Information Theory and Aerospace & Electronic Systems (VITAE), Aalborg, 2014, pp. 1-5

[32] https://openfmb.gitlab.io

[33] https://grid-io.com/2018/04/25/openfmb/

[34] Aleksandar Vukojevic, "Microgrid Protection and Control Strategies at Duke Energy" 2018 72nd Georgia Tech Protective Relaying Conference, Atlanta, GA

[35] https://selinc.com/products/

[36] Srdjan Lukic, Short Course on Microgrids Power Electronics, FREEDM Systems Center, Spring'19

[37] https://www.multisim.com/help/components/pulse-width-modulation-pwm-components/

APPENDIX A: NOMENCLATURE FOR ANALOG OUTPUTS

SEL AI Module 2245-22	Typhoon I/O Board	Box No
AI_Node1_CB_V_ECAT - VA	AO-1	1
AI_Node1_CB_V_ECAT - VB	AO-2	1
AI_Node1_CB_V_ECAT - VC	AO-3	1
AI_Node1_CB_V_ECAT - VN	AO-4	1
AI_Node1_CB_I_ECAT - IA	AO-5	1
AI_Node1_CB_I_ECAT - IB	AO-6	1
AI_Node1_CB_I_ECAT - IC	AO-7	1
AI_Node1_CB_I_ECAT - IN	AO-8	1
AI_Node1_HPOI_V_ECAT - VA	AO-9	1
AI_Node1_HPOI_V_ECAT - VB	AO-10	1
AI_Node1_HPOI_V_ECAT - VC	AO-11	1
AI_Node1_HPOI_V_ECAT - VN	AO-12	1
AI_Node1_HPOI_I_ECAT - IA	AO-13	1
AI_Node1_HPOI_I_ECAT - IB	AO-14	1
AI_Node1_HPOI_I_ECAT - IC	AO-15	1
AI_Node1_HPOI_I_ECAT - IN	AO-16	1
AI_Node1_UPOI_V_ECAT - VA	AO-17	1

AI_Node1_UPOI_V_ECAT - VB	AO-18	1
AI_Node1_UPOI_V_ECAT - VC	AO-19	1
AI_Node1_UPOI_V_ECAT - VN	AO-20	1
AI_Node1_UPOI_I_ECAT - IA	AO-21	1
AI_Node1_UPOI_I_ECAT - IB	AO-22	1
AI_Node1_UPOI_I_ECAT - IC	AO-23	1
AI_Node1_UPOI_I_ECAT - IN	AO-24	1
AI_Node1_MPOI_V_ECAT - VA	AO-25	1
AI_Node1_MPOI_V_ECAT - VB	AO-26	1
AI_Node1_MPOI_V_ECAT - VC	AO-27	1
AI_Node1_MPOI_V_ECAT - VN	AO-28	1
AI_Node1_MPOI_I_ECAT - IA	AO-29	1
AI_Node1_MPOI_I_ECAT - IB	AO-30	1
AI_Node1_MPOI_I_ECAT - IC	AO-31	1
AI_Node1_MPOI_I_ECAT - IN	AO-32	1

Table A.1: Nomenclature for naming Analog input/output cards-1

Table A.2: Nomenclature for naming Analog input/output cards-2

SEL AI Module 2245-22	Typhoon I/O Board-1	Typhoon Box No
AI_Node1_GPOI_V_ECAT - VA	AO-33	2
AI_Node1_GPOI_V_ECAT - VB	AO-34	2
AI_Node1_GPOI_V_ECAT - VC	AO-35	2
AI_Node1_GPOI_V_ECAT - VN	AO-36	2
AI_Node1_GPOI_I_ECAT - IA	AO-37	2
AI_Node1_GPOI_I_ECAT - IB	AO-38	2
AI_Node1_GPOI_I_ECAT - IC	AO-39	2
AI_Node1_GPOI_I_ECAT - IN	AO-40	2
AI_Node1_PCC12_V_ECAT - VA	AO-41	2
AI_Node1_PCC12_V_ECAT - VB	AO-42	2
AI_Node1_PCC12_V_ECAT - VC	AO-43	2
AI_Node1_PCC12_V_ECAT - VN	AO-44	2
AI_Node1_PCC12_I_ECAT - IA	AO-45	2
AI_Node1_PCC12_I_ECAT - IB	AO-46	2
AI_Node1_PCC12_I_ECAT - IC	AO-47	2
AI_Node1_PCC12_I_ECAT - IN	AO-48	2
AI_Node1_PCC34_V_ECAT - VA	AO-49	2
AI_Node1_PCC34_V_ECAT - VB	AO-50	2
AI_Node1_PCC34_V_ECAT - VC	AO-51	2
AI_Node1_PCC34_V_ECAT - VN	AO-52	2
AI_Node1_PCC34_I_ECAT - IA	AO-53	2
AI_Node1_PCC34_I_ECAT - IB	AO-54	2
AI_Node1_PCC34_I_ECAT - IC	AO-55	2
AI_Node1_PCC34_I_ECAT - IN	AO-56	2

APPENDIX B: NOMENCLATURE FOR DIGITAL INPUTS & OUTPUTS

Table B.1: Nomenclature for naming Digital input/output cards-1

Digital outputs in SEL 2244-3	Digital Input Terminals	Typhoon Box No
1-CB-DO (Group A)	DI-1	1
2 - HPOI-DO (Group-A)	DI-2	1
3 - UPOI-DO (Group-A)	DI-3	1
4 - GPOI-DO (Group-A)	DI-1	2
5 - MPOI-DO (Group-A)	DI-4	2
6 - PCC12-DO (Group-A)	DI-2	2
7 - PCC34-DO (Group-A)	DI-3	2

Table B.2: Analog Output Pins configuration

Description		Sensor Data	Analog Output Pins in Box-1
Substation Circuit Breaker	Substation CB phase-A voltage	CB_VA	AO-1
	Substation CB phase-B voltage	CB_VB	AO-2
	Substation CB phase-C voltage	CB_VC	AO-3
	Substation CB neutral voltage	CB_VN	AO-4
	Substation CB phase-A current	CB_IA	AO-5
	Substation CB phase-B current	CB_IB	AO-6
	Substation CB phase-C current	CB_IC	AO-7
	Substation CB neutral current	CB_IN	AO-8
Hybrid Energy Storage System (HESS)	HESS POI phase-A voltage	HPOI_VA	AO-9
	HESS POI phase-B voltage	HPOI_VB	AO-10
	HESS POI phase-C voltage	HPOI_VC	AO-11
	HESS POI neutral voltage	HPOI_VN	AO-12
	HESS POI phase-A current	HPOI_IA	AO-13
	HESS POI phase-B current	HPOI_IB	AO-14
	HESS POI phase-C current	HPOI_IC	AO-15

Table B.3: Analog Output Pins Configuration - Cont'd

Description		Sensor Data	Analog Output Pins in Box-1
	HESS POI neutral current	HPOI_IN	AO-16
Upstream Point of Interaction (UPOI)	UPOI phase-A voltage	UPOI_VA	AO-17
	UPOI phase-B voltage	UPOI_VB	AO-18
	UPOI phase-C voltage	UPOI_VC	AO-19
	UPOI neutral voltage	UPOI_VN	AO-20
	UPOI phase-A current	UPOI_IA	AO-21
	UPOI phase-B current	UPOI_IB	AO-22
	UPOI phase-C current	UPOI_IC	AO-23
	UPOI neutral current	UPOI_IN	AO-24
Microgrid Point of Interaction (MPOI)	MPOI phase-A voltage	MPOI_VA	AO-25
	MPOI phase-B voltage	MPOI_VB	AO-26
	MPOI phase-C voltage	MPOI_VC	AO-27
	MPOI neutral voltage	MPOI_VN	AO-28
	MPOI phase-A current	MPOI_IA	AO-29
	MPOI phase-B current	MPOI_IB	AO-30
	MPOI phase-C current	MPOI_IC	AO-31
	MPOI neutral current	MPOI_IN	AO-32

Table B.4: Analog Output Pins Configuration - Cont'd

Description		Sensor Data	Analog Output Pins in Box-2
Current Source Generating Point of Interaction (GPOI)	GPOI phase-A voltage	GPOI_VA	AO-33
	GPOI phase-B voltage	GPOI_VB	AO-34
	GPOI phase-C voltage	GPOI_VC	AO-35
	GPOI neutral voltage	GPOI_VN	AO-36
	GPOI phase-A current	GPOI_IA	AO-37
	GPOI phase-B current	GPOI_IB	AO-38
	GPOI phase-C current	GPOI_IC	AO-39
	GPOI neutral current	GPOI_IN	AO-40
PCC12 Point of Interaction (PCC12-POI) (Inside Microgrid)	PCC12 phase-A voltage	PCC12_VA	AO-41
	PCC12 phase-B voltage	PCC12_VB	AO-42
	PCC12 phase-C voltage	PCC12_VC	AO-43
	PCC12 neutral voltage	PCC12_VN	AO-44
	PCC12 phase-A current	PCC12_IA	AO-45
	PCC12 phase-B current	PCC12_IB	AO-46
	PCC12 phase-C current	PCC12_IC	AO-47
	PCC12 neutral current	PCC12_IN	AO-48
PCC34 Point of Interaction (PCC12-POI) (Inside Microgrid)	PCC34 phase-A voltage	PCC34_VA	AO-49
	PCC34 phase-B voltage	PCC34_VB	AO-50
	PCC34 phase-C voltage	PCC34_VC	AO-51

Table B.5: Analog Output Pins configuration

Description	Sensor Data	Analog Output Pins in Box-2
PCC34 neutral voltage	PCC34_VN	AO-52
PCC34 phase-A current	PCC34_IA	AO-53
PCC34 phase-B current	PCC34_IB	AO-54
PCC34 phase-C current	PCC34_IC	AO-55
PCC34 neutral current	PCC34_IN	AO-56

Table B.6: Digital input terminals in Box-1 & Signal name

	Digital input terminals in Box-1	Signal name
Substation CB	DI-1	CB-DI
HESS POI	DI-2	HESS-DI
Upstream POI	DI-3	UPOI-DI
Microgrid POI	DI-4	MPOI-DI

Table B.7: Digital input terminals in Box-2 & Signal name

	Digital input terminals in Box-2	signal name
Current Source Generation POI	DI-1	GPOI-DI
PCC12 Recloser	DI-2	PCC12-DI
PCC34 Recloser	DI-3	PCC34-DI